# DISSERTATION

submitted to the

Combined Faculties for the Natural Sciences and for Mathematics

of the Ruperto-Carola University of Heidelberg, Germany

for the degree of

DOCTOR OF NATURAL SCIENCES

presented by

Master of Science, Vianihuini Figueroa Vázquez

born in Puebla, Mexico

Oral-examination:

# Functional characterization of BRAF mutations in multiple myeloma

Referees:

Prof. Dr. Robert B. Russell

PD. Dr. med. Marc-Steffen Raab

# Table of Contents

# Summary

Activating BRAF mutations are frequently found in diverse types of cancer, including multiple myeloma. Moreover, current targeted therapy can abrogate mutant BRAF kinase activity although drug resistance mechanisms are still a challenge. However, this mutation has not been functionally characterized in multiple myeloma and biological consequences along BRAF inhibitor resistance mechanisms are unknown.

Here we show that BRAF V600E expression in multiple myeloma leads to an active MAPK/ERK pathway and eventual DNA damage. This mutation can be targeted with BRAF inhibitors (BRAFi). Nevertheless, we demonstrate that BRAF wild type under BRAFi leads to paradoxical activation. To overcome this effect a MEK inhibitor was employed for an effective pathway abrogation in multiple myeloma.

Furthermore, to identify mechanisms that contribute to BRAFi resistance, whole exome sequencing of a BRAFi-resistance model of MM was performed. We identified a novel mutation in the transcription factor EGR-1 followed by its protein functional characterization. This showed that the mutant protein (p. 332fs) along the wild type protein is overexpressed in our *in vitro* model and mutant EGR-1 influences its own subcellular localization. Overexpression of the mutant EGR-1 conferred complete resistance to BRAF inhibition.

# Zusammenfassung

Aktivierende Mutationen in der BRAF Kinase werden in verschiedenen Krebsarten mit unterschiedlicher Häufigkeit nachgewiesen, unter anderem auch im Multiplen Myelom. Ferner sind die derzeitigen zielgerichteten Therapien in der Lage, die Kinaseaktivität des mutierten BRAFs zu unterbinden, wobei jedoch auftretende Medikamentenresistenzen eine Herausforderung darstellen. Diese Mutation wurde jedoch beim Multiplen Myelom noch nicht funktionell charakterisiert und die biologischen Folgen von Resistenzmechanismen gegen BRAF-Inhibitoren sind unbekannt.

In dieser Arbeit zeigen wir, dass die Expression von BRAF V600E im Multiplen Myelom zu einer Aktivierung des MAPK/ERK Signalwegs führt und schließlich in DNA-Schäden resultiert. Diese Mutation kann mit BRAF Inhibitoren (BRAFi) gezielt spezifisch gehemmt werden. Dennoch zeigten wir wie es unter BRAFi-Exposition des BRAF-Wildtyps zu einer paradoxen Aktivierung kommt. Um diese Wirkung zu umgehen wurde ein MEK-Inhibitor für eine effektive Signalwegblockade im Multiplen Myelom eingesetzt.

Außerdem wurde eine vollständige Exomsequenzierung eines BRAFi-Resistenzmodells durchgeführt, um Mechanismen zu identifizieren, die zur BRAFi-Resistenz beitragen. Wir identifizierten eine neue Mutation im Transkriptionsfaktor EGR-1, woraufhin eine funktionelle Charakterisierung dieses Proteins erfolgte. Diese zeigte, dass das mutierte Protein (p. 332fs) zusammen mit dem Wildtyp-Protein in unserem in vitro Modell überexprimiert wird und die EGR-1 Mutation die subzelluläre Lokalisation des Proteins beeinflusst. Zusätzlich führt die fehlerhafte Proteinexpression alleine zu einer Dabrafenib-Resistenz im Multiplen Myelom.

# Acknowledgements

# 1

---

# Introduction

## Multiple myeloma

Multiple myeloma (MM) is a clonal disease of malignant plasma cells characterized by the excess of plasma cells in the bone marrow, along with high monoclonal protein levels in the blood or urine, osteolytic bone lesions, renal disease and immunodeficiency.

On a worldwide scale, MM is estimated to represent approximately 1% of all new cancer cases and about 10% of hematologic malignancies. It is also considered to be the second most frequent blood neoplastic disease, accounting for 0.9% of all cancer-related deaths per year [1]. The incidence of MM is higher in the industrialized regions of Europe, North America, Australia and New Zealand than in the rest of the world. Ethnically, it occurs almost double as frequent in blacks compared to whites, and in terms of age at diagnoses, the median ranges from 63 to 71 years. In regard to gender, this disease is more predominant in males than in females. Currently, the median overall survival is about 5 years [2].

MM is regularly preceded by a premalignant state, termed monoclonal gammopathy of undetermined significance (MGUS). The pathogenesis of MM is

thought to embrace a multistep process from early genetic events such as hyperdiploidy and immunoglobulin translocations, followed by secondary genetic events such as copy number abnormalities (gain and losses of entire DNA regions), acquired mutations and DNA hypomethylation that lead to tumor cell diversity and disease progression (Figure 1) [3–5].

The most predominant chromosomal aberrations include translocations of the Heavy Chain Locus (IGH@) on chromosome 14 as a result of switch recombination or somatic hypermutation causing spiked expression of oncogenes positioned near Ig enhancers [6]. Some reported translocations that lead to an upregulated gene expression are, t(4;14) FGFR3 and MMSET, t(6;14): CCND3, t(11:14): CCND1, t(14;16): MAF, t(14;20): MAFB[3,4].

The secondary genetic events comprehend mutations, overexpression or activation of functional sequelae such as G1/S transition, proliferation, resistance to apoptosis, NF-κB pathway, bone disease, abnormal plasma differentiation, abnormal DNA repair, RNA editing, epigenetic abnormalities [7].

Moreover, genetic abnormalities affect the expression of adhesion molecules in myeloma cells, responsible for the interaction with bone marrow stromal cells and the extracellular matrix proteins. This can influence cell migration, survival, growth and drug resistance. As it has been described for other types of cancer, interaction with the microenvironment results in the upregulation of cell cycle and antiapoptotic proteins, leading to disease progression [8].

The current treatment is based on proteasome inhibitors like bortezomib and carfilzomib, immunomodulatory drugs including thalidomide, lenalidomide and pomalidomide, and conventional chemotherapy drugs such as melphalan. However, relapse occurs inevitably and it becomes harder over time to provide an effective therapy since tumor cells acquire resistance [9]. Thus, new therapeutic

approaches are urgently needed to overcome treatment resistance in multiple myeloma.
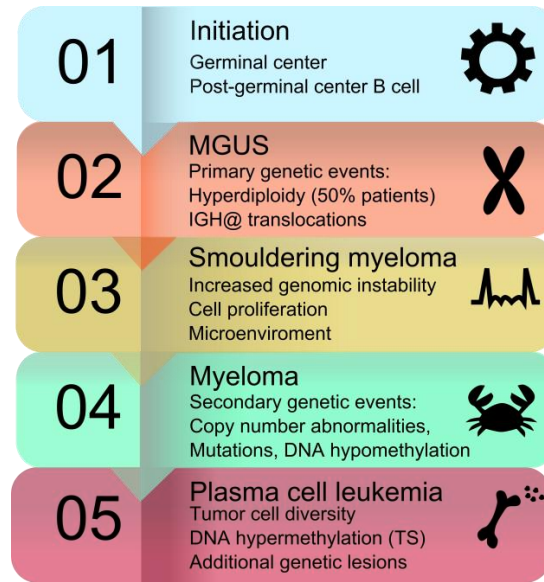


**Figure 1. Pathogenesis of multiple myeloma.** Early aberrations occur in the germinal center of B cells, which lead to MGUS with hiperdiploidy and IGH@ translocations. These last contribute to increased genomic instability and to secondary genetic events found in MM. Additional genetic lessions cause the terminal phase called plasma cell leukemia.

# The MAPK/ERK pathway

The mitogen-activated protein kinase (MAPK) pathway is involved in the regulation of cell differentiation, proliferation, and survival. The activation of this pathway is triggered by diverse cytokines, such as interleukin-6 (IL-6) and interleukin-21(IL-21), vascular endothelial growth factor (VEGF), tumor necrosis factor-α (TNFα), stromal cell derived factor-1 (SDF-1) or the insulin-like growth factor-1 (IGF-1)[10–12] .

These mitogens activate the membrane receptors of the respective receptor tyrosine kinases (RTK) family such as fibroblast growth factor receptor (FGFR), epidermal growth factor receptor (EGFR) and platelet-derived growth factor

receptors (PDGF-R). Once bound to the ligand the receptor auto-phosphorylates tyrosine residues and recruits docking proteins like SHC, GRB2, and SOS allowing the activation of the guanosine triphosphate (GTP) dependent RAS protein. In consequence, membrane-associated RAS-GTP recruits and activates the RAF family kinases (A, B and C-RAF), leading to the dimerization of RAF molecules. These dimers phosphorylate and activate the MAPK/ERK kinase (MEK 1/2) that in turn phosphorylates ERK 1/2 on residues T202/185 and Y204/187 (Figure 2). Active ERK1/2, targets hundreds of downstream substrates that regulate the expression of genes involved in proliferation, cell cycle progression, differentiation and in the MAPK negative feedback, (Figure 2) [13,14]. There are more than 650 direct targets of ERK identified, including transcription factors (c-Jun, c-Fos, STAT1/3, c-Myc, N-Myc, UBF, ATF2 , Elk1), kinases and phosphatases (BRAF, CRAF, MEK1/2, RSK1-4, MKP3, MSK1/2) cytoskeletal proteins (Paxillin, Annexin XI, Laminin B2), signaling proteins (EGFR, IRS1, LAT, PLCβ, TSC2), apoptotic proteins and proteinases (Bad, Bim-EL, Caspase 9, MCL-1) among other targets[15–18].

Regarding the MAPK negative feedback loop of the MAPK/ERK pathway, it comprises diverse regulators of the same pathway such as dual-specificity phosphatases (DUSP) and Sprouty proteins (Spry)[19–21].
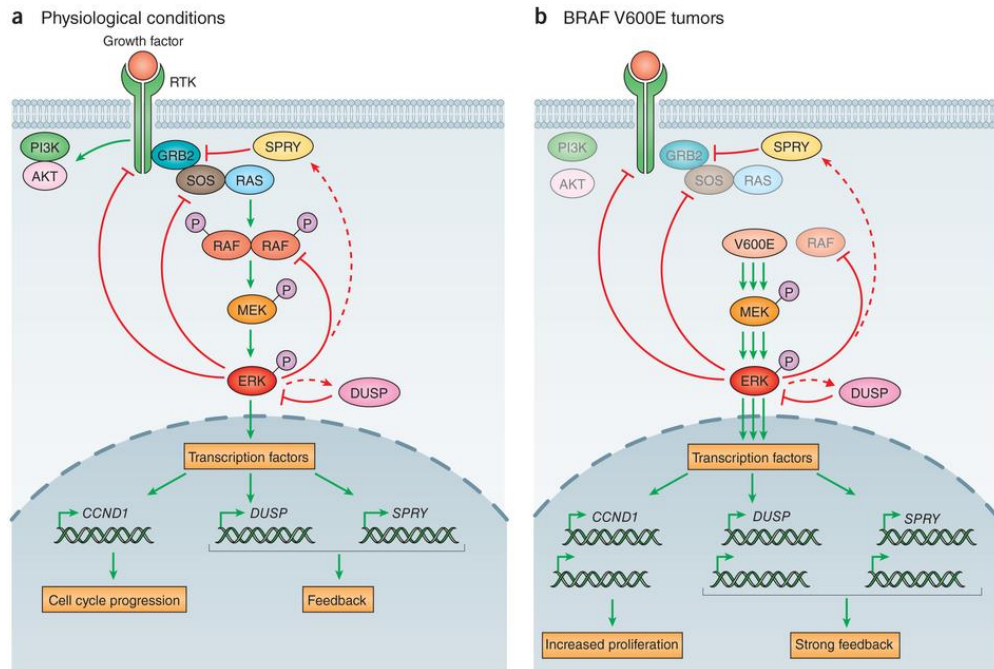
**Figure 2 Overview of the MAPK/ERK pathway.** The phosphorylation events on the kinases, precedes the phosphatases activity which regulate the pathway. Activated ERK is translocated to the nucleus where it phosphorylates transcription factors such as Elk-1. Crosstalk activation of the PI3K/AKT pathway is also shown[31].. Copyright 2017 by Nature Publishing Group. Reprinted with permission

# The MAPK/ERK pathway in multiple myeloma

Recently, tumor genome sequencing data has shed light on the mutational status of different genes that contribute to the pathogenesis of multiple myeloma. The Ras pathway has the most noticeable rate of recurrent mutations being detectable in about 50% of the patients, highlighting the importance of the study of these genes along with the respective signaling pathways to discern a better understanding of this disease.

Remarkably, in 4% of newly diagnosed and 8% refractory multiple myeloma patients the gene encoding for the serine-threonine kinase, BRAF was mutated mainly at the V600E position, conferring activation of this protein [22–25].

Importantly, MM patients refractory to all approved therapeutic options with multiple extramedullary lesions have successfully been treated with the mutation-specific BRAF inhibitor vemurafenib. Low doses of this compound were able to induce a stable remission of more than 8 months. This is the first evidence of the clinical and therapeutic relevance of the BRAF V600E mutation in multiple myeloma, proving the principle of specific inhibition of driver mutations in this disease [23,26]. Nevertheless, resistance to vemurafenib is still a challenge in MM, recent results of the follow-up of the one patient showed acquired spatially heterogeneous NRAS mutations G13R, G12A, and Q61H, yet clonal within the lesions[27].

Recent studies in other types of cancer that contain the BRAF V600E mutation, like malignant melanoma and hairy cell leukemia, had demonstrated the benefit of targeting this mutation with specific drugs such as vemurafenib [28–30]. However, single agent treatment with BRAF inhibitors, as shown in several malignancies, carries the risk of tumors developing early drug resistance[31,32]

# Serine/threonine-protein kinase BRAF

Originally, the characterization of the RAF oncogenes was derived from the discovery of the murine sarcoma virus 3611 (MSV) and the avian retrovirus Mill Hill 2(MH2) and were found to transform epithelial cells and fibroblasts, inducing rapidly accelerated fibrosarcomas (RAF) in mice [33]. The human homolog C-RAF was discovered in 1985, shortly followed by A-Raf (1986) and BRAF (1988). Since then many studies have contributed to the current knowledge about these kinases in normal and pathological conditions.

The v-Raf murine sarcoma viral oncogene homolog B (*BRAF*) is a human gene located on chromosome 7 at position 7q34 containing 21 exons that encode an

mRNA of 2480 base pairs. The BRAF protein has 766 amino acids and a molecular weight of approximately 86 kDa.

## BRAF structure

BRAF contains three conserved domains, Ras-GTP binding domain, a serine-rich hinge region and a catalytic domain The protein has two lobes; the N-lobe residues 457-530 binds adenosine triphosphate (ATP) while C-lobe residues 535-717 bind to substrate proteins. The active site is located within the cleft between both lobes (Figure3) [34,35] . The kinase domain contains a DFG motif formed by D594, F595, and G596, and it is involved in the inactive and active state of the enzyme by regulating its interaction with ATP's phosphate groups[36].

Furthermore, to be fully activated, BRAF has to dimerize via hydrogen bonding and electrostatic interactions of its kinase domains to another monomer of C-RAF or BRAF [10] .
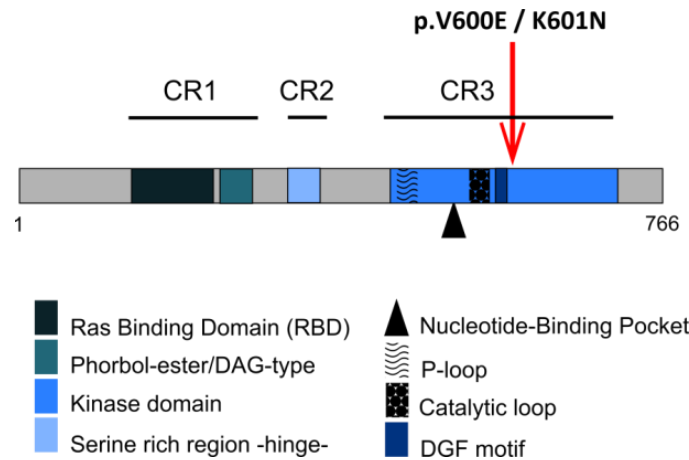


**Figure 3 BRAF protein scheme.** BRAF has three conserved domains, CR1 with a Ras-GTP binding domain, CR2 with a serine-rich hinge region and CR3 with the catalytic domain. For membrane docking the enzyme has a phorbol-ester/DAG type motif. The P-loop stabilizes the non-transferable phosphate groups of ATP, while ATP is anchored to the Nucleotide Binding Pocket and the DGF motif allows transferring the phosphate group to enzyme's substrates[37,131,132].

## Mutant BRAF in cancer

In 2002, Davies and colleagues described, for the first time, mutations in the BRAF gene in a wide range of human cancers [37]. Almost 90% of BRAF mutations account for the substitution of valine (V) for glutamic acid (E) at position V600. This point mutation occurs within the activation segment of the protein, which leads to a constitutively active state of BRAF in a monomeric form. Another recurrent hotspot is the substitution of lysine (K) for asparagine (N) at the position K601 (0,2% in melanoma )[38]. Upon mutation, the mutant kinase becomes independent of upstream signals leading to a strong activation of the MAPK pathway, enhancing its oncogenic effect [39].

Inactivating BRAF mutations have also been reported but are quite sporadic, some of them are the kinase-inactive variants BRAF D594A/V and K483M. Importantly, the combination of an activating Ras mutation with an inactive BRAF kinase can lead to tumor progression upon BRAF inhibition in mice [40].

# RAS/MAPK pathway inhibitors

## BRAF inhibitors

BRAF inhibitors (BRAFi) are divided into two types, based on selectivity towards the kinase. Type 1 inhibitors are designed to selectively target mutant activated BRAF (active conformation "DGF-in") two examples used in this work are described below.

Vemurafenib (PLX4032, marketed as Zelboraf,) is a selective BRAF V600E that binds to the DFG-in (Asp-Phe-Gly) motif of the activation loop in the active kinase, blocking MEK/ERK phosphorylation [14,28,31].

This BRAFi can induce upon inhibition of ERK phosphorylation cascade, the expression of Bim, which triggers caspase 9 leading to subsequent caspase 3 activation enhancing apoptosis. Vemurafenib also up-regulates endoplasmic reticulum (ER) stress-related genes as, p8, CHOP, TRB3, ATF4, and ATF3 by blocking sarco/endoplasmic reticulum $Ca^{2+}$ ATPase (SERCA) and increasing the concentration of cytosolic calcium. As result of higher expression of pro-apoptotic proteins and ER-stress related genes, the BRAF mutated cells go into apoptosis [41].

During phase III trials of vemurafenib, it was demonstrated its clinical efficacy in malignant melanoma patients with a BRAF V600E mutation at six months under treatment with a confirmed overall response rate of 84% in the vemurafenib group and 64% in the dacarbazine group (control arm) and a median progression-free survival of approximately 5 months for vemurafenib and 2 months for dacarbazine [28,30].

Dabrafenib (GSK2118436, trade name Tafinlar,) is a reversible ATP-competitive RAF inhibitor, which has a wider target spectrum than vemurafenib, targeting BRAF V600E (IC50 0.8nM), BRAF wild type (IC50 3.2nM and C-RAF (5nM)[42]. Preclinical data proved that dabrafenib inhibits the MAPK pathway in BRAF V600E *in vitro* and *in vivo* models by decreasing proliferation and inducing tumor regression in xenografts mice models [42,43]. Clinical studies in melanoma showed its benefits, with a median progression-free survival of 5 months for dabrafenib and 2.7 months for dacarbazine (control arm) and a response rate of 50% for dabrafenib and 6% for control arm [44,45].

In contrast, type 2 inhibitors bind to kinase's inactive conformation known as "DFG-out" where F595 blocks ATP binding of the enzyme's nucleotide-binding pocket [36]. Nevertheless, these drugs failed to show clinical efficacy for BRAF inhibition, an example is Sorafenib, a first generation of BRAF inhibitor, that targets C-RAF, BRAF wild type, BRAF mutant, vascular endothelial growth factor

receptor 2 (VEGFR2), vascular endothelial growth factor receptor 3 (VEGFR3), platelet-derived growth factor (PDGF) , p38 MAPK, FLT, cKIT, FMA, and RET [46].

Along with the discovery of specific BRAF inhibitors, downstream MAPK inhibitors have been developed to specifically block MEK1/2 and ERK1/2 activity.

## MEK inhibitors

Trametinib is a competitive allosteric MEK inhibitor (MEKi) which was the first of its kind to be approved for clinical use. Trametinib clinical data in metastatic melanoma patients carrying a BRAF V600E/K mutation disclosed median progression-free survival of approximately 5 months and 1.5 months in the chemotherapy group (control arm). At 6 months, the overall survival was >80% in the trametinib group and <70% in the chemotherapy group [47,48]. Moreover combined therapy with dabrafenib and trametinib showed a better outcome in melanoma patients (BRAF V600E/K) with a response rate of 76% in comparison to 59% single dabrafenib treatment and 40% single trametinib treatment and median progression-free survival was of 9.4 months for combined therapy while for dabrafenib alone was 6.9 months and trametinib alone was 5.7 months [48,49].

## ERK inhibitors

ERK upstream therapy focuses in abrogating ERK phosphorylation, therefore a next logical step in inhibitor development is to target directly ERK with small molecule inhibitors such as SCH772984, GDC-0994, Ulixertinib, etc. Nevertheless, information on safety, drug combinations, and resistance mechanisms are still under investigation [50,51].

## Paradoxical RAF activation

The characterization of the crystal structure of BRAF was a breakthrough step in understanding physiological dimerization of the protein and how certain mutations such as V600E or K601N can change the enzymatic conformation to an activated state. Moreover, it led to the discovery of specific BRAF inhibitors.

BRAF inhibitors can induce transactivation of wild type BRAF because they change the enzyme conformation to an "open state" leading to its dimerization. For example, vemurafenib binds only to one monomer provoking an allosteric transactivation of the drug-free monomer and downstream sequelae of the RAS/MAPK pathway are activated. Transactivation of BRAF caused by BRAFi can be even further enhanced in tumors already carrying a RAS activating mutation, since active RAS-GTP also promotes BRAF dimerization. Strategies to prevent/overcome this paradoxical activation include an increased BRAFi dose that blocks both RAF monomers and their kinase activity (Figure 4), however toxicity is still a clinical dare, and also continuous dosis can lead to faster drug resistance. For this reason different therapeutic strategies have been developed such as drug holiday or re-challenge of BRAF/MEK inhibitor [52–55].

Recent findings showed that BRAF inhibition can lead to the development or promotion of second primary neoplasias, such as cutaneous squamous cell carcinoma (cuSCC) and keratoacanthomas (KA). This secondary effect is mainly due to insufficient dose of the drugs leading to transactivation of BRAF wild type giving a paradoxical activation of the MAPK/ERK pathway mainly observed in presence of pre-existing RAS mutations which also promotes RAF dimerization and activates the same pathway. The incidence of cuSCC for vemurafenib-treated patients is 20-26% and dabrafenib-treated is 6-11%. Combined BRAFi and MEKi therapy diminishes cuSCC to 7% of patients receiving both drugs but it was not exempt [56]. For this reason, a new class of RAF inhibitors was recently developed. One of this is the paradox breaker 04 (PB04/PLX7904) which blocks

ERK1/2 activation in mutant BRAF cells and did not enhance ERK1activation in NRAS and HRAS cell lines, or even in BRAF/NRAS co-expressing melanoma cells this occurs because this molecule was design to bind to the enzyme similarly as vemurafenib does but the difference is that PB04 along aminoacid Leu505 on the enzyme interact to each other and leads to a slight change of conformation, disrupting a RAF dimer formation which does not occur in the case of other BRAFi's[57,58].
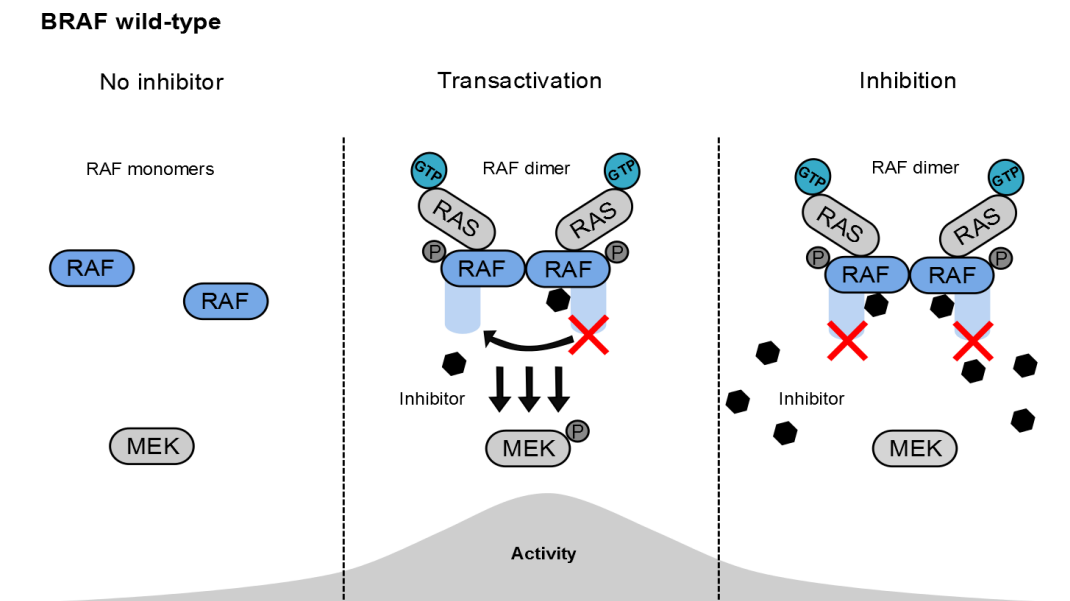


**Figure 4 Paradoxical RAF activation.** At baseline, BRAF wild type without stimulation remains inactive. While upon addition of non-saturating concentrations of the inhibitor BRAF is transactivated leading to an overactive MAPK/ERK pathway. In contrast, high inhibitor concentrations efficiently abrogate downstream signaling.

# BRAF inhibitors mechanism of resistance

The striking initial responses to BRAF inhibitors fascinated the scientific and clinical community because it meant a great achievement in cancer targeted

therapy. Nonetheless, the main obstacle of this targeted therapy drug resistance, mainly due to reactivation of the ERK signaling which promotes tumor re-growth in almost all patients with a median progression-free survival of 5-7 months.

**Tumor microenvironment**

A recent study demonstrated that innate BRAF inhibitor resistance is mainly due to the secretion of hepatocyte growth factor (HFG) by stroma cells of the tumor microenvironment. The secretion of this cytokine results in the MET activation, which in turn triggers a sustained signaling of both MAPK and PI3K/Akt pathways facilitating cell proliferation in BRAF inhibitor resistant cell lines. Additionally combination treatment *in-vitro* with BRAF inhibition and MEK inhibition was not sufficient to overcome HGF-induced resistance [59].

**NF1 loss**

NF1 is mainly a RAS GTPase activating protein (RAS GAP) that inhibits RAS activity.

Moreover preclinical models on vemurafenib resistance showed RAS activation after the loss of the tumor suppressor NF1 reducing the sensitivity to BRAFi in BRAF V600E cells [60,61]. About 4% BRAF mutant melanoma patients contain inactivating NF1 mutations. Active RAS is sufficient to induce BRAFi resistance in BRAF V600E cells [62].

**BRAF copy number gain**

A screening study compared baseline versus disease progression in melanoma patients after BRAF inhibitor treatment and found that 20% of the relapse samples had a BRAF gene amplification with copy-number gains from 2-13 fold. Moreover, higher doses of specific inhibitor or treatment with a MEK inhibitor in

preclinical cell models overexpressing BRAF V600E, have shown to overcome a hyperactivated MAPK/ERK pathway [63,64].

**BRAF splicing variant**

The expression of the p61 BRAF V600E isoform had been reported in a vemurafenib-resistant cell line SKMEL-238. This protein variant lacks exons 4-8 corresponding to the encoding region of RBD in BRAF. This isoform leads to the high dimerization of the protein, thereby activating MEK. Although the enzyme retains sensitivity towards BRAFi, the high RAS-independent dimerization strongly triggers the MAPK/ERK pathway. In addition, other in-frame splice variants derived from patients with acquired vemurafenib resistance had been documented such as p41, p48 and p55 which all contain an active kinase domain [65].

**Activation of tyrosine kinase receptors**

Upregulation and activation of tyrosine kinase receptors (RTK) as Axl, ERBB2, PDFGRB, IGF1-R1 have been described as a secondary event under BRAFi treatment favoring cancer cell survival. Additionally, the activation of these receptors may be due to an increased intrinsic tumor cell ligand secretion or paracrine ligand production by stromal cells[66].

**NRAS mutations**

Several studies in different types of cancer like leukemia, colorectal cancer, thyroid cancer and melanoma demonstrated that secondary activating RAS mutations can promote RAF dimerization and confer resistance to BRAF inhibitors by sustained activation of the MAPK/ERK pathway promoting tumor growth independently of upstream activation. Moreover, the PI3K pathway is a main effector of RAS contributing to cell growth, cell cycle progression and cell

survival. NRAS mutations like G12D, G13R and Q61K have been detected in 18% of progressive melanoma tumors while KRAS mutations such as G12C, G12R and Q61H were found in 7% of progressive melanoma tumors [57,67–69]. A recent study in a multiple myeloma patient carrying a BRAF V600E mutation treated with low dose vemurafenib developed a disease relapse due to clonal heterogeneity of tumor cells since 3 different lesions harbored 3 independent clonal NRAS mutations (G12A, G13R and Q61H), to overcome/prevent further development of resistance the patient was treated with a combination of BRAF and proteasome inhibitors[23,70].

**C-RAF over-expression**
Studies *in vitro* had demonstrated that melanocytes under BRAF inhibitor switched BRAF dependency to C-RAF over-expression which increases phosphorylated ERK 1/2 levels resulting in an active MAPK/ERK pathway [71,72].

**COT over-expression**
In a selective RAF kinase inhibitor study, the gene MAP3K8 (encoding COT) was identified as an *in vitro* resistance mechanism due to its ability to constitutively activate ERK through a MEK-dependent mechanism that bypasses RAF signaling even in presence of the inhibitor. Furthermore, COT expression has been observed in tissues from relapsing patients after BRAFi or MEKi treatment [73].

**MEK mutations**
Secondary activating MEK1/2 mutations can confer BRAFi resistance because they can trigger the MAPK/ERK pathway independently of upstream signals. Some of the reported mutations include Q56P, K57E, V60E, C121S, G128V, E203K for MEK 1 and V35M, L46F, F57C, C125S, N126D for MEK2[14,74–76].

**PTEN Loss**

*In vivo* studies demonstrated that concurrent expression of BRAF V600E and silencing of the tumor suppressor PTEN gene led to development and metastasis of tumors in all mice [77]. In the clinic, >10% of melanoma patients (BRAF V600E/K) present a loss of this phosphatase. An *in-vitro* study demonstrated that the absence of this enzyme facilitates AKT expression triggering cell survival even in the presence of BRAFi[78].

**Cyclin D1 overexpression**

Cell cycle deregulation is a common feature in cancer, it occurs when there is an abnormal expression of cyclins and cyclin-dependent kinases (CDKs) which in consequence lead to uncontrolled proliferation, genomic instability (GIN) and chromosomal instability (CIN) favoring further disease progression [79,80].

Cyclin D1 regulates cyclin dependent kinases (CDKs) 4 and 6 which form a complex which phosphorylates the retinoblastoma protein (Rb) promoting cell cycle progression. A mutational screening in BRAF inhibitor resistant melanoma cells identified that resistance was mainly due to a CDK4 mutation (R24C, R24L, and K22Q) and CCND1 amplification. Of clinical relevance, CCND1 is amplified in almost 20% of BRAF V600E melanoma patients and multiple myeloma patients independently of BRAF status[81,82]. In the case of MM, CCND1 gene amplification is also associated to higher expression of MDR1 in comparison to CCND1 negative patients. To our knowledge aberrant expression of cyclin D1 and mutant BRAF along with BRAF inhibitor resistance in MM has not been described.

## Overcome BRAF inhibitor resistance

Several studies, using different BRAFi as monotherapy, have reported a short duration of response. Therefore, it is important to develop more effective strategies such as combination and sequential therapies with other inhibitors.

A common strategy is targeting the same MAPK/ERK pathway with a combination of a BRAF inhibitor and a MEK inhibitor, for example in a phase II study in metastatic melanoma the combination of dabrafenib and trametinib improved the median progression-free survival (PFS) of 9.4 months compared with 4-6 months for single-agent treatment [49]. Nevertheless, in approximately 50% of the patients treated with dabrafenib and trametinib resistance mechanisms could be identified at disease relapse , conferred by BRAF amplification (36%), activating NRAS mutations (18%) and MEK2 mutation C125S (9%) [83].

Furthermore, targeting multiple signaling pathways simultaneously could avoid possible cancer cell dependence on other cell survival signaling. *In vitro* studies demonstrated that combination of dabrafenib, trametinib and GSK2126458, a phosphoinositide 3-kinase/mTOR inhibitor, improved cell growth inhibition in BRAF mutant cell lines [84]. Phase I studies testing multi-targeted combinations with the PI3K inhibitor and trametinib showed that patient safety is still a clinical challenge [85]. Currently, there are also other open phase I/II trials exploring combination therapies with the Akt inhibitor GSK2141795 and trametinib [86].

# 2

---

# Research Objectives

Recent clinical studies have reported activating BRAF mutations in 4- 10% MM patients, which can be successfully treated with targeted therapy. However, drug resistance occurs rapidly, limiting the duration of response. Moreover, the activating role of BRAF mutations in MM pathophysiology is poorly defined. Therefore, a better understanding of the biological impact of these aberrations and the resistance mechanisms against BRAF inhibitors in MM is of utmost importance to rationalize targeted therapy.

The aim of this study was to decipher the cellular consequences of activating BRAF mutations in MM and, especially, to elucidate cell specific resistance mechanisms to BRAF inhibitors.

For this purpose, two *in vitro* cellular models were developed and characterized, one focusing on conditional overexpression of BRAF wild type or V600E and another model to examine resistance mechanisms to pharmaceutical BRAF inhibition.

# 3

---

# Materials and Methods

## Materials

### Biological materials

### Eukaryotic cell lines

**Table 1. Cancer cell lines**

| Cell Line | Description | Source / Reference |
| --- | --- | --- |
| OPM-2 | Multiple myeloma cell line with wild type Ras pathway | Katagiri et al. 1985 |
| U266 | Multiple myeloma cell line with mutation BRAF K601N | Nilsson et al. 1970 |
| HeLa | adenocarcinoma | Gey 1952 |
| A375 | malignant melanoma | Giard et al. 1973 |
| Lenti-X™ 293T | kidney | Clontech, Takara Bio Company |

## Bacterial material

**Table 2. Bacterial material**

| Name | Genotype | Source / Reference |
|------|----------|--------------------|
| E.coli DH5 alpha | *F- φ80lacZΔM15 Δ(lacZYA argF) U169recA1endA1 hsdR17 (rKmK+) phoA supE44 thi-1gyrA96 relA1 λ-* | Stratagene, La Jolla, California, USA |
| E. coli SCS110 | *rpsL thr leu endA thi-1 lacY galK galT ara tonA tsx dam dcm supE44 Δ(lac-proAB)* | Agilent Technologies, Inc., Cedar Creek, Texas, USA |

## Genetic material

## DNA primers

Primers for sequencing and polymerase chain reaction (PCR) were obtained from Eurofins MWG Operon (Ebersberg, Germany).

**Table 3. Primers**

| Name | Usage | Sequence |
|------|-------|----------|
| 5prBRAFNheI | For production of vector pLV.MIR-Neo TRE BRAF | GGAGCTAGCATGGCGGCGCTGAGC |
| 3prNheIBRAFmut | For production of vector pLV.MIR-Neo TRE cBRAF V600E | GGAGCTAGC  TCAGTGGACAGGAAACGC |
| 3prBRAFXbaI | For production of vector pLV.MIR-Neo TRE cBRAF WT | GGATCTAGATCAGTGGACAGGAAACGC |
| Q5SDM_2/11/2016_F | Mutagenesis | CCCCCCCCACGAACGCCCTT |

| | | |
|---|---|---|
| Q5SDM_2/11/2016_R | | CGTCTTGCTGGGCCGGTTG |
| 3prBRAF FLAG-C | | GTTGTAAAACGACGGCCAGT |
| 5pr_rtTAM2 | | ATG TCT AGA CTG GAC AAG AGC AAA GTC |
| 3pr_rtTAM2 | PCR | TTA CCC GGG GAG CAT GTC AAG GTC AAA |
| 5pr_BRAFV600E in FLAG-C | | AGAACCCTCCTTGAATCGGG |
| 3pr_BRAFV600E in FLAG-C | | AGAGAGCTATGACGTCGCAT |
| ACTB_FWD | | CATGTACGTTGCTATCCAGGC |
| ACTB_REV | | CTCCTTAATGTCACGCACGAT |
| FWD_N-EGR1 | Semiquantitative | TGACCGCAGAGTCTTTTCCT |
| REV_N-EGR1 | PCR | TGGGTTGGTCATGCTCACTA |
| FWD_C-EGR1 | | AAAGTGTTGTGGCCTCTTCG |
| REV_C-EGR1 | | GGGGAACAGAGGAGTACGTG |
| EGR-1_FWD | | GCCCTCAATACCAGCTACCA |
| EGR-1_REV | | AAGTTGCGCATGCAGATG |
| STK36_FWD | | GGGCTATGAGCACCAATACAATG |
| STK36_REV | Sequencing | AAAGCAGGGACTGATGGTTG |
| CACNA2D3_FWD_2 | | ACGGTTATGCCTTTGCAATC |
| CACNA2D3_REV_2 | | CGTTTCCCTTTGTCCACTGT |
| 5' EGR1_dupC 994 | | CCAGCAAGACGCCCCCCCCACGAAC |
| 3' EGR1_dupC 994 | | GTTCGTGGGGGGGGCGTCTTGCTGG |

## Expression constructs

### Table 4. Expression plasmids

| Name | Backbone | Vector type | Antibiotic resistance | Insert | Source |
|---|---|---|---|---|---|
| pLV.MIR-Neo | pLV Tet-IRES-mCherry | Mammalian Expression, Lentiviral | Ampicillin /Neomycin | - | Dr. Daniel Novak, Clinical Cooperation Unit Dermato-Oncology, |
| FUdeltaGW-rtTA | FUdeltaGW | | Ampicillin /Zeocine | reverse tetracycline | |

| | | | | transactivator (rtTA) | German Cancer Research Center, Heidelberg, Germany |
|---|---|---|---|---|---|
| pCMV- EGR1 cDNA clone | pCMV-ORF | Mammalian Expression | Ampicillin /Hygromycin | EGR1 cDNA clone | Sino Biologicals Inc. Catalog No. HG11870-G-N |

**Table 5. Expression constructs used for mammalian cell transduction or transfections**

| Backbone | Vector Name | Vector type | Antibiotic resistance | Insert | Source |
|---|---|---|---|---|---|
| pLV.MIR-Neo TRE BRAF WT | pLV Tet-TRE BRAF WT-IRES-mCherry | Mammalian Expression, Lentiviral | Ampicillin /Neomycin | BRAF wild type | Produced during this work |
| pLV.MIR-Neo TRE BRAF MUT | pLV Tet-TRE BRAF V600E-IRES-mCherry | | | BRAF V600E | |
| pCMV-EGR1 MUT | pCMV-ORF | Mammalian Expression | Ampicillin /Hygromycin | EGR1 dupC944 | |
| pLenti EGR-1 | pLenti EGR-1 IRES GFP | Mammalian Expression | Ampicillin/ Blasticidin | EGR1 wt or mut | |

# Antibodies

# Primary Antibodies for Western Blot

### Table 6.  Primary antibodies used for western blot

| Antigen | Clone | Species | Clonality | Dilution | Source |
|---------|-------|---------|-----------|----------|--------|
| MCM7 | 141.2 | mouse | monoclonal | 1:1000 | Santa Cruz |
| Alpha tubulin | DM1A | mouse | monoclonal | 1:1000 | Abcam |
| Erk1/2 (p44/42 MAPK) | - | rabbit | ployclonal | 1:1000 | Cell Signaling Technologies |
| phospho-ERK 1/2 (Thr202/204) | - | rabbit | ployclonal | 1:1000 | Cell Signaling Technologies |
| Phospho-BRAF (Ser445) | - | rabbit | polyclonal | 1:1000 | Cell Signaling Technologies |
| BRAF  (N-terminus) | H-145 | rabbit | polyclonal | 1:1000 | Santa Cruz |
| BRAF  (C-terminus) | C-19 | rabbit | polyclonal | 1:1000 | Santa Cruz |
| BRAF V600E | VE-1 | mouse | monoclonal | undiluted | Dr. med. David Capper, Pathology Institut, Neuropathology, Heidelberg University |
| phospho-MEK1/2 (S217/221) | - | rabbit | polyclonal | 1:1000 | Cell Signaling Technologies |
| MEK1/2 | - | Rabbit | polyclonal | 1:1000 | Cell Signaling Technologies |
| EGR-1 | 44D5 | rabbit | monoclonal | 1:1000 | Cell Signaling Technology |

## Secondary Antibodies for Western Blot

**Table 7. Secondary antibodies used for western blot**

| Antigen | Specifications | Species (clonality) | Dilution | Source |
|---------|----------------|---------------------|----------|--------|
| Mouse IgG | HRP-conjugated | Goat (p) | 1:5000 | Santa Cruz |
| Rabbit IgG | HRP-conjugated | Goat (p) | 1:5000 | Santa Cruz |

## Enzymes

**Table 8. Enzymes**

| Name | Source |
|------|--------|
| T4 DNA ligase | New England Biolabs, Ipswich, UK |
| Restriction endonucleases | New England Biolabs, Ipswich, UK |
| DNAse I | Sigma-Aldrich Munich, Germany |
| Phusion® High-Fidelity DNA Polymerase | Thermo Fisher Scientific, Lafayette, CO, USA |
| Shrimp Alkaline Phosphatase | Thermo Fisher Scientific, Lafayette, CO, USA |
| RNAse A | VWR International GmbH, Darmstadt, Germany |

## Molecular weight markers

**Table 9. Molecular weight markers used for agarose electrophoresis or western blot**

| Name | Source |
|------|--------|
| LowRanger DNA Ladder | Thermo Fisher Scientific (Fermentas Life Science), Waltham, MA, USA |
| HighRanger DNA Ladder | Norgen Biotek, Ontario, Canada |
| Precision Plus Protein ™Dual Color Standards | Bio-Rad Laboratories, Hercules, CA, USA |

# Kits

**Table 10. Kits used in this work**

| Name | Source |
| --- | --- |
| Quick Start TM Bradford Protein Assay | Bio-Rad Laboratories, Hercules, USA |
| iScript™ cDNA Synthesis Kit | |
| Q5® Site-Directed Mutagenesis Kit | New England Biolabs, Ipswich, UK |
| Cell Titer-Glo® Luminescent Viability Assay | Promega, Madison, USA |
| Midi/Maxi Plasmid Purification Kit | Qiagen, Hilden, Germany |
| QIAamp DNA Mini Kit | |
| QIAprep® Spin Miniprep Kit | |
| QIAQuick® Gel Extraction Kit | |
| RNeasy Mini Kit | |
| High Pure PCR Product Purification Kit | Roche, Basel, Switzerland |
| Pierce® ECL Western Blotting Substrate | Thermo Scientific, Waltham, USA |
| Vectashield® | Vector Laboratories, Burlingame, USA |
| Vectashield® with DAPI | |
| Lenti-X™ GoStix™ | Clontech Laboratories, Inc. A Takara Bio, Shiga Japan |
| Senescence β–galactosidase staining kit | Cell Signaling Technology, Danvers, MA, USA |

# Chemicals

List of sources for molecular biological grade or purest reagents (chemicals, antibodies, enzymes, etc.) employed during this work.

Abcam Cambridge, UK; AppliChem Darmstadt, Germany; BD Biosciences Heidelberg, Germany; Biochrom Berlin, Germany; Bio-Rad Munich, Germany; Biozym Scientific GmbH Oldendorf, Germany; Carl Roth Karlsruhe, Germany; Cell Signaling Technology Danvers, USA; Dyomics Jena, Germany, Eppendorf Hamburg, Germany; Exbio Prague, Czech Republic; GE Healthcare Buckinghamshire, UK; Gibco Eggenstein, Germany; Ibidi Munich, Germany; Life

Technologies Darmstadt, Germany; Merck Millipore   Bedford,   USA;   New England Biolabs Frankfurt, Germany; Proteintech Manchester, UK; QiagenHagen, Germany; Roche Basel, Switzerland; Roche Diagnostics   Mannheim,   Germany; Santa Cruz Heidelberg, Germany; Selleck Chemicals München, Germany; Serva Heidelberg, Germany; Sigma-Aldrich Munich, Germany;  Thermo Fisher Scientific Lafayette, CO, USA and Vector Laboratories Burlingame, USA.

## Consumables

GE Healthcare Chalfont St Giles, UK; Greiner Bio-One Kremsmuenster, Austria; Starlab   Hamburg,   Germany;   Sarstedt   Nuembrecht,   Germany;   Eppendorf Hamburg, Germany.

## Media, buffers and solutions

## Media for bacterial culture

**LB medium:**  1% w/v Trypton,  0.5% w/v Yeast extract,  pH 7.2
**LB-agar:**  LB medium,  1% w/v NaCl,  1.5% w/v Agar, stored 4°C
**SOC medium:** 2% w/v Trypton,  0.5% w/v Yeast extract, 0.05% w/v NaCl,  2.5 mM KCl10,  mM MgCl2,  20 mM Glucose,  pH 7.0

## Media and solutions for cell culture

**Table 11. Media and solutions for cell culture**

| Name | Source |
| --- | --- |
| TC10 Trypan Blue Dye 0,4% | Bio-Rad Laboratories GmbH, Munich, Germany |
| Trypsin/EDTA-solution | 0,25% (v/v) Pig-trypsin (Gibco®/Invitrogen, Carlsbad, USA) in PBS/EDTA |

| | |
|---|---|
| PBS/EDTA | 2 mM EDTA in PBS |
| Fetal Calf Serum (FCS) | Biochrom, Merck Millipore, Berlin Germany |
| L-Arginine | Fisher Scientific |
| L-Lysine Dihydrochloride | |
| L- Arginine:HCl (13C6; Arg+6) / Arg+6 | |
| L-Lysine: 2HCl (4,4,5,5-D4; Lys+4) / Lys+4 | |
| L-Arginine:HCl (U-13C6, 15N4; Arg+10)/ Arg+10 | |
| RPMI 1640 | Gibco®/Invitrogen, Carlsbad, USA |
| DMEM | |
| OptiMEM | |
| Fetal Bovine Serum dialyzed (dFCS) | Sigma-Aldrich St. Louis, USA |
| Poly-L-Lysine | |
| SILAC RPMI | Thermo Scientific (Life Technologies) |
| PrestoBlue® Cell Viability Reagent | |

# Buffers and reagents

## Table 12.  Buffers and reagents

| Name | Description/Source |
|---|---|
| 10X Methanol transfer buffer | Tris 50mM |
| | Glycine 40mM |
| | SDS 3,7g |
| | ddH2O 1000mL |
| 1X Methanol transfer buffer | 10X Methanol transfer buffer 100mL |
| | Methanol 200mL |
| | ddH2O 700mL |
| 10X Running Buffer for SDS-PAGE | Glycin  30,3g |
| | Tris 144,1g |
| | SDS 10g |
| 1X Phosphate-buffered saline | 137 mM NaCl |

| | |
|---|---|
| (PBS) | 2,7 mM KCl |
| | 10 mM Na2HPO4 |
| | 1,7 mM KH2PO4 |
| | pH 7,4 |
| 1X RIPA buffer | 50 mM Tris/HCl pH 7.5 |
| | 150 mM NaCl |
| | 0.25% w/v Sodium-deoxycholate |
| | 1% v/v Nonidet P40 |
| | 1 mM EDTA |
| | 1 Tablets/10 ml Complete protease inhibitor, Roche, Basel, Switzerland |
| 1X TBS | 10mM Tris-HCl |
| | 150mM NaCl |
| | pH 8.0 |
| 1X TBTS | 1X TBS |
| | 0.1% (v/v) Tween-20 |
| 6X SDS loading buffer | Tris/HCl pH 6.8 240 mM |
| | B-mercaptoethanol 30% v/v |
| | SDS 6% w/v |
| | Glycerol 30% v/v |
| | Bromophenol blue 0.002% w/v |
| 6X DNA loading dye | 100 mM Tris/HCl pH 7.5 |
| | 200 mM EDTA |
| | 0.01% w/v Bromophenol blue |
| | 0.01% w/v Xylencyanol |
| | 30% v/v Glycerol |
| Borate transfer buffer | Boric acid 20 mM |
| | EDTA 1.3 mM |
| | pH 8.8 |
| NP40-Lysis-buffer | 50 mM Tris-HCl pH 7,5-7,8 |
| | 150 mM NaCl |
| | 0,5% NP40 |
| | 5 mM NaF |
| | 1 mM Na3VO4 |

| | |
|---|---|
| | 1 Tablets/10 ml Complete protease inhibitor, Roche, Basel, Switzerland |
| Trihydrocloride, trihydrate Hoechst 33342 | Life Technologies Darmstadt, Germany |
| Acrylamide/ Bis 37.5:1 solution (30% w/v) | Serva Electrophoresis, Germany |
| Ammonium Persulfate (APS) | Carl Roth GmbH, Germany |
| Blocking buffer immunofluorescence | 10% Goat serum  in 1X PBS |
| Blocking buffer Western Blot | 5% Bovine serum albumin in PBST |

## Antibiotics

**Table 13.  Antibiotics used during this work**

| Name | Source |
|---|---|
| Carbemicillin | Serva, Heidelberg, Germany Final concentration: 100µg/mL |
| Geneticin (G418) | PAA Laboratories GmbH (Austria) |
| Zeocine | Sigma-Aldrich St. Louis, USA |
| Tetracycline hydrochloride | |
| Doxycycline hydrochloride | VWR International GmbH, Darmstadt, Germany |

## Drugs

**Table 14.  Chemicals used for cell culture experiments**

| Chemical | Source |
|---|---|
| **Vemurafenib (PLX4032)** | Selleck Chemicals, München, Gemany |
| **Dabrafenib (GSK2118436)** | |
| **Trametinib (GSK1120212)** | |

| | |
|---|---|
| **Etoposide** | Promokine, Heidelberg, Germany |
| **5-Fluoroacil** | Sigma-Aldrich St. Louis, USA |
| **Cytochalasin B** | |
| **Cisplatin** | |
| **Doxorubicin hydrochloride** | Biomol GmbH, Hamburg, Germany |
| **Vincristine sulfate** | |
| **Paclitaxel** | |

**Table 15. Doxycycline concentration used for transgene induction**

| Cell line | Doxycycline concentration |
|---|---|
| **OPM-2 BRAF WT** | 1 µg/mL |
| **OPM-2 BRAF V600E** | 1 µg/mL |

# Laboratory equipment

**Table 16. Equipment used during this work.**

| Name | Source |
|---|---|
| BD Accuri C6 Flow cytometer | Becton Dickinson, San Jose, USA |
| Mini-PROTEAN® Tetra Cell | Bio-Rad Laboratories Hercules, CA, USA |
| Mini Trans-Blot® Electrophoretic Transfer Cell Bio-Rad Laboratories | |
| TC20™ automated cell counter | |
| Fluorescence microscope Axiovert 200M equipped with AxioCam MRm | Carl Zeiss, Jena, Germany |
| Fluorescence microscope Axioskop equipped with AxioCam MRc | |
| PCR-Machine „Mastercycler gradient" | Eppendorf Hamburg, Germany |
| PCR-Machine „Mastercycler personal" | |
| Photometer | |
| Centrifuge 5417R Eppendorf | Hamburg, Germany |
| Centrifuge Megafuge 1.0R | Heraeus, Hanau, Germany |
| UV Table | Konra Benda, Wiesloch,Germany |

| | |
|---|---|
| Confocal Microscope Leica TCS SP5 | Leica Wetzlar, Germany |
| pH-Meter SevenMulti | Mettler Toledo, Giessen, Germany |
| Spectrophotometer "NanoDrop" | PeqLab Biotechnologie Erlangen, Germany |
| Shandon Cytospin III | Thermo electron corporation,Pittsburg, USA |
| Centrifuge Sorvall RC6Plus | Thermo Scientific, Waltham, USA |

## Software

AxioVision Version 4.7.2 Carl Zeiss, Göttingen, Germany; BD Accuri C6 Becton Dickinson, San Jose, USA; ImageJ Wayne Rasband, USA;  Microsoft Office 2010 Microsoft Corporation, Redmond, USA;  NEBaseChanger™ New England Biolabs, Ipswich, UK;  SerialCloner 2.6.1 SerialBasics, http://serialbasics.free.fr;  ZEN lite 2011 Carl Zeiss, Göttingen, Germany; Chipster    Helsinki, Finland;  Ingenuity® Pathway      Analysis      IPA®,      QIAGEN      Redwood      City,      USA, www.qiagen.com/ingenuity;  DAVID Bioinformatics  Resources 6.7      National Institute of Allergy and Infectious Diseases (NIAID), NIH, Maryland, USA.; Panther University of Southern California, Los Angeles, USA;  InkscapeSoftware Freedom Conservancy, Inc., New York, USA; GraphPad Prism version 7 for Windows, GraphPad Software, La Jolla California USA, www.graphpad.com.

# Methods

## Molecular biology methods

## Isolation of plasmid DNA

To analyze recombinant DNA, the isolation of plasmids was performed from the host cell. Briefly, transformed bacteria colonies were isolated and transferred to liquid cultures at 37°C in LB medium. For small scale preparation (mini-prep) 5mL of liquid culture was incubated for 8 hours while for larger scale preparation (maxi-prep) 1 mL of mini-prep culture was then transferred to 100 mL liquid culture and incubated overnight.

## Cultivation of bacteria

*E. Coli* DHα were cultured in lysogeny broth (LB) or plated on LB-agar and grown at 37°C under continuous shaking. Bacteria were selected under appropriate antibiotics. Depending on the preparation scale, purified DNA was obtained either using QIAprep Spin Miniprep Kit (Qiagen, Hilden, Germany) or QIAGEN Plasmid Maxi Kit (Qiagen, Hilden, Germany) and followed according to manufacturer's instruction. DNA concentration was determined by measuring the 260/280 nm absorbance ratio using a NanoDrop 2000 spectrophotometer (PeqLab Biotechnologie, Erlangen, Germany).

## Cloning

BRAF genes were isolated from plasmids pCMV BRAF C-FLAG and pCMV BRAF V600E C-FLAG, generously provided by Dr. David Capper from Pathology

Institute, Neuropathology from Heidelberg University. Once the sequence was verified, the BRAF genes were amplified by polymerase chain reaction (PCR) with primers containing NheI and XbaI restriction sites. Afterward, the correct size fragments (2,3kb) were visualized in a 1% agarose gel. The PCR products were purified by column using the High Pure PCR Product Purification Kit (Roche, Basel, Switzerland).

## Digestion

Digestion of the vector was done with NheI and XbaI restriction endonucleases enzymes (New England Biolabs, Ipswich, UK) as indicated by the manufacturer. Then, the digested vector was dephosphorylated with 10UI Shrimp Alkaline Phosphatase (Thermo Fisher Scientific, Waltham, MA, USA) at 25°C for 2 hours. The digested vector was purified by agarose gel electrophoresis and gel extraction using the QIAQuick Gel Extraction Kit, according to manufacturer's instructions.

## Ligation

The insert and the vector were ligated with T4 DNA ligase (New England Biolabs, Ipswich, UK) by setting up the reaction as follows, 2µL 1010X T4 DNA Ligase Buffer, 100ng vector DNA, 75ng insert DNA, 1µL T4 DNA Ligase and up to 20µL Nuclease-free water. As negative control same reaction was perform except with insert. The ligation was incubated at 16°C overnight. Next day, the enzyme was inactivated at 65°C for 10 minutes. A 1-5µL product of ligation was used for bacterial transformation. All reactions were assembled on ice.

## Bacterial transformation

10-100ng of DNA from ligations or vectors was used for bacterial transformation. Briefly, 50μL of competent bacteria were thawed on ice. The DNA was added to the thawed bacteria and samples were incubated on ice for 1 hour. Subsequently, heat shock was employed by exposure to the bacteria to 42°C for 45 seconds and immediate ice incubation for 2 minutes. Then, 250-500μL of SOC medium was added, and samples were incubated at 37°C shaking horizontally at 1400rpm for 1 hour. Bacteria were centrifuged at 3000rpm for 4 minutes and resuspended in 100μL of SOC medium, plated in LB plates with antibiotics. LB plates were incubated at 37°C overnight.

## Site-directed mutagenesis

Mutagenesis of pCMV- EGR1 cDNA clone was done using the Q5® Site-Directed Mutagenesis Kit (New England Biolabs, Ipswich, UK) as indicated by the manufacturer. To design the primers to insert a base pair, the software NEBaseChanger™ was employed.

**Table 17. Example of PCR protocol**

| Component | 25 μL reaction | Final conc. |
|---|---|---|
| Q5 Hot Start High-Fidelity 2X Master Mix | 12.5 μL | 1X |
| 10 μM Forward Primer | 1.25 μL | 0.5 μM |
| 10 μM Reverse Primer | 1.25 μL | 0.5 μM |
| Template DNA (1–25 ng/μL) | 1 μL | 1-25 ng |
| Nuclease-free water | 9.0 μL | |

| Step | Temp | Time |
|---|---|---|
| Initial Denaturation | 98°C | 30 seconds |
| 25 Cycles | 98°C | 10 seconds |
| | 50–72°C* | 10–30 seconds |
| | 72°C | 20–30 seconds/kb |

| | | |
|---|---|---|
| Final Extension | 72°C | 2 minutes |
| Hold | 4–10°C | |

## Agarose gel electrophoresis

For DNA size fragment separation, agarose gel electrophoresis was performed. 1% - 2% agarose gels were prepared with 0.1 µL/mL ethidium bromide in TAE buffer. DNA samples were prepared with 6X loading dye and were run at 100V for 1 hour in an electrophoresis chamber (Bio-Rad Laboratories, Hercules, USA). DNA fragments were visualized by UV light in a gel documentation system.

## RNA extraction and cDNA synthesis

Total RNA extraction was done using RNeasy Mini Kit (Qiagen, Hilden, Germany), following manufacturers specifications. RNA concentration and purity was measured at 260nm/280nm in a NanoDrop 2000 Spectrophotometer. RNA was subjected to DNAse I treatment (Sigma-Aldrich Munich, Germany), agreeing manufacturer's specifications. For the complementary DNA synthesis (cDNA), the iScript™ cDNA Synthesis Kit Bio-Rad (Munich, Germany) was employed according manufacturer's instructions.

## Polymerase chain reaction (PCR)

To amplify interest regions of genomic DNA or cDNA, a polymerase chain reaction (PCR) was performed using Phusion® High-Fidelity DNA Polymerase (Thermo Fisher Scientific, Lafayette, CO, USA), following manufacturer's instructions.

## Gene expression profiling

Gene expression profiling (GEP) of induced cell lines expressing BRAF WT or V600E and U266 Dabrafenib resistant cell lines was performed. The inducible OPM-2 cell lines BRAF wild type or V600E were under doxycycline (1µg/mL) for 24h. U266-R cells were washed and subsequently total RNA (RNeasy Mini Kit, Qiagen, Hilden, Germany),) from both cell lines was extracted. RNA concentration of 50ng/µL and 500 ng in total was sent to the microarray unit of the DKFZ Genomics and Proteomics Core Facility for providing the Gene Expression Profiling which was carried on the Illumina HT12v4 platform. The data was processed in chipster [91]. The selection of genes from microarray was within a defined fold range of greater than 1.5-fold and less than 0.75-fold. Statistical significance was analyzed by two group empirical Bayes test. The value of P<0.05 was considered significant.

## Sanger sequencing

30-80ng/µL purified PCR or plasmids dissolved in 20µL nuclease-free water were sent for Sanger sequencing (GATC Biotech, Konstanz, Germany). Analysis of the sequence was performed in Chromas Lite 2.01 (Technelysium Pty Ltd, South Brisbane Australia) software.

## Next generation sequencing

50ng/µL of total DNA from cell lines with a was extracted with the QIAamp DNA Mini Kit (Qiagen, Hilden, Germany) with a final volume of 20µL and then for the next generation sequencing (NGS) the Ion AmpliSeq™ Cancer Hotspot Panel v2 with Ion Torrent Next Generation Sequencing was employed by A. Böhnisch or

A. Brütgens from the Molecular Diagnostics department at the Institute of Pathology Heidelberg (IPH).

## Whole exome sequencing

Total DNA was extracted with the QIAamp DNA Mini Kit (Qiagen, Hilden, Germany), and a concentration of 50ng/µL and 3µg in total was sent to High Throughput Sequencing Unit of the DKFZ Genomics and Proteomics Core Facility. For library preparation "Exome-seq SureSelectXT Human v5+UTRs" was used and for sequencing an Illumina sequencing system "HiSeq 2000" with a paired-end read of 100bp length was employed. Whole exome sequencing (WES) data was kindly processed by Sadaf Mughal and Dr. Benedikt Brors from the Division Applied Bioinformatics, DKFZ and NCT Heidelberg, Heidelberg, Germany.

## Methods in cytogenetics

### Interphase FISH

$1-5 \times 10^4$ cells per sample were diluted in 200µL 1XPBS, and transferred to the sample chambers and immobilized on glass slides by cytospin centrifugation (Thermo Fisher Scientific, Lafayette, CO, USA) at 400rpm for 5 minutes. Then cells were air dried and fixed with ice-cold methanol: glacial acetic acid for 10 minutes. Interphase FISH with probes for 5q31/5q33/6cen and 13q14/18q21/21q22 and quantification of at least 200 cells was performed by Michaela Brough or Dr. Anna Jauch from the Institute of Human Genetics, University Hospital Heidelberg.

## Metaphase spread of human myeloma cell lines

70% confluent cells were used in a final volume of 20ml media. Then cell were treated with 10µg/ml colcemid for 2h at 37°C followed by centrifugation at 1200rpm for 10min. Hypotonic treatment of the samples with KCl 0,55%, 0.075M was slowly added and incubated for 10min. Cells were fixed with 2ml of methanol / glacial acetic acid, 3:1 and centrifuged for 10min at 1200rpm. Cell pellets were resuspended in 5ml supernatant. Second step of 20ml fixative was followed and centrifuged three times at same speed and time as previously mentioned. For dropping, the cells were added to clean slides from 50cm height and spread over waterbath at 56°C. Control of mitotic index (1-2 mitoses/field) was perfomed at bright field microscope (20X objective). Samples were stored at -20°C.

## Multicolor FISH and karyotyping

Multiplex fluorescence in situ hybridization of myeloma cell lines (U266 parental and U266R) were prepared. Fifteen metaphase spreads were analyzed and presented as multicolor karyograms. These experiments were perfomed by Brigitte Scholer in the laboratory of Prof. Dr. Anna Jauch, Department of Human Genetics at Heidelberg University.

## Methods in protein biochemistry

## Protein lysates for western blot analysis

Suspension cells were harvested by centrifugation and then washed once with 1XPBS. Cell pellets were resuspended in RIPA buffer supplemented with Complete Protease Inhibitor (Roche, Basel, Switzerland) and PhosSTOP

Phosphatase Inhibitor Cocktail (Roche, Basel, Switzerland). The samples were incubated on ice for 30 minutes and then centrifuged at 10,000rpm for 10 minutes. The supernatant was transferred into new tubes and stored at -80°.

## Bradford protein assay

The colorimetric protein Bradford assay was employed to determine protein concentration. 1mL dye reagent for the Quick Start Bradford Protein Assay (Bio-Rad, Munich, Germany) and 1μL of the protein lysate was mixed and incubated for 5 minutes. Then absorbance at 595nm was measured by spectrophotometry (Eppendorf, Hamburg, Germany) using a BSA standard curve as reference

## Sodium-dodecyl-sulfate polyacrylamide gel electrophoresis (SDS-PAGE)

SDS-PAGE gels self-made were used to separate proteins according to their molecular weight. Usually 10-12% acrylamide running gels (1,5 M Tris pH 8.8 0.4 % SDS) with stacking gels (1,0 M Tris pH 6.8 0.4 % SDS). 30μg of protein in 1X SDS loading buffer were incubated at 95°C for 5 minutes and then loaded to the gel. Separation of proteins was at 120V in Mini-Protean Tetra cells (Bio-Rad, Munich, Germany) filled with 1X Running buffer for SDS-PAGE.

## Western blot

Separated proteins from the SDS-PAGE were transferred onto a nitrocellulose blotting membrane (GE Healthcare Life Sciences, Chalfont St Giles, UK). An assembled sandwich ((cathode) fiber pad, filter paper, membrane, gel, filter paper and fiber pad (anode)) was collocated in the electrode module of the Mini

Trans-Blot Electrophoretic Transfer cell (Bio-Rad, Munich, Germany) along ice cold transfer buffer and transfer was performed at 400 mA for 70 minutes.

After transfer, the membranes were blocked for with 5% skimmed milk powder in 0.1% Tween-20 with TBS (TBS-T) for 1 hour. Primary antibodies were diluted in blocking solution and incubated with membranes overnight. Then the membranes were rinsed three times with TBS-T for 5 minutes. They were incubated with horseradish peroxidase (HRP)-conjugated secondary antibody solution at room temperature for 1 hour. Three more washes with TBS-T were followed.

The signal from HRP-conjugated secondary antibodies was identified by enhanced chemiluminescence method with Pierce ECL western blotting substrate (Thermo Fisher Scientific, Lafayette; USA) according to manufacturer's instructions. Photographic films (Amersham Hyperfilm ECL GE Healthcare Buckinghamshire, UK) were exposed to HRP signal and developed. Alternatively, the membranes were developed in a ChemiDoc touch Imaging System (Bio-Rad Laboratories, Inc., Hercules/California, USA) following manufacturer's instructions. Image analysis was performed in the Image Lab (Bio-Rad Laboratories, Inc., Hercules/California, USA) software.

## Methods  in cell biology

## Cell cultures

A complete list of the cell lines employed in this work is provided in Table 18
All cell lines were maintained at 37°C with 5% $CO_2$ atmosphere. Cells were cultured in cell culture flasks or dishes with appropriate growth medium as described in Table 18.

**Table 18. Cell culture media and supplements Medium RPMI and DMEM**

| Medium | Supplements | Selection antibiotics | Cell line |
|---|---|---|---|
| RPMI-1640 *(2 mM L-glutamine, 10 mM HEPES, 1 mM sodium pyruvate, 4500 mg/L glucose, and 1500 mg/L sodium bicarbonate)* | 10% FCS, | None | OPM-2, U266, |
| RPMI-1640 | 10% FCS, | 1,25µM Dabrafenib | U266 dabrafenib resistant cell lines (U266-R): clones 3C, 3F, 5E, 7E and 9D |
| RPMI-1640 | 10% tetracycline-free FCS | 300µg/mL Zeocin 400µg/mL G418 | OPM-2 conditional BRAF WT: clones 9 and 16  or BRAF V600E: Clones 2, 4G, 12 and 19 |
| DMEM *(4 mM L-glutamine, 4500 mg/L glucose, 1 mM sodium pyruvate, and 1500 mg/L sodium bicarbonate)* | 10% FCS | None | HeLa, A375 |
| DMEM | 10% FCS 100 IU/mL Penicillin 100 µg/mL Streptomycin | None | Lenti-X™ 293T |
| Light SILAC RPMI 1640 | 10% dFCS 100 IU/mL Penicillin and 100 µg/mL Streptomycin 0.131 mM L-Arginine | None | OPM-2, U266 |

| | 0.315 mM L-Lysine Dihydrochloride | | |
|---|---|---|---|
| Medium SILAC RPMI 1640 | 10% dFCS<br>100 IU/mL Penicillin and 100 µg/mL Streptomycin<br>0.132 mM L-Arginine:HCl (13C6; Arg+6) / Arg+6<br>0.32 mM L-Lysine: 2HCl (4,4,5,5-D4; Lys+4) / Lys+4 | None | OPM-2 BRAF WT clones |
| Heavy SILAC RPMI 1640 | 10% dFCS<br>100 IU/mL Penicillin and 100 µg/mL Streptomycin<br>0.133 mM L-Arginine:HCl (U-13C6, 15N4; Arg+10)/ Arg+10<br>0.313mM L-Lysine: 2HCl (13C6, 15N2) / Lys+8 | None | OPM-2 BRAF V600E clones and U266-R clones |

Growth media were stored at 4°C.

Subcultures of suspension cell lines, the cultures were maintained by addition or replacement of fresh medium.  Cell density was preserved between 3*10^5 and 1x10^6 cells/mL.

Subculture of adherent cells, growth medium was removed and cells were rinsed with PBS-EDTA.

Trypsin-EDTA solution was added and incubated at 37°C until cells were detached from the vessel.  Fresh medium was transferred to inhibit trypsin

activity. The subsequent cultivation ratio was 1:3 or 1:8 and they were seeded in a new vessel.

## Cryopreservation of cell lines

To store cells, cell cultures were harvested and centrifuged for 5 minutes at 800 x g. Growth medium was removed and cells were suspended in an ice-cold freezing medium (90% FCS and 10% DMSO) at $1*10^6$ cells/mL 1 mL aliquots were transferred to cryovials. Cryovials were transferred to -80°C overnight and then moved to liquid nitrogen.

## Poly-l-lysine coating

Sterile coverslips were placed in a 10cm dish, followed by 100µL of Poly-l-lysine (Sigma-Aldrich, Munich, Germany) for 20 minutes at room temperature. Then three washes with sterile ddH2O were performed and the coated coverslips were stored at 4°C until use.

## Cell growth curves

Cell growth was evaluated by Trypan blue exclusion cell count and PrestoBlue® Cell Viability Reagent proliferation assay. Cells were plated in a 24-well plate for Trypan blue exclusion cell count and 96-well plates for the PrestoBlue® proliferation assay. Cells were counted at 24-h intervals. PrestoBlue® was detected by luminescence (excitation 560nm and emission 590nm) in a microplate reader Infinite® 200 PRO series (Tecan Trading AG, Männedorf, Switzerland). Samples were in triplicates.

## Drug-response curves

For drug response curves 0.5*10^4 or 1*10^4cells per well with 50µL media were seeded in a 96 well plate. Then the drug was serially diluted and 50µL (2X of final concentration) were added to cells and incubated at 37°C, 5% $CO_2$. After 24, 48, 72, 96 or 120 hours a luminescent viability assay with Cell Titer Glo (Promega Mannheim, Germany) was performed in a microplate reader Infinite® 200 PRO series (Tecan Trading AG, Männedorf, Switzerland). Statistical analysis of the data was performed using Excel software (Microsoft Corporation, Redmond, USA).

## *In vitro* development of dabrafenib drug-resistant cell line

 0.3x10^6 cells/mL in 5mL of RPMI 1640 medium were seeded in 25 cm² flasks. As the control, a flask named "parental" was untreated and maintained along the duration of the experiment. A flask of cells derived from same cell population was named "R1" and exposed to a starting dose (500nM) of the BRAF inhibitor. The drug concentration was increased up to 1.25µM dabrafenib.  After 4 months of continued exposure to the drug, the resistant polyclonal R6 cell line was obtained. From the R6 resistant cell line, single cell cloning was performed and derived into 5 dabrafenib resistant clones: 3C, 3F, 5E, 7E and 9D.

## Single cell cloning by limited dilution of suspension cells

1x10^6 cells in 3mL of complete growth media in a 6 well plate, were seeded. Then 100µL aliquot of the cells was diluted 1:20 in 2mL of conditioned media (50% of 20% FCS RPMI 1640 and 50% sterile stroma cell medium). Then four vials containing 5mL of conditioned media were prepared, and from the 1:20

stock different dilutions were transferred: 1:500, 1:250, 1:166 and 1:125. After mixing, 96 well plates (4 plates in total) were prepared for each dilution containing 50μL/per well. Cells were incubated at 37°C 5%CO2 and cryopreserved until use.

## Senescence-associated β-galactosidase (SA-β-gal) assay

$1x10^6$ cells in 3mL of complete growth media in a 6 well plate, were seeded. For positive control, cells were treated with 75μM H2O2 for 2h followed by a wash and further incubation for 4 days then coverslips were fixed with 1 × fixative solution using the Senescence β-galactosidase staining kit. Staining of cells fixed on coverslips was performed according to manufacturer's instructions. Lastly, 200 μL β-galactosidase staining solution was added to each coverslip then samples were incubated at 37 °C without $CO^2$ for 16 h. The coverslips were washed twice with 1 × PBS, fixed in 100% ethanol and air-dried. Coverslips were mounted with Vectashield. Images were taken using a Zeiss Axiovert microscope[92].

## Development of tetraploid U266 cells

U266 cells were seeded with a density of $1.5x10^6$ cells/mL in RPMI1640 with 10%FCS, until reach approximately $30x10^6$ cells in total. Then cells were treated with 5μM cytochalasin B (Sigma, Aldrich, Munich, Germany) for 16h and released for 48h to interrupt cytokinesis and induce tetraploidy. After that, live-cell staining was performed with 1:1000 Hoechst 33342 (10mg/mL) for 40 minutes at 37°C and 5%CO2.

## Phosphoproteomics

## Preparation of SILAC media

Cell culture media SILAC RPMI 1640 was prepared for stable isotope labeling with amino acids (SILAC) as indicated in the table. The fetal calf serum dialyzed (dFCS) was heat inactivated at 56°C for 30 minutes, and centrifuged at 4500rpm for 10 minutes. It was stored at -20°C until use.

## Double SILAC

The protein expression profiling of the U266-R cells was performed as follows, the starting culture was with $3x10^6$ cells in flasks 25cm$^2$ with 10mL SILAC media; for the parental cell line (untreated) was labeled with light amino acids while, the resistant clones (treated) were labelled with heavy amino acids. 2 to 5mg of proteins was required which is obtained harvesting $5x10^7$-$10^8$ cells in total.

## Triple SILAC

For the protein expression profiling of the OPM-2 BRAF WT/V600E, $3x10^6$ cells in flasks 25cm$^2$ with 10mL SILAC media, the OPM-2 cells were labeled with light amino acids, OPM-2 BRAF WT were labeled with medium amino acids and OPM-2 BRAF V600E with heavy amino acids. Cells were expanded until harvesting $5x10^7$-$10^8$ cells in total.

## SILAC protein lysates

Harvested cells were washed with 1X PBS and resuspended in an appropriate volume of NP40-Lysis buffer (20µL lysis buffer per $10^6$ cells). Then the samples were incubated on ice for 20 minutes.  Samples were centrifuged at 15000rpm for 10 minutes at 4°C. The supernatant was transferred to a new tube and subjected to sonication (Branson Ultrasonics, Danbury, Connecticut, USA) at 15W output with 3 burst of 10 seconds each. Then lysates were stored at -80°C. Electrospray Ionisation Mass Spectrometry of the samples was kindly managed by Dr. Diego Yepes and Dr. Thomas Oellerich from the Hematology Oncology Department of the Frankfurt am Main University Clinic, DKTK/DKFZ Germany. Data was analyzed through the use of QIAGEN's Ingenuity® Pathway Analysis (IPA®, QIAGEN Redwood City,USA).

## High-throughput data analysis

High-throughput data from gene expression microarray and proteomics were analyzed in different bioinformatics software packages as the database for annotation, visualization and integrated discovery (DAVID),  PANTHER database and QIAGEN's Ingenuity® Pathway Analysis (Huang, Lempicki, and Sherman 2009; Thomas et al. 2003, IPA® QIAGEN Redwood City,USA).

## Flow cytometry

Suspension cells were washed with 1XPBS and resuspended in 250µL of 1XPBS. Then 700µL of ice-cold methanol were added dropwise, while slowly vortexing the tube. The fixed cells were incubated at 4°C for at least 1 hour.

Equally number of cells per sample (1x106 cells) were washed with 10mL 1XPBS. A propidium iodide (PI) working solution was prepared 1:100 PI (1mg/mL) in 1XPBS, and with 1:40 RNase A 10mg/mL). 200μL of the working PI solution was added to the samples, followed by incubation at room temperature for 30 minutes.

The collection of data was done in an Accuri C6 flow cytometer (BD Biosciences, Heidelberg, Germany) and the analysis of cell cycle was through the BD Accuri C6 software (BD Biosciences, Heidelberg, Germany).

## FACS sorting of cells

Samples before sorting were resuspended with high density in PBS 1X and 15ml receiving tubes were prepared with 3mL media. Sorting of cells was done with 100μM nozzle and drop delay was calculated per experiment in a FACS BD Aria I or FACS BD Fusion I sorters (Becton Dickinson, Franklin Lakes, NJ, USA) and performed by Klaus Hexel or Tobias Rubner from the Core Facility Flow Cytometry at DKFZ, Heidelberg, Germany.

## Indirect immunofluorescence

Cells grown on coverslips were briefly rinsed with PBS and then fixed in ice-cold methanol/acetone for 7 minutes. Coverslips were blocked in 10% goat serum in PBS for 30 minutes and incubated with primary antibodies for 1 hour.

A complete list of the primary antibodies used for immunofluorescence is provided in Table.

**Table 19. Primary antibodies used for immunofluorescence**

| Antigen | Clone | Species | Clonality | Dilution | Source |
|---------|-------|---------|-----------|----------|--------|
| EGR-1 | 44D5 | rabbit | monoclonal | 1:400 | Cell Signaling |

| | | | | | |
|---|---|---|---|---|---|
| | | | | | Technology |
| **BRAF** | C-19 | rabbit | polyclonal | 1:200 | Santa Cruz |
| **BRAF V600E** | VE-1 | mouse | monoclonal | undiluted | Dr. med. David Capper, Pathology Institute, Neuropathology, Heidelberg University |

Followed of primary antibody incubation, the coverslips were washed three times for five minutes in 1X PBS and incubated with appropriate species-specific secondary antibodies. Proceeded with three 1XPBS washes, and washed once with ddH2O. Coverslips were mounted in Vectashield antifade mounting medium (Vector Laboratories, Burlingame, CA, USA) with DAPI for Fluorescence or DNA was counterstained with Hoechst 33342 (10 mg/mL), diluted 1:1000 in 1XPBS. Coverslips were analyzed by fluorescence microscopy on a Zeiss Cell Observer.Z1 system equipped with an AxioCam MRm camera (Carl Zeiss, Göttingen, Germany), or an Axiovert 200M equipped with an AxioCam MRm camera (Carl Zeiss, Göttingen, Germany). Then for image analysis the software ZEN lite 2011 (Carl Zeiss, Göttingen, Germany) was employed.

A complete list of the secondary antibodies used for immunofluorescence is provided in Table 20.

**Table 20. Secondary antibodies used for immunofluorescence**

| Antigen | Fluorochrome | Species | Clonality | Dilution | Source |
|---|---|---|---|---|---|
| **Mouse IgG** | Alexa Fluor 488 | Goat | polyclonal | 1:1000 | Molecular Probes Life Technologies |
| **Rabbit IgG** | Alexa Fluor 488 | | | | |
| **Mouse IgG** | Cy3 | | | | Dianova (Jackson immuno Research) |
| **Rabbit IgG** | Cy3 | | | | |

# Gene transfer techniques

## Transduction

### Lentiviral production – transfection of 293t cells

The day before transfection, $1\times10^6$ Lenti-X™ 293T cells were seeded in a 10cm dish in 10mL fresh medium to obtain 50-80% confluency on the day of lentiviral production.

Immediately before transfection in 6 cm plate, a mixture of 3 plasmids was prepared with 1.8µg of packaging plasmid (psPAX2), 300ng envelop plasmid (pMD2.G) and 3µg expression plasmid along with 20µL RPMI 1640. The cell transfection was performed with TransIT®-LT1 Transfection Reagent (Mirus Bio LLC, Madison Wisconsin, USA) according to manufacturer's instructions. TransIT®-LT1 is a cationic polymer that forms stable positively charged complexes with DNA, allowing its delivery to cells. The transfection reagent was diluted with RPMI 1640 and incubated 5 minutes at room temperature. Then the plasmid mixture was diluted with the transfection reagent and incubated 20 minutes at room temperature. The mix was added to 6mL of fresh DMEM medium. The medium in the cells was removed and replaced with the mix, followed by incubation at 37°C overnight.

Next day, the medium was replaced with 2,7mL DMEM + 30% FCS with Pen/Strep. On the third day, harvesting of the virus was collected and stored at 4°C; cells received fresh media. On the fourth day, a second harvesting was performed and filtered with 0.22µm filters (Millipore, Bedford, USA). The presence of virus (>5 x 105 IFU/ml) was confirmed by Lenti-X™ GoStix™ according to manufacturer's instructions (Clontech Laboratories, Inc. A Takara Bio, Shiga Japan). 1mL viral soup aliquots were stored at -80°C.

## Lentiviral infection of human cell lines

The cells to be infected were plated in a 6 well culture plate, and 0.8μL of Polybrene (10mg/mL, Santa Cruz Biotechnology Heidelberg, Germany), were added per 1mL medium. Then 300μL of viral soup was transferred to 1.5x10^5 cells in 1mL and incubated at 37°C overnight. The following day, the medium was replaced with fresh medium and after 48h cells were under antibiotic selection.

## Transfection

Transfection of adherent cell lines was performed with a cationic polymer, Lipofectamine® 3000 Reagent (Thermo Fisher Scientific, Lafayette; USA), according to manufacturer's instructions. The day before transfection, 1x10^5 cells were seeded on coverslips in 6 well plates (Greiner-Bio-One GmbH, Frickenhausen Germany) with 3mL fresh RPMI or DMEM.

## Statistical analysis

Statistical analysis was performed using Excel software (Microsoft Corporation, Redmond, USA) and GraphPad Prism 7 software (GraphPad Software La Jolla, CA, USA). Experiments consisted in technical and biological replicates and were in triplicates unless otherwise is specified. Microarray statistical significance was analyzed by two group empirical Bayes test. For biological and functional gene analysis the right-tailed Fisher's exact test was performed. Significances were calculated by two-tailed t test or two-way ANOVA methods. False discovery rate (FDR) <0.05. The value of P<0.05 was considered significant.

# 4

---

# Results

## Conditional BRAF V600E OPM-2 model

In order to investigate biological sequelae of BRAF V600E expression in multiple myeloma, we established an inducible model system. MM cell lines that are available in the laboratory were sent for targeted sequencing of genes that included: KRAS, NRAS, and BRAF. The MM cell line OPM-2 was chosen among other myeloma cell lines such as RPMI-8226, U266, L363, MM1.S, SKMM.1, and INA-6 because of its wild type KRAS, wild type NRAS, and wild type BRAF status. In the Tet-On system, gene expression is conditionally obtained upon addition of tetracycline (Tet) or doxycycline (Dox) to the cell culture medium. The RAS/RAF-WT OPM-2 cells were co-transduced with both vectors containing the regulatory plasmid and response plasmid, and conditional target gene expression (c: conditional, cBRAF-WT or cBRAF V600E, respectively) was examined in presence of Dox by immunofluorescence or immunoblotting (Figure 5). Conditional overexpression of the mutant cBRAF V600E was detected using a mutation-specific antibody. Likewise, the inducible cBRAF WT expression was confirmed by immunoblotting, serving as control of the mutant protein. Once that the presence of the inducible protein was confirmed, the conditional cells

were under clonal selection by limiting dilution to generate conditional stable clones

## Characterization of mutant BRAF in MM cells

In order to reveal the consequences of conditional BRAF expression, we examined cell growth, gene expression, protein expression and phosphorylation profile of both cells overexpressing BRAF wild type or mutant.

Although MAPK/ERK pathway mutations in MM have been identified, the mechanism of action by which activated BRAF contributes to this disease needs to be further elucidated. Therefore, we investigated gene expression of the human myeloma OPM-2 cell line with conditional expression of BRAF V600E by cDNA microarray analysis and compared their gene expression patterns to OPM-2 cBRAF wild type. In total, 1788 genes were differentially expressed in OPM-2 cBRAF V600E compared to OPM-2 cBRAF WT cells (log2FC <-1 and >1, p-value <0.05 and FDR 0.05). Of these, 1014 genes were down- and 774 were upregulated in cBRAF V600E compared to cBRAF WT MM cells (Figure 7 ).

 Ingenuity Pathway Analysis (IPA) software was used to sort differentially expressed transcripts to functional categories (data not shown). The most significantly canonical pathways included diverse hints towards DNA damage response (Figure 7). It has been reported that mutant BRAF can lead to oncogenic stress which induces DNA damage and subsequently can result in oncogene-induced senescence (Vredeveld et al. 2012). Moreover, using the Database for Annotation, Visualization and Integrated Discovery (DAVID) we classified the functionally related genes by their enrichment score (ES)[93]. Prominent gene groups revealed were, for example, negative cell growth (ES: 2.16), programmed cell death (ES: 1.63) and microtubules (ES: 1.36), etc. (Figure 7).

To test the effect on proliferation of the conditional model, OPM-2 cells were maintained in 10% FCS RPMI 1640 and induced with Dox, but no differences were observed upon overexpression of either cBRAF wt or cBRAF V600E (Figure 5E). AS OPM-2 cells might depend on other pathways to proliferate and survive irrespective of their BRAF status, we subjected the cells to starvation media 1% FCS RPMI 1640 followed by Dox treatment. However, no growth differences were observed(data not shown). The mutated kinase does not offer any growth advantages and there was no slowdown in the growth in the mutant clones. In addition, to find out if senescence was a result of conditional BRAF overexpression, a senescence-associated β-galactosidase (SA-β-gal) assay was performed. However, no changes were observed in induced cBRAF V600E in comparison to cBRAF wild type or uninduced despite the suggestive gene expression profiling (Figure 6B).
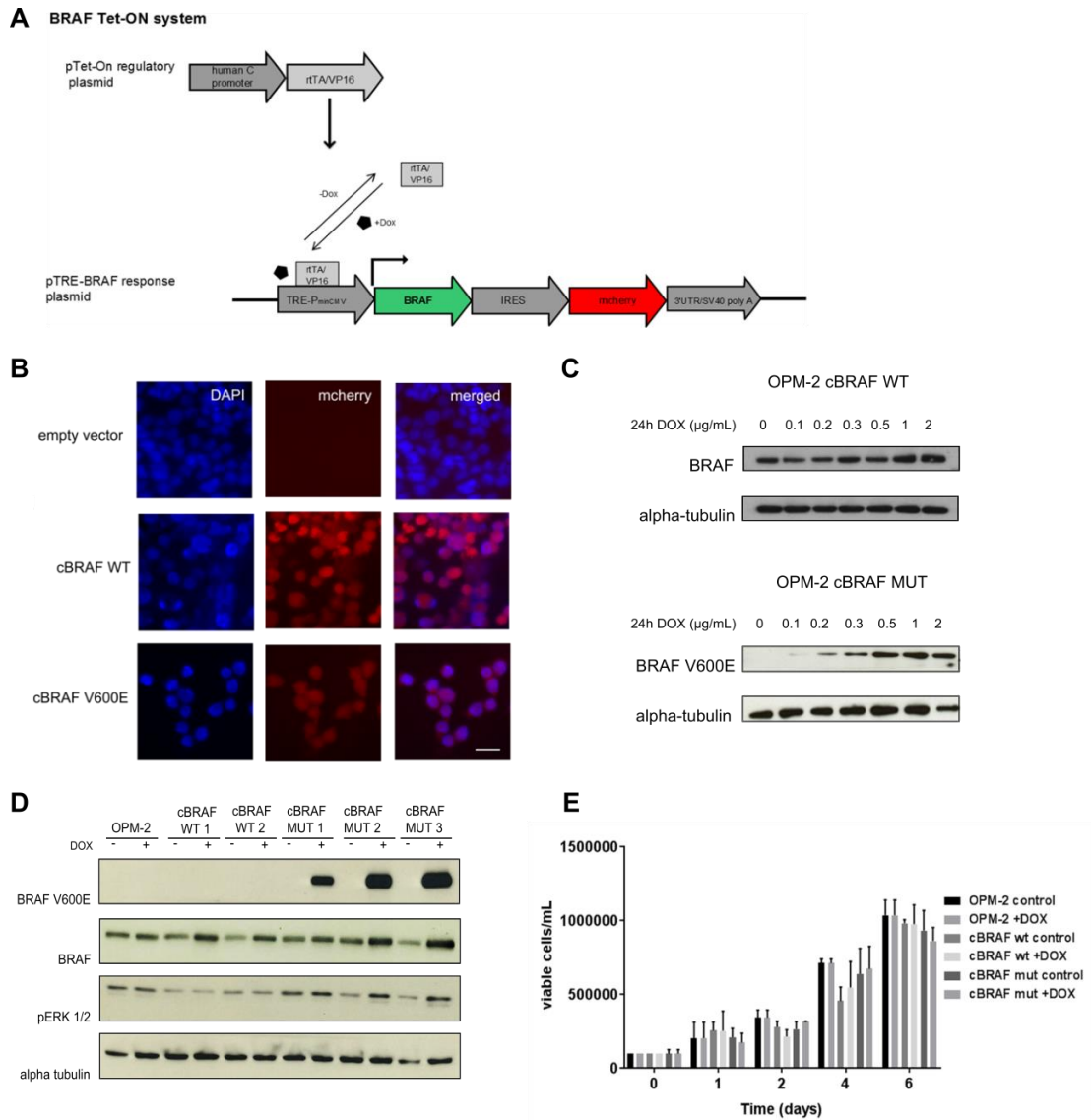
**Figure 5. Inducible expression system of BRAF wild type or mutant in multiple myeloma.** A. BRAF Tet-On system. B Immunofluorescence of induced cBRAF wild type and mutant IRES mcherry and DAPI for nucleus. C. Immunoblot of dependence of protein expression level on concentration of doxycycline. D. After single cell cloning of the transduced parental cell lines, the clones obtained were induced with doxycycline and the expression of the conditional proteins was confirmed by immunoblotting. Unmodified OPM-2 cell line was included as control. D. Growth of inducible BRAF OPM-2 cell lines. Trypan blue exclusion growth measurements were generated from OPM-2 cBRAF cells. There were no significant growth differences among the groups.
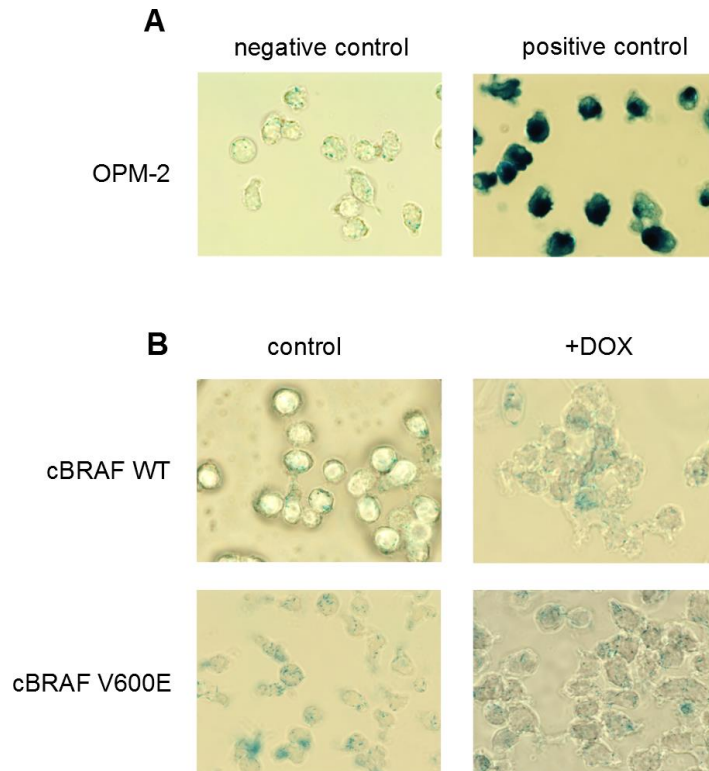
**Figure 6. Senescence in conditional BRAF wild type or mutant in multiple myeloma.** A. β-Galactosidase staining on normal OPM-2 at population doubling 30 (left) and stress-induced premature senescence induced using 75μM peroxide hydrogen (H2O2) for 2h, followed by a wash and further incubation for 4 days. B. Cells were induced with 1μg/mL doxycycline for 24h followed by wash and further incubation for 48h. No oncogene induced senescence was observed in the cBRAF model.
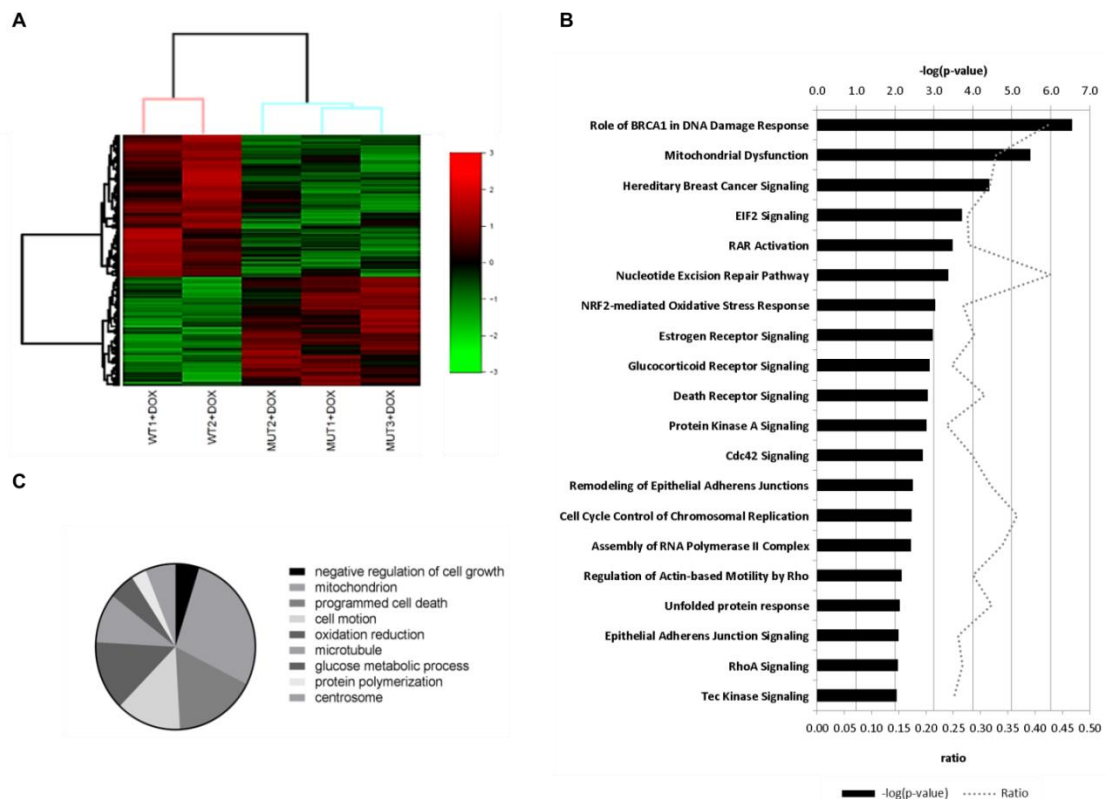
**Figure 7. Gene expression profiling of induced cell lines expressing cBRAF WT or V600E.** A. The inducible OPM-2 cell lines cBRAF wild type or V600E were under doxycycline (1μg/mL) for 24h, subsequently RNA was extracted and the gene expression profile was assessed using the Illumina HT12v4 platform followed by hierarchical clustering in Chipster (M Aleksi., et al. 2011). B. Analysis of canonical pathways in Ingenuity Pathway Analysis (IPA, Qiagen). D. DAVID Top ten functional clusters (Huang DW et al. 2009). Log2FC <-1 to >1 and FDR p-value <0.05.

## Protein expression profiling and phosphoproteomics of cBRAF OPM-2

In order to understand the biological consequences of BRAF V600E in MM, differential protein and phosphoproteome expression of the wild type versus mutant kinase was performed by using stable isotope labeling by aminoacids in cell culture (SILAC) in combination with protein enrichment and LC-MS/MS analysis. The distribution histograms of the protein expression profiling and

phosphoproteome of SILAC cBRAF OPM-2 fit a Gaussian distribution, which satisfies the criteria for protein quantification (Supp. Figure 21). Follow up on the analysis demonstrated upregulation of EGFR signaling including proteins related to MAPK/ERK pathway and molecules associated with DNA replication were downregulated (Figure 8). The differential expression of BRAF V600E versus BRAF wild type showed active proteins involved in the MAPK/ERK pathway such as BRAF, MEK1/2 ERK2 and ELK-1, which is consistent with our previous results (Figure 9).

An integrative assessment of our analyses of the transcriptome, proteome, and phosphoproteome indicates that conditional expression of mutant BRAF promotes DNA damage response through diverse signaling including nucleotide excision repair (NER), DNA double–strand break repair by NHJE, BRCA1 in damage response, etc. (Figure 7B, 10A and 10B). Nevertheless, OPM-2 cBRAF V600E cell proliferation showed no difference in comparison to BRAF wild type (Figure 5E). This is potentially explained by the mutational background of OPM-2 which affects main effectors of growth arrest such as p53 and CDKN2A.
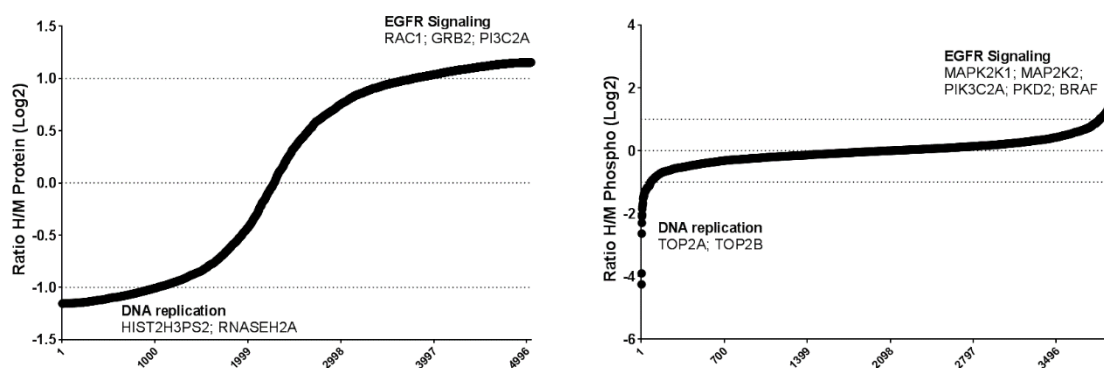


**Figure 8. Distribution of protein expression profiling and phosphorylation in OPM-2 cBRAF V600E.** SILAC labeling of OPM-2 cells expressing cBRAF V600E (H) compared against cells expressing cBRAF *wild type* (M). The expression was normalized against non-modified OPM-2 cells (L). Log2 plot for quantified proteins and phosphopeptides.
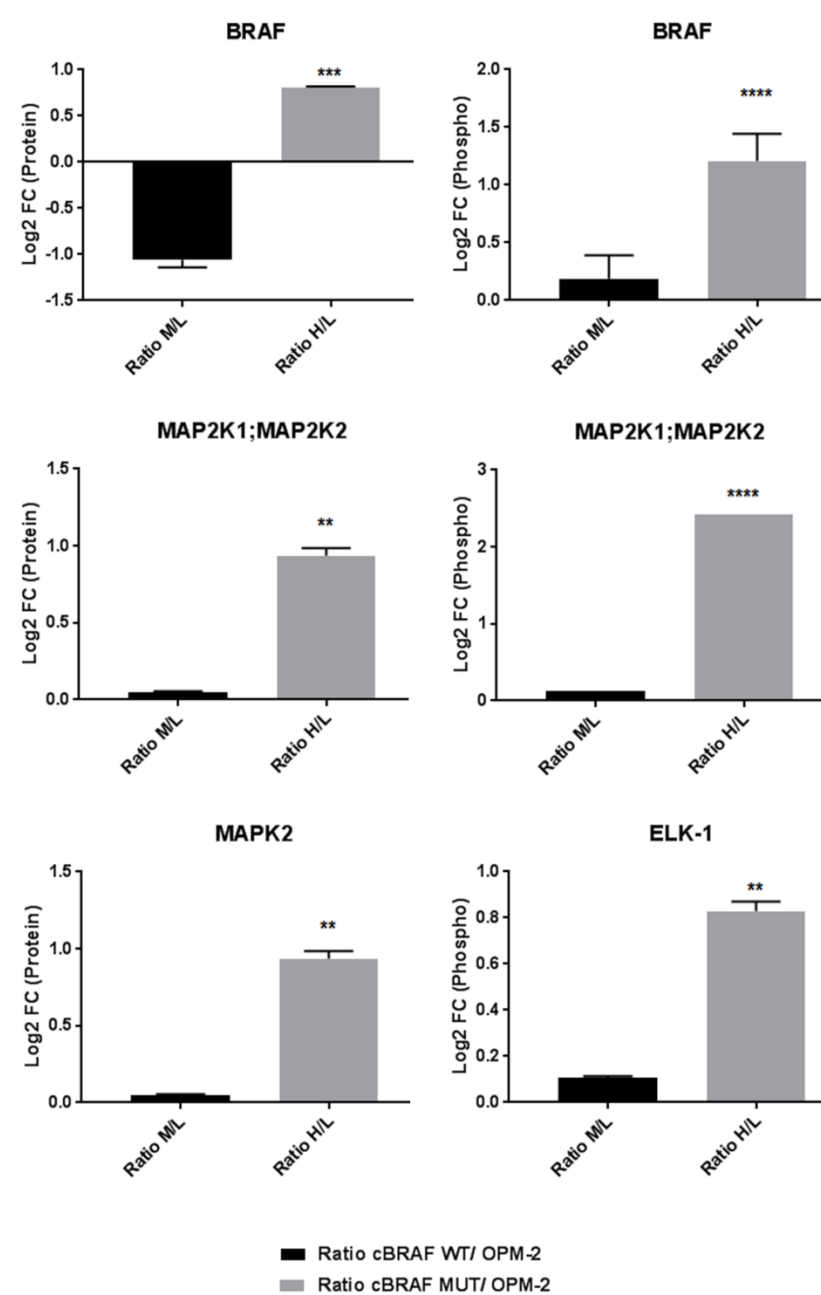
**Figure 9. Quantitation of MAPK/ERK proteins in OPM-2 cBRAF V600E by SILAC**. The histograms represent the quantitative data obtained for cBRAF V600E (H) normalized to OPM-2 cells (L) and compared to cells expressing cBRAF wild type (M) normalized to OPM-2 cells (L). Log2 fold change plot for quantified protein and phosphopeptides. p>0.01, **- 0.01≥p>0.001, *** - p≤ 0.001,**** p≤ 0.0001
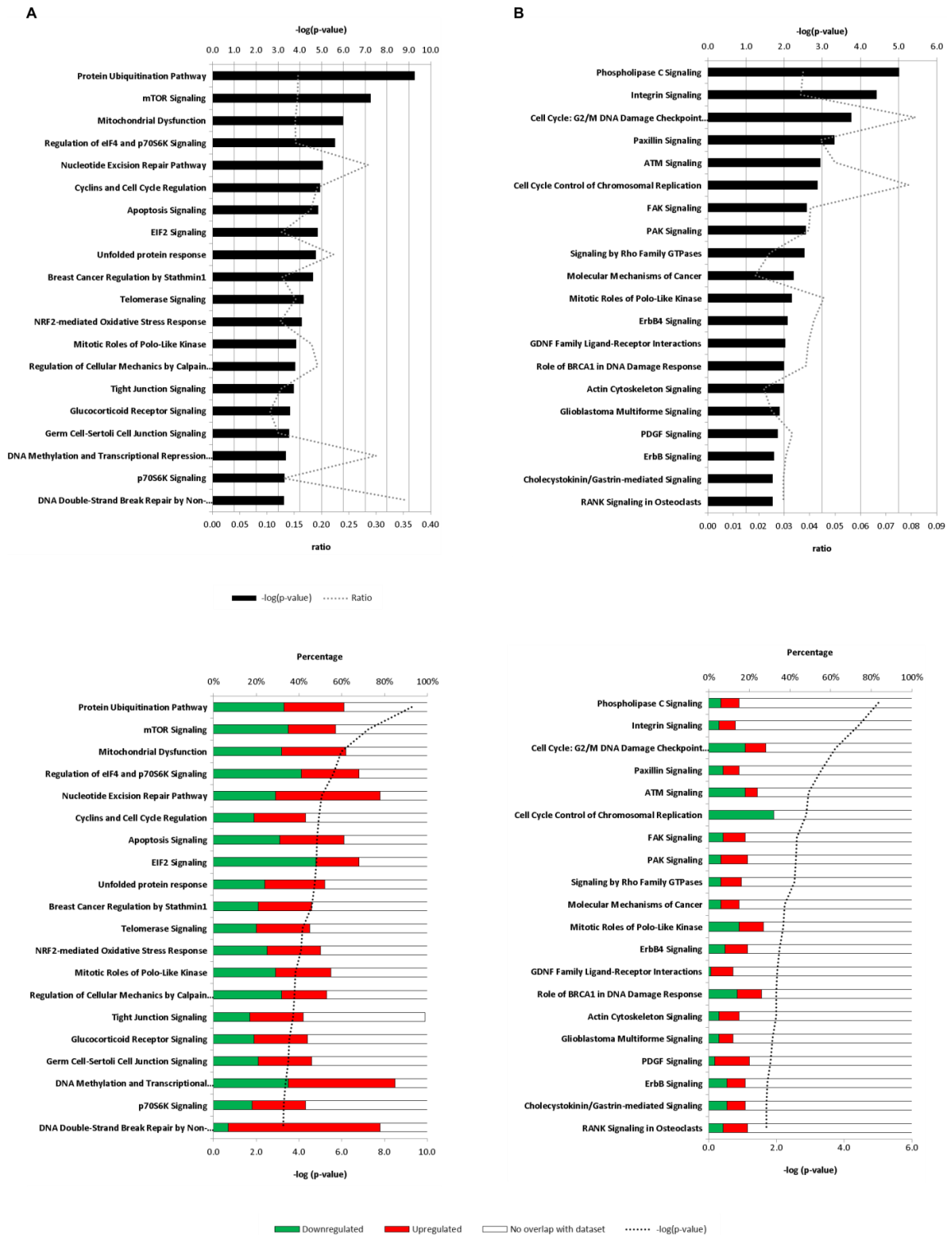
**Figure 10. Canonical pathways in OPM-2 cBRAF V600E.** A. Ingenuity's canonical pathways of protein expression profiling and stack bars showing the percentage of down- (green) and upregulated (red) protein expression. B. IPA analysis of canonical pathways of phosphoproteome and stack bar showing lower phosphorylation (green) or high phosphorylation (red).

## BRAF inhibition and MEK inhibition in cBRAF OPM-2.

To explore cell response under BRAF inhibitors, mutant cells were treated either with vemurafenib, a BRAF V600E specific inhibitor or dabrafenib, a mutant BRAF V600 inhibitor but with wider target range including wild type B-RAF and C-RAF. In both cases, we observed the paradoxical activation of the native BRAF protein in the immunoblot by downstream ERK phosphorylation, although this activation occurs more moderately in cells under dabrafenib. This effect has also been observed in melanoma which is associated with the induction of neoplasia such as cutaneous squamous cell carcinoma (cuSCC) [55] (Figure 11 ). This is caused by BRAF inhibitor-mediated homodimerization and heterodimerization of non-mutant RAF isoforms, leading to pathway activation rather than inhibition. Interestingly, the presence of BRAF V600E by the conditional expression is fully abrogating the paradoxical activation of the still present WT BRAF kinase (Figure 11A and 11B). Importantly, the employment of downstream inhibitors, such as the MEK inhibitor trametinib (Figure 11C), abrogates the activation of the pathway without the paradoxical activation, supporting the combination of both inhibitor families, as approved for melanoma and also now under clinical investigation in multiple myeloma.
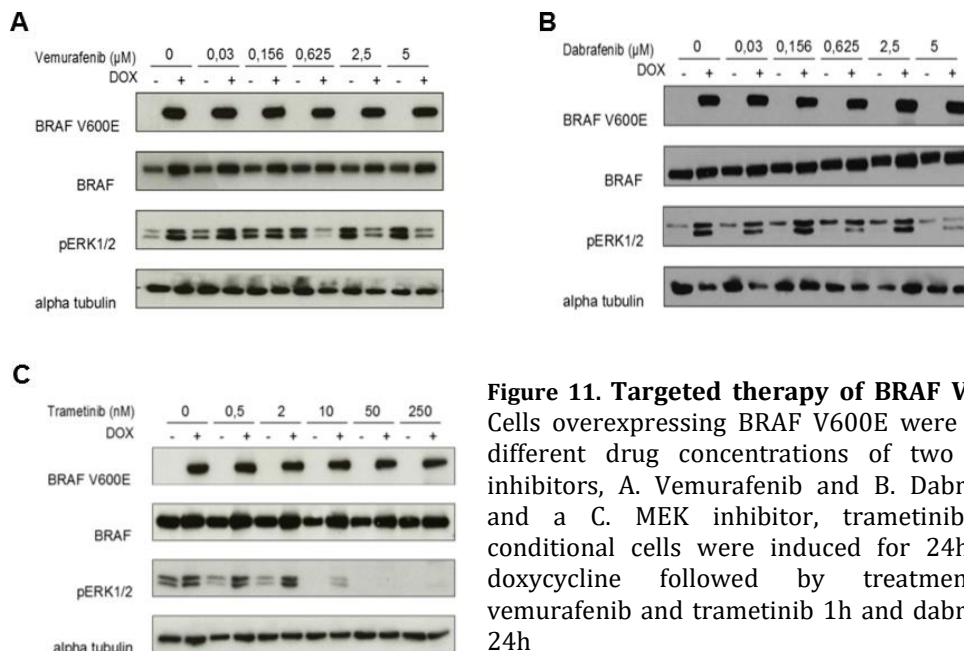


**Figure 11. Targeted therapy of BRAF V600E.** Cells overexpressing BRAF V600E were under different drug concentrations of two BRAF inhibitors, A. Vemurafenib and B. Dabrafenib and a C. MEK inhibitor, trametinib. The conditional cells were induced for 24h with doxycycline followed by treatment of vemurafenib and trametinib 1h and dabrafenib 24h

# Dabrafenib resistant multiple myeloma model

To understand possible mechanisms underlying clinical drug resistance in MM, a Dabrafenib resistant model was established using the multiple myeloma U266 cell line carrying the BRAF K601N mutation, which we confirmed by panel sequencing. U266 is the only known MM cell line carrying an activating BRAF mutation [95,96]. A U266 resistant cell line (U266 R6) was created by long-term exposure to increasing concentrations of the kinase inhibitor. In addition, parental U266 cells (not exposed to dabrafenib) were kept in culture in parallel to U266 R6 over the same period of time to serve as controls (Figure 12A). Then U266 R6 cell growth was analyzed and similar growth patterns were observed in comparison to parental cells (Figure 12B).

From the resistant polyclonal cells U266 R6, single cell clones (U266R) were obtained by limiting dilution. To confirm specific resistance to the BRAF inhibitor, the cells were exposed to other chemotherapeutic agents to test for unspecific resistance through efflux pumps, increased drug metabolism, altered drug targets, etc.. Paclitaxel, Etoposide, 5-Fluoroacil, Vincristine, Doxorubicin and Cisplatin (Figure 13) were used as such control agents and we obtained five clones (1C-5C) with confirmed specific resistance to dabrafenib (Figure 12C). Specific resistance was also maintained after freeze and thaw cycles of the cell lines.

**A**



**B**



| Sample | Population doubling time | Fold clone vs. parental |
|---|---|---|
| U266 Par | 2.15 | 1 |
| Clone 1 | 2.51 | 1.1 |
| Clone 2 | 2.87 | 1.3 |
| Clone 3 | 2.57 | 1.1 |
| Clone 4 | 3.25 | 1.5 |
| Clone 5 | 3.47 | 1.6 |

**C**
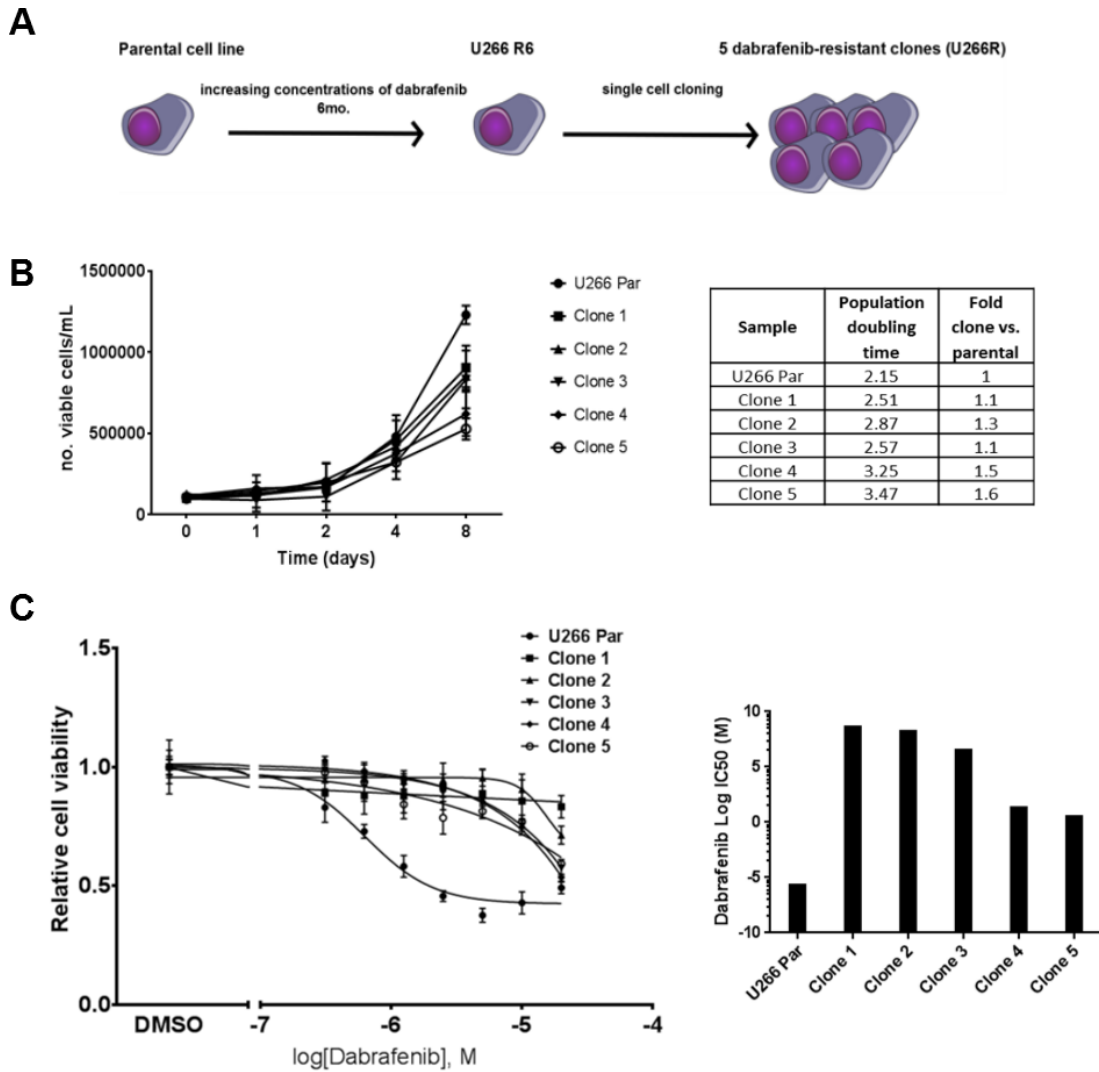


**Figure 12. U266 resistant clones to dabrafenib.** A. Scheme of development of the model. B. Growth curves of U266R and table showing the population doubling time. C. Dose response curves where U266R cells were exposed to the indicated concentrations of dabrafenib for 72h and cell viability was measured by CellTiterGlo and expressed relative to control untreated cells (left panel). IC50 of dabrafenib in U266R cells (right panel).
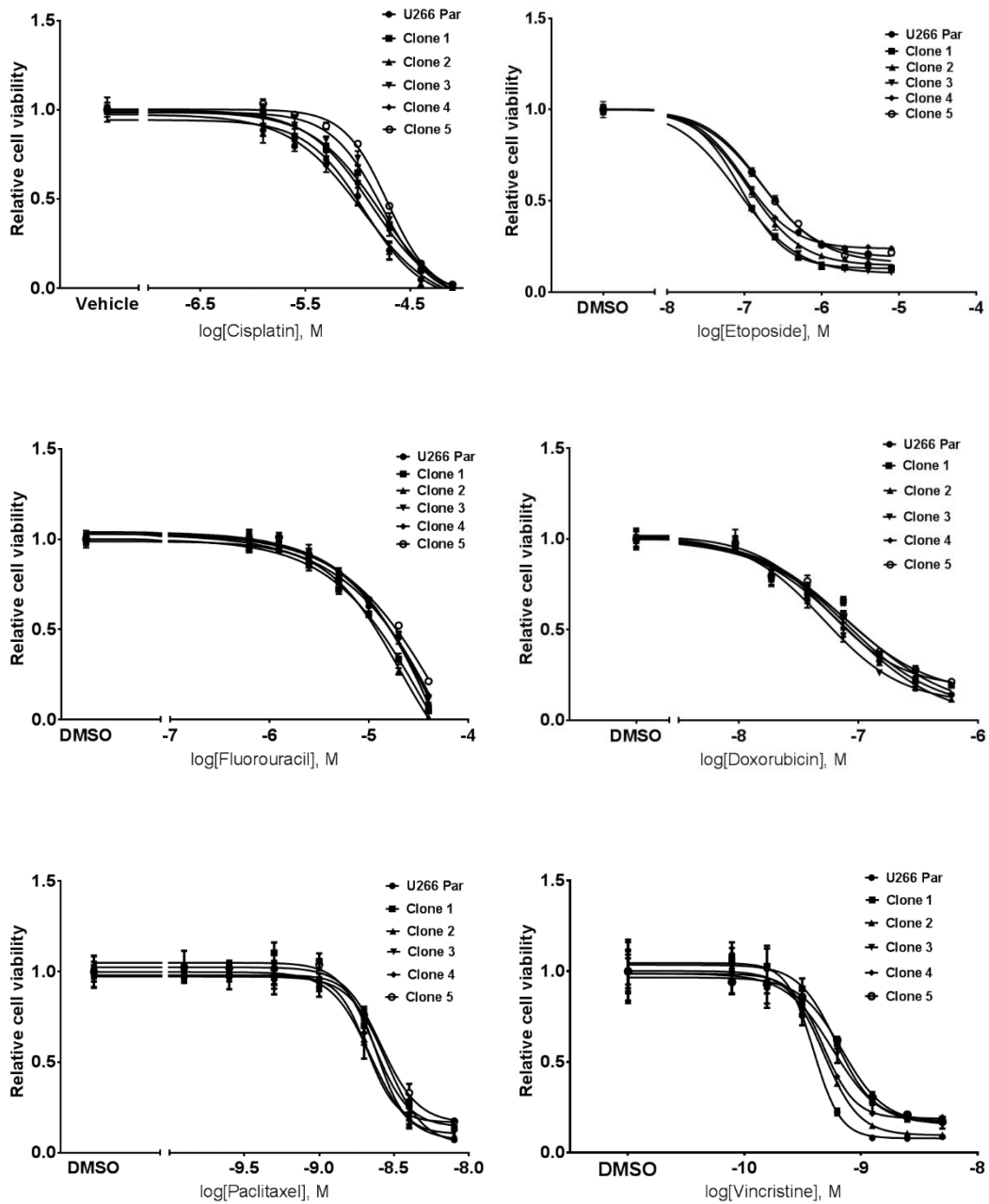
**Figure 13. U266R resistant clones and chemotherapeutic agents.** Proliferation of U266 resistant clone cells following 72h with the indicated chemotherapeutic agents. Cell viability was measured by CellTiter Glo and expressed relative to control untreated cells.

## Whole Exome Sequencing in dabrafenib U266R resistant clones

Once specific resistance to BRAF inhibitors was confirmed, next-generation sequencing was performed to identify mechanisms of drug resistance in the U266R model. A total of 96 SNVs and 45 indels were detected in exonic regions that were present in one or more resistant clones (Figure 14A and 14B). We focused on heterozygous mutations that were identically present in all resistant clones, and 3 candidates for dabrafenib resistance were identified. These were the serine/threonine kinase 36 (STK36), the calcium channel, voltage-dependent, alpha 2/delta subunit 3 (CACNA2D3) and the Early Growth Response 1 (EGR-1) (Supp. Table 21). Subsequently, these aberrations were confirmed by Sanger sequencing. The drug resistance candidate gene chosen for further study was EGR-1 because it is downstream of the MAPK/ERK pathway (Figure 16A). Interestingly, the tumor variant frequency was approximately 20-25% in all cases, which suggests that U266 resistant cell clones became tetraploid. Results from FiSH analyses in this regard confirmed tetraploidy (>80%) of resistant clones.

From the whole exome sequencing of U266R differences in structural DNA rearrangement, copy number variations (CNVs) were detected in comparison to the reference genome of untreated parental cells (Figure 15). CNVs could contribute to the U266R phenotypic variation as an adaptative trait to dabrafenib treatment. Pathogenic CNVs are frequently related to an imbalance in gene dosage, such as gene amplification which is associated with drug resistance. Whether the selective pressure in our model with the BRAFi and the environmental conditions directly played a role in the generation of "somatic" CNVs in U266R or if it was due to a stochastic process is yet to be determined.
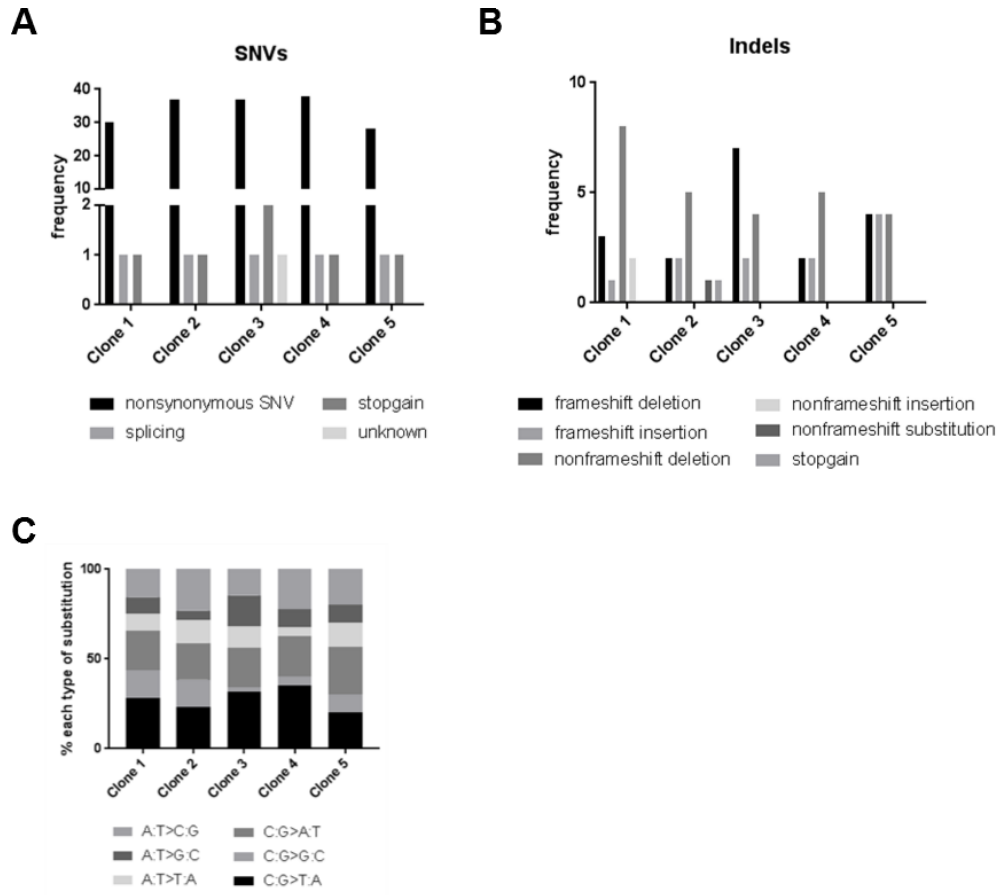
**Figure 14. Whole exome sequencing U266 dabrafenib resistant cells**. Frequency of A. single nucleotide variants and  B. indels in U266R. C. Pattern of nucleotide substitutions in all samples.
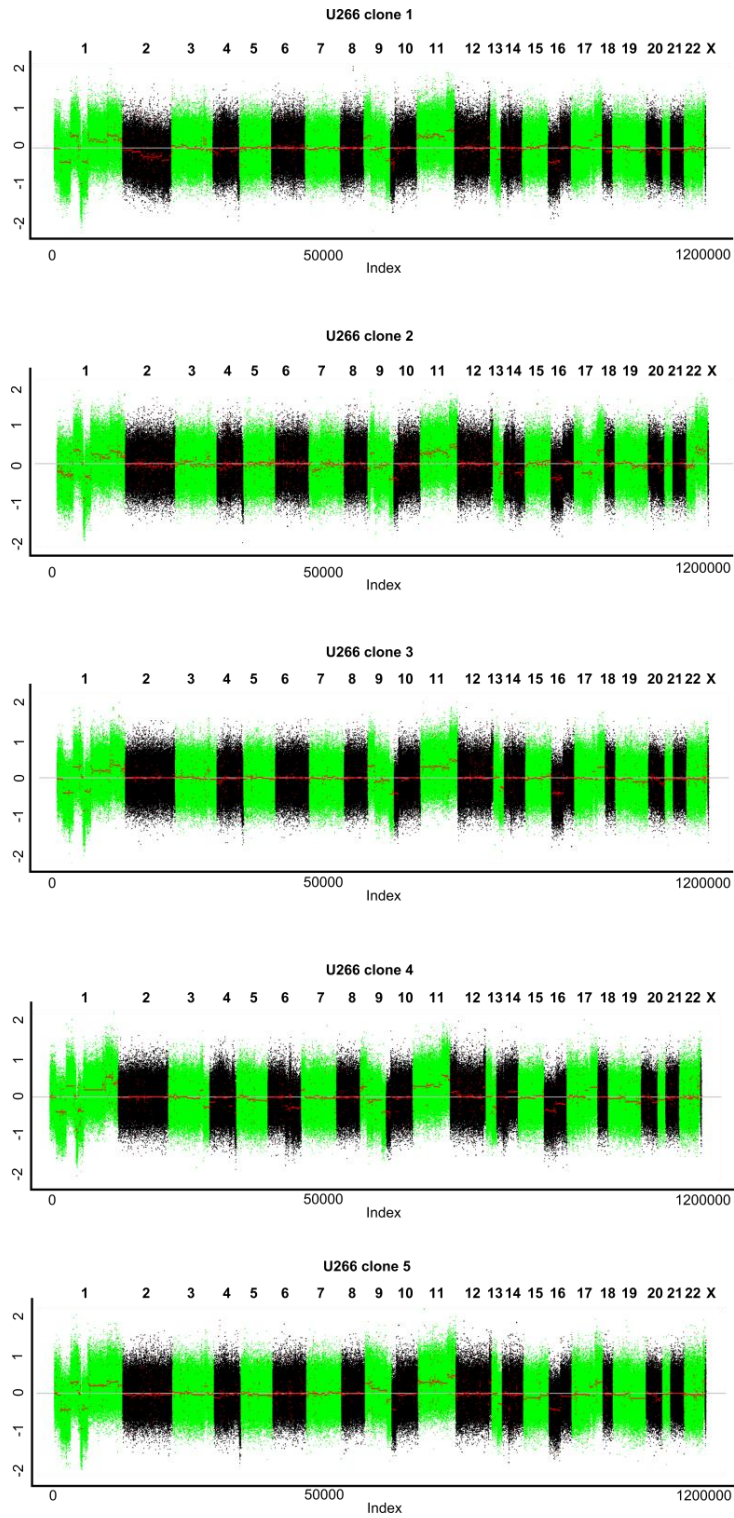
**Figure 15. U266-R DNA copy number variants.** Whole-exome view of U266 dabrafenib resistant clones. Coverage data are indicated as Normalized Log2 Ratios. Alternated green and black colors represent specific chromosomes from 1 (left) to X (right).

## Hyperdiploidy in U266R

After whole exome sequencing of U266R, a low, yet consistent tumor variant frequency was detected (20-25%) in all resistant clones, suggesting that cells acquired a tetraploid karyotype. To characterize the resistant clones, DNA ploidy analysis was performed by interphase FISH and metaphase FISH (Figure 16) and these experiments confirmed that U266 dabrafenib resistant clones developed a near-tetraploid karyotype in comparison to the near-diploid karyotype of parental untreated cells.

To explore whether dabrafenib resistance was due to polyploidy, U266 cells were treated with a cytokinesis inhibitor, cytochalasin B. Then the DNA content was analyzed by flow cytometry and samples were sorted for tetraploidy content (purity >80%). Sorted cells were treated with dabrafenib for 72h. No significant differences were observed for these generated tetraploid cells in comparison to control cells (Figure 16C). Overexpression of EGR-1 was observed in purified tetraploid (purity after sorting 86.2%)  cells but not in cells before sorting (purity 1.7%) or overexpression of control proteins as alpha tubulin or RAS was not observed (data not shown).Thus, tetraploidy per se did not contribute to resistance it was observed in U266R.
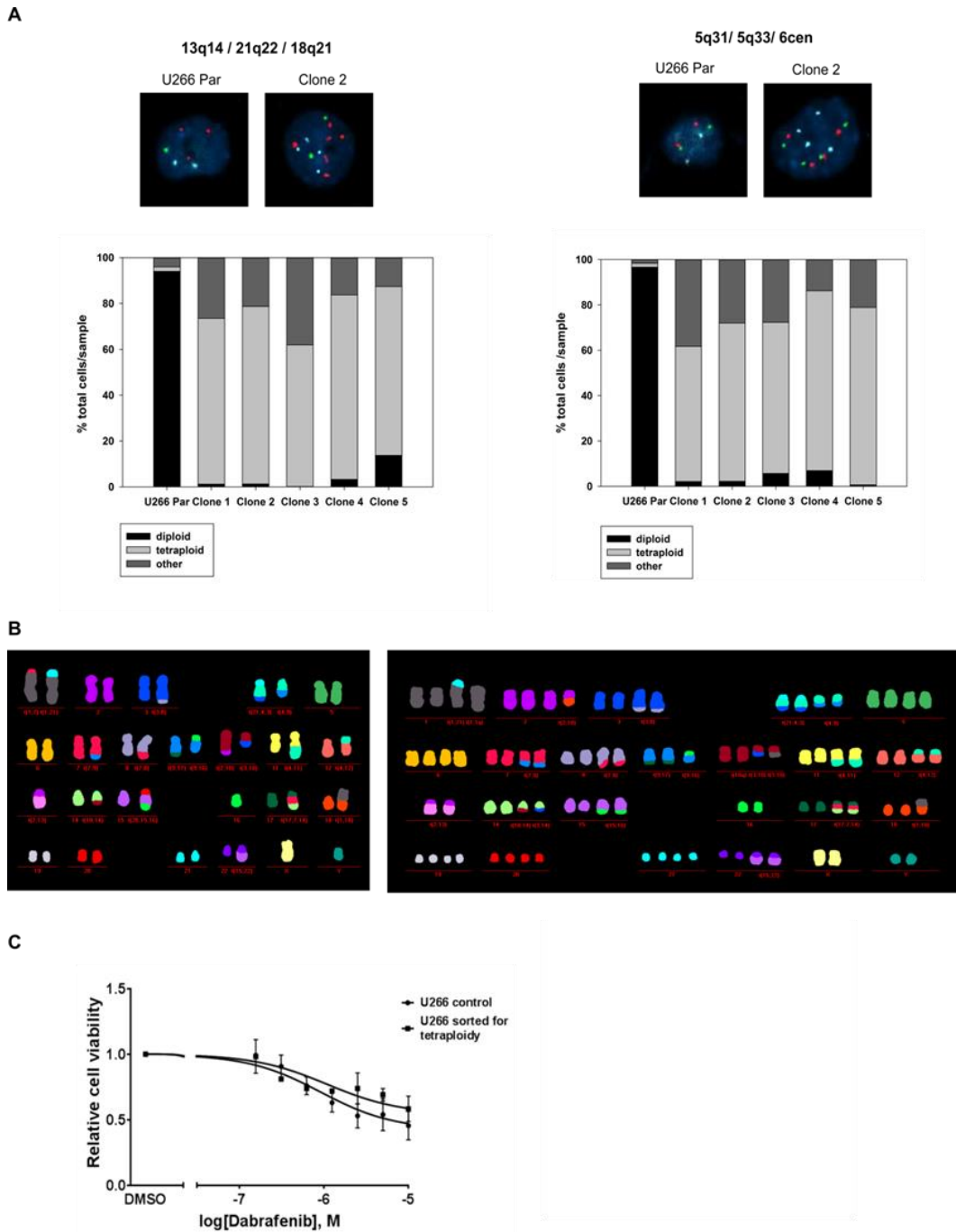
**Figure 16. Tetraploidy in U266R.** A. Fluorescence *in situ* hybridization of U266R cell lines. Top: Representative FISH results shows duplicated gene copy number in a U266R clone in comparison to parental cells. Bottom: quantification of ploidy in U266R clones. Cytogenetic probes used PS 13-g 21-r, 18-b (1) and AML MDS 5q31-R 5q33-G 6cen-B (2). B. M-FISH images of U266. Parental cells (left) with near diploid karyotype (n=44) and U266R clone 1 (right), showing near tetraploid karyotype with numerical and structural chromosomal instability. C. drug response curves of tetraploid sorted cells. No significative differences were observed.

## Aberrant expression of EGR-1 confers dabrafenib resistance in U266R

In this study, whole exome sequencing of U266R cells identified the frameshift insertion 994dupC (p. P332fs) in EGR-1, a candidate for dabrafenib resistance.

The Early Growth Response 1 (EGR-1) is a nuclear protein and a member of the EGR family of C2H2-type zinc-finger proteins which binds to DNA motifs with the sequence 5'-GCG(T/G)GGGCG-3'. The gene is encoded on plus strand of chromosome 5 from 137,801,169 to 137,805,103 and contains 1 intron and 3 exons. As protein it is described as a transcriptional regulator with 543 aminoacids (Figure 17B). EGR-1 expression is induced by growth factors, mitogens, ischemia, and tissue injury. Then it binds to DNA and activate the transcription of several genes that are required for mitogenesis and differentiation [97–99].

The frameshift insertion 994dupC (p. P332fs) found by whole exome sequencing was confirmed by Sanger sequencing (Figure 18A). This aberration results in a premature stop codon which leads to the expression of a truncated transcript of 292 amino acids losing the C-terminus of the protein. Our results demonstrated aberrant expression of EGR-1 in U266R with overexpression of wild type protein but also expression of a truncated protein which is observed at 50kDa in the immunoblot, while the wild type protein has a molecular weight of ~85KDa depending on posttranslational modifications (Figure 18B and 18C).
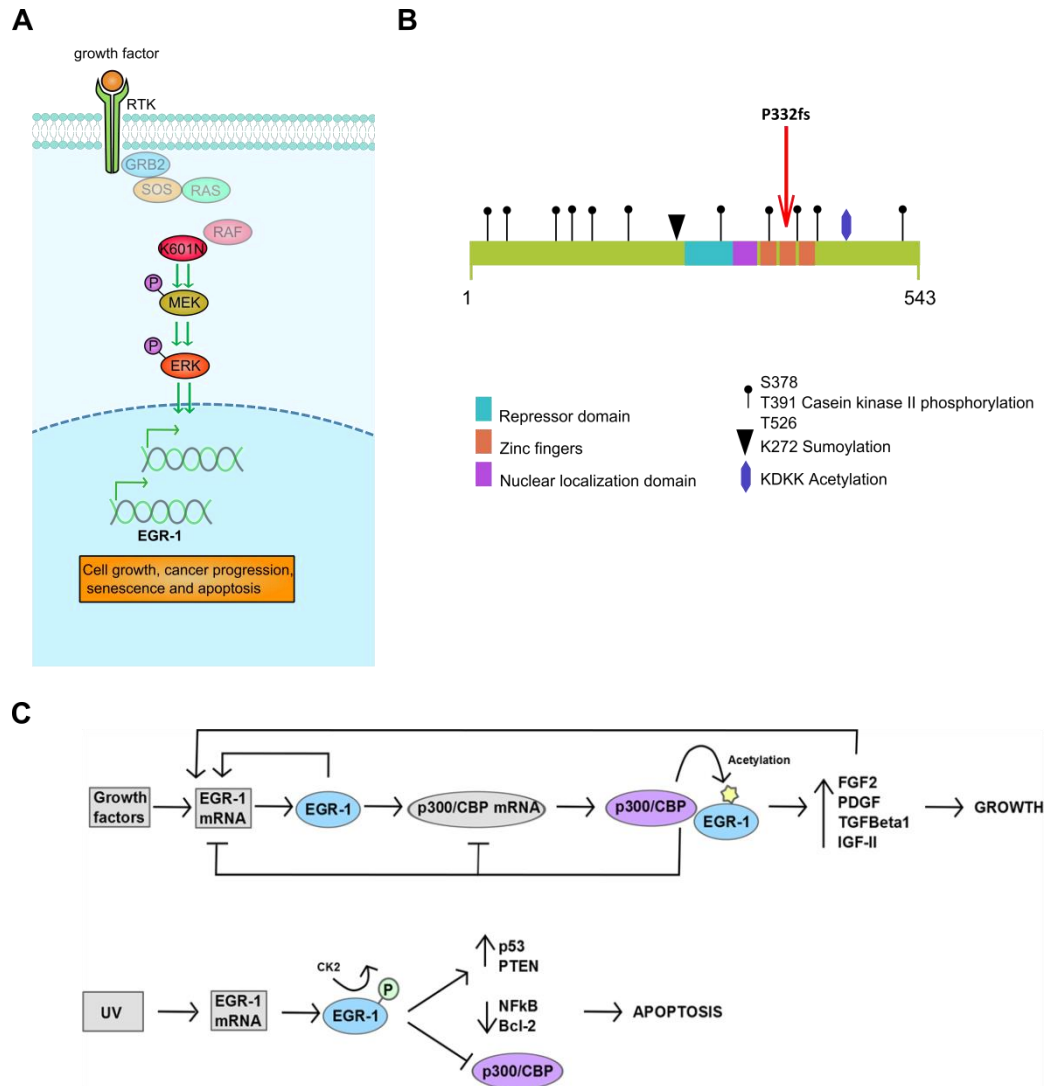
**Figure 17. EGR-1 in MAPK pathway.** A. scheme of MAPK pathway. Active mutant BRAF K601N promotes activation of downstream players of MAPK pathway including the transcription factor EGR-1. B. Scheme of EGR-1 protein, it contains a repressor domain. It has a nuclear localization domain followed by three zinc finger that bind to DNA. EGR-1 has diverse posttranslational modifications sites such as phosphorylation, sumoylation and acetylation sites. C. The overall effect of this transcription factor is mainly determined by posttranslational modifications. Acetylation of EGR-1 by p300/CBP leads to cell growth, while phosphorylation by CSKII promotes apoptosis. Red arrow indicates indel 994dupC p.P332fs in U266R cells[133].Copyright 2017 by Molecular Cell. Modified and reprinted with permission

To explore EGR-1 expression under dabrafenib, cells were treated for 24h with increasing concentrations of the inhibitor followed by nuclear and cytoplasmic fractionation. Overexpression of wild type protein is observed in the nucleus in the resistant clone, along with expression of a truncated protein in nucleus and cytoplasm and both cell lines respond to the highest concentrations in comparison to parental cells (Figure 19A). To identify what occurred first during the development of this model, EGR-1 mutation or hyperdiploidy, samples from previous time points (2-3 months (R1 and R3, respectively) vs. 6 months (R6) under dabrafenib treatment) were studied by interphase FISH (5q31_5q33_6cen R1 with 90.85% positive tetraploid cells and 9-18% CIN and R3 with 77.98% positive tetraploid cells and 21-25% CIN) and by immunoblot (EGR-1 overexpression, and expression of EGR-1 truncated), and both abnormalities were detected in the earliest steps of U266R development (data not shown).

Further characterization of the aberrant EGR-1 expression in U266R was performed by treatment with actinomycin D, a transcription inhibitor and cycloheximide, a translation inhibitor, to distinguish the effect of these drugs on transcript levels and protein stability between wild type EGR-1 and truncated EGR-1. Downregulation of both wild type and the mutant EGR-1 was observed, therefore its overexpression is transcriptionally regulated (Figure 19 B and 19C). Moreover, near-tetraploid U266 cells, generated by inhibiton of cytokinesis, showed an increased expression of this protein but not in the controls, suggesting that overexpression of EGR-1 in U266R could be caused by a gene-dosage effect (Figure 16D).

In order to elucidate if the aberrant expression of EGR-1 could confer resistance to dabrafenib, U266 cells were transduced with a lentiviral IRES GFP$_{nuc}$ vector to overexpress either wild type EGR-1 or truncated EGR-1. To analyze gene of interest expression, immunofluorescence microscopy and immunoblots were performed (Figure 20A and 20B). We observed differences in protein

localization, overexpressing EGR-1 wild type protein was co-localized in the nucleus, and however, truncated EGR-1 protein was mainly localized in the cytoplasm. This is likely to occur due to the loss of the zinc fingers so in consequence the protein cannot bind to DNA and its function as a transcription factor is abrogated. Of note, growth curves of transduced cells were similar to non-transduced U266 cells (Figure 20C). Another consideration is the loss of posttranslational modifications such as phosphorylation at the C-terminus and acetylation which play a main role in the direction of the effect of this protein.

It has been described in previous studies that EGR-1 can bind to p300/CBP, which acetylates the protein and promotes the transcription of growth-related factors such as FGF2, PDGFA, TGF- β and IGF-2. In contrast, when the protein is only phosphorylated it can promote the expression of factors associated with apoptosis like p53, PTEN, NF-κβ and BCL-2 [100].

To test if ectopic EGR-1 expression in U266 parental cells contributes to dabrafenib resistance, drug response curves of transiently transduced U266 cells (FACS-sorted to > 95% purity) showed increased BRAFi resistance in cells overexpressing wild type EGR-1. Strikingly, nearly complete resistance was observed in cells expressing truncated EGR-1 (Figure 20D).

To know if this is an exclusive mechanism of resistance for cells with BRAF K601N, preliminary experiments in A375 melanoma cell line carrying BRAF V600E transfected with EGR-1 wild type or mutant showed no difference in viability when cells were under dabrafenib (data not shown), therefore the interplay between mutation BRAF K601N and aberrant EGR-1 has to be elucidated.
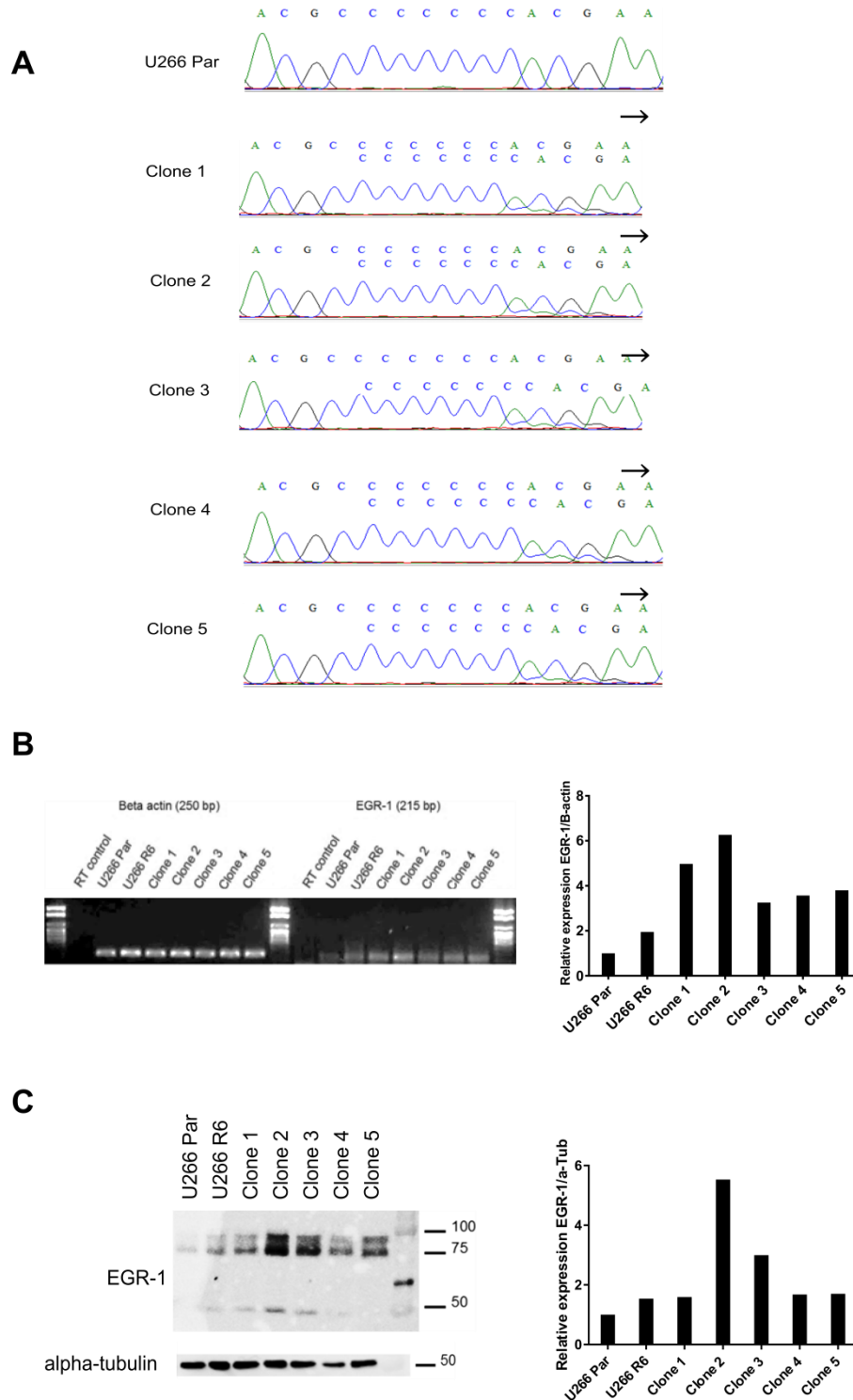
**Figure 18. Identification and analysis of indel EGR-1 found in U266 resistant clones.** A. Sanger sequencing of U266R confirmed indel c.994dupC in gene EGR-1. As is observed in the chromatograms, the frameshift is present in the resistant clones but not in the parental U266 non-treated cells. B. RT-PCR and C. western blot of EGR-1 expression in U266R.
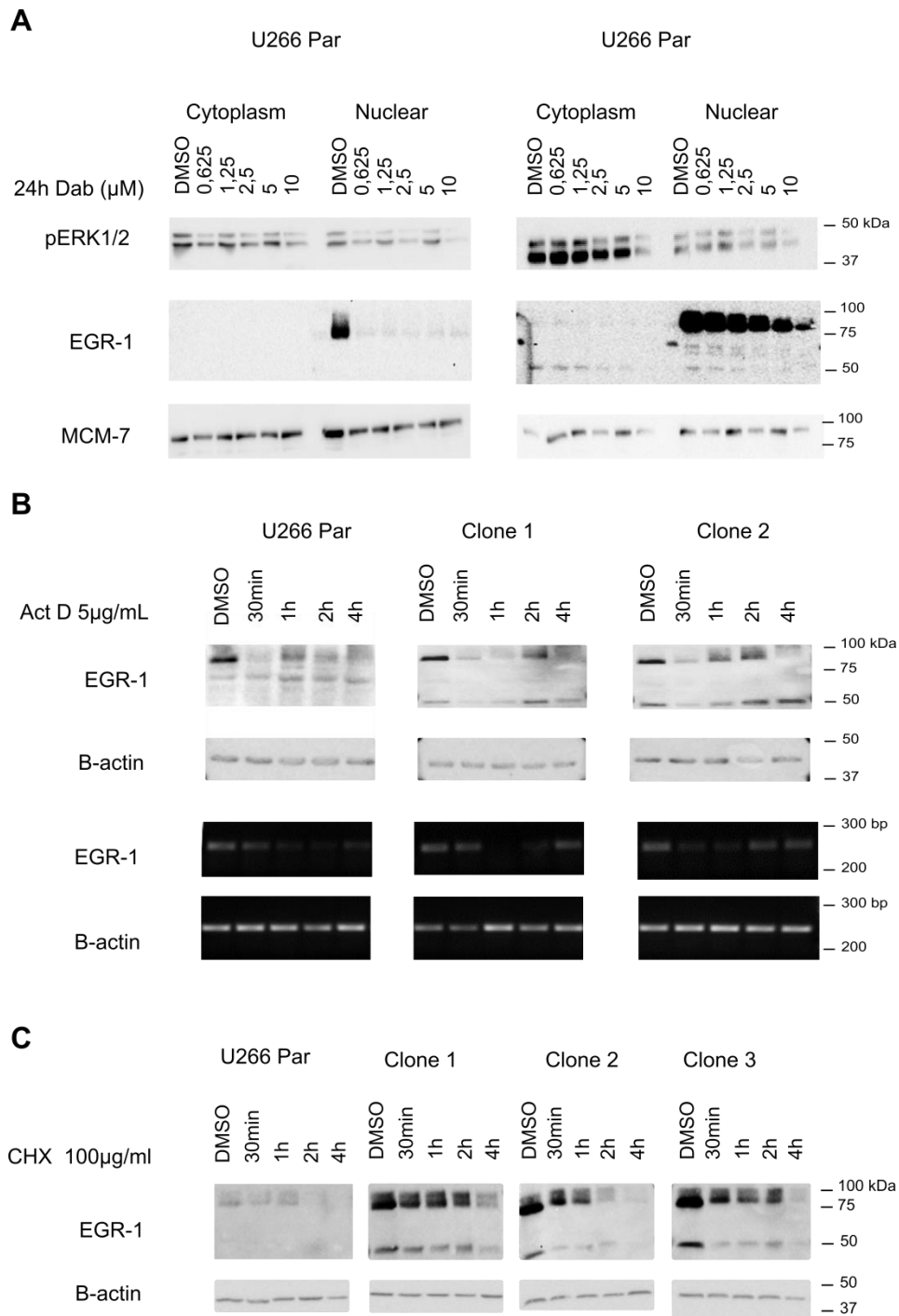
**Figure 19. Characterization of EGR-1 expression in U266R cells.** A. Immunoblot of nuclear and cytoplasmic fractions of U266 parental cells and a resistant clone treated with increasing concentrations of dabrafenib for 24h. Overexpression of EGR-1 wild type in U266R is mainly found in the nucleus while mutant protein is also found in cytoplasm. Higher ERK1/2 phosphorylation is observed in resistant clone. B. Immunoblot (up) and RT-PCR (down) of time course of U266R cells treated with 5μg/ml actinomycin. Decreased expression of EGR-1 is observed at 30min in all samples. C. Western blot of EGR-1 expression in U266R under a time course with 100μg/ml cycloheximide. Downregulation of EGR-1 expression is observed at 2h across samples.
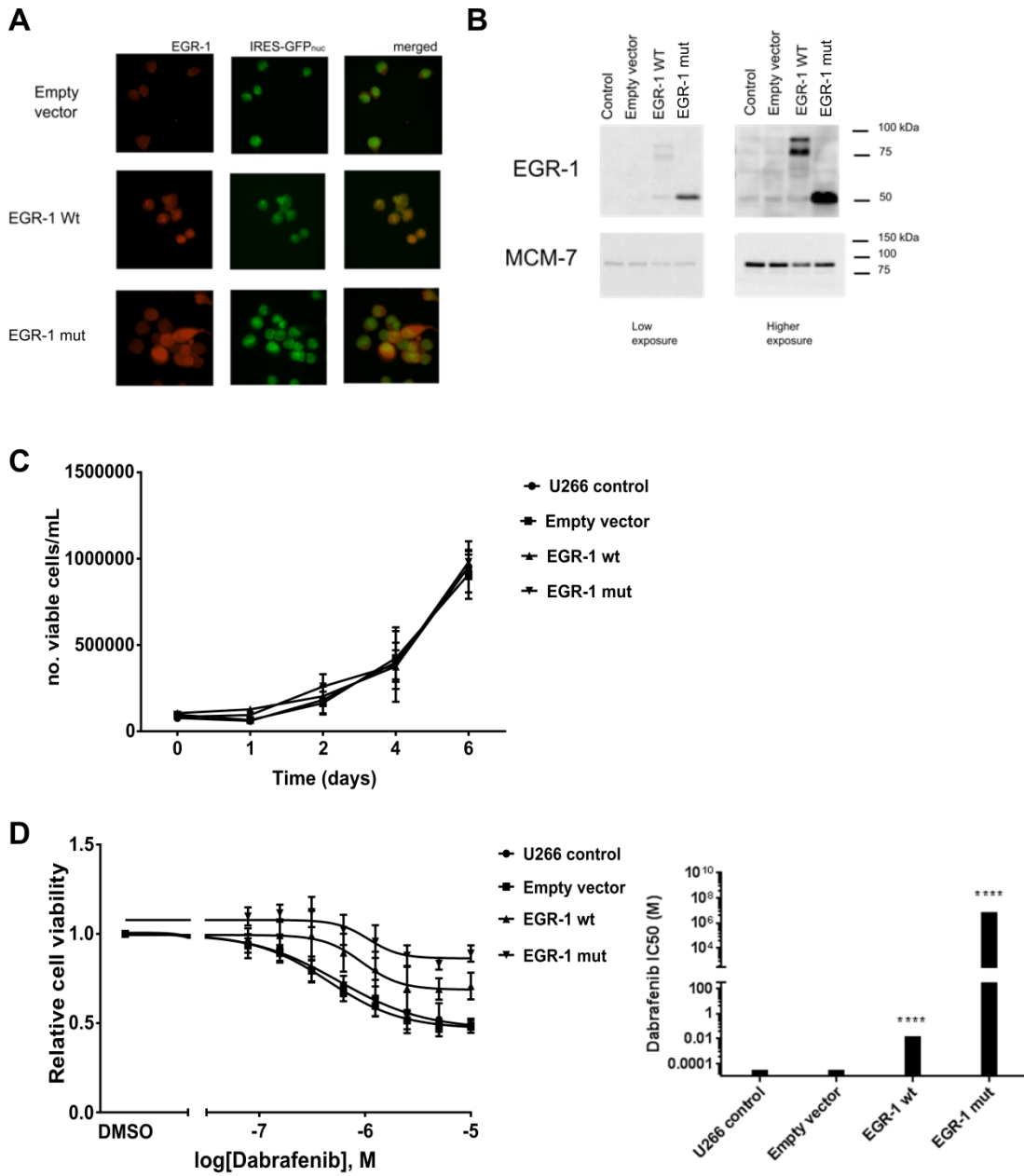
**Figure 20. EGR-1 overexpressed in U266 cells.** A. Immunofluorescence of lentiviral transduced U266 cells with EGR-1 IRES GFPnuc vector. B Western blot of U266 overexpressing EGR-1 wild type or mutant. C. Growth curve of U266 EGR-1 showed no difference in comparison to controls. D. Drug response curves of U266 EGR-1 under Dabrafenib for 72h and IC50 showed significant differences in cells overexpressing EGR-1 wild type and EGR-1 mutant in contrast to controls.

# 5

---

# Conclusions and Discussion

## BRAF mutations in multiple myeloma

BRAF mutations are found in a variety of solid and hematological tumors. These aberrations occur more frequently in the activation domain of this kinase conferring hyperactivation of the MAPK/ERK pathway which triggers cell proliferation, differentiation and survival.

Recurrent aberrations in BRAF have been described mainly in hairy cell leukemia, melanoma, and thyroid cancer, among other malignancies, which has allowed for the development of successful targeted therapies. However, rapid drug resistance can develop, and a high number of resistance mechanisms have been discovered. Therefore, it is important to overcome this resistance with new therapeutic strategies.

Recently, activating BRAF mutations have been reported in multiple myeloma patients while the functional characterization of these mutations in this disease remains elusive.

The work presented here demonstrates the potential biological impact of BRAF V600E mutation and a novel BRAF inhibitor resistance mechanism in multiple myeloma.

## BRAF V600E in OPM-2 multiple myeloma cells

In this study, an *in vitro* model conditionally expressing BRAF wild type or BRAF V600E was developed and used to subsequently investigate the influence of this aberration on the biology of myeloma cells.

Previous studies have shown that constitutive activation of the MAPK/ERK pathway in immortalized human fibroblasts harboring the BRAF V600E mutation can induce either cell cycle progression or cell cycle arrest in the G1 or G2-M phases depending on expression of tumor suppressors such as p19[ARF] or p16[INK4a] which hinder the activity of cyclin-dependent kinases (CDKs), thereby preventing DNA replication. For example, silencing a tumor suppressor by using p16INK4a shRNA, in the same cells abolished cell cycle arrest and increased cell proliferation [101,102].

In melanoma, the mutated kinase is associated with proliferative advantages and cellular differentiation.  What is more, in 50% of melanoma cases, present loss of function of p16INK4a and ARF genes.[103] *In vitro* melanoma studies abrogating the function of the tumor suppressors p53, RB and ARF, resulted in unlimited cell proliferation and oncogenic transformation[102].

However, in a conditional BRAF V600E model in rat thyroid PCCL3 cells, expression of the mutant kinase leads to increased DNA synthesis, chromosomal instability, dedifferentiation, and apoptosis [104].

Oncogenic stress can be caused hyperactivation of the MAPK/ERK pathway due to an activating BRAF mutation which could lead to hyper-replication, causing replication factor exhaustions; fork stalling/collapse and triggering DNA damage, promoting growth arrest.

The MAPK/ERK pathway also plays a role in DNA damage response (DDR) by facilitating DNA repair through the regulation of ataxia-telangiectasia mutated (ATM) and Rad3-related kinase (ATR)[105]. Furthermore, it has been

demonstrated that low levels of DNA strand breakings (DSBs) increased ERK and AKT phosphorylation through the ATM-AKT-ERK path as a pro-survival signaling. However, the pro survival signaling is overridden in case of excessive DNA damage due to the triggering of ATM-independent phosphatases that inhibit ERK signaling [106,107].

In multiple myeloma, our conditional model of overexpression of BRAF V600E resulted in a highly active MAPK/ERK pathway, however, changes in either proliferation or senescence were not observed in comparison to controls. The most likely explanation for this lack of phenotype is that we introduced the BRAF mutation as secondary event in late stage MM cells, i.e. a MM cell line, already depend on other oncogenic mechanisms and have already acquired mechanisms to overcome checkpoints against malignant transformation.

The OPM-2 cell line used here, for example, has a p53 mutant (R175H) protein which abolishes the wild type tumor suppression function of this protein [108].  In addition, OPM-2 has a CDKN2A mutation (H83Y) which leads to reduced ability to promote cell cycle arrest [109]. Both of these proteins are main regulators of the cell cycle progression, hence if there is an oncogenic insult without sustained p53/Rb activation cBRAF (c: conditional BRAF expression) V600E OPM-2 cells may not be able to undergo growth arrest and are likely to escape from senescence.

This would be in line with our results showing diverse simultaneous activations of DNA repair pathways by overexpression of BRAF V600E. Of note, no mutations of participating molecules in DNA repair pathways are present in OPM-2 cells. In consequence, it is possible that cBRAF V600E induced DNA damage can be solved by the DNA repair machinery in OPM-2 cells.

The mutational background of the OPM-2 cells may also compensate pro-apoptotic signals related to stress by DNA damage through different means. For

example, PTEN loss present in OPM-2 contributes to apoptosis resistance since it is a direct regulator of the PI3K/Akt pathway, which mediates survival in cancer cells [110]. Furthermore, OPM-2 harbors mutant FGFR3 K650, which confers activation of this receptor being associated with activation of the MAPK/ERK pathway likely contributing to OPM-2 cell proliferation [111,112].

## Dabrafenib resistance in multiple myeloma

Currently, targeted therapy with BRAF inhibitors such as vemurafenib and dabrafenib are first line treatments for several mutant BRAF cancers. Nevertheless, drug resistance in BRAF inhibitors-treated patients frequently developed within the first year of treatment. Understanding the mechanisms of resistance is critical for the development of better therapeutic strategies. Frequently single BRAF inhibitor treatment resistant mechanisms include continuous MAPK/ERK pathway activation[65,72,81,83,113].

The activating BRAF K601N/E is a mutation found in melanoma, colorectal cancer, bladder cancer, prostate cancer, lung adenocarcinoma among others types of cancer [96,114]. In contrast to BRAF V600E there is only very limited data on resistance mechanisms of BRAF K601N/E positive cells after initial response to dabrafenib.

We developed an *in vitro* model of resistance using the U266 MM cell line, which harbors BRAF K601N, by long-term culture under increasing concentrations of dabrafenib, followed by limiting dilution single cell seeding to generate the U266R stable resistant clones. In this work, U266R was established as an *in vitro* dabrafenib resistant model was established and was characterized by whole exome sequencing, cytogenetics, and proteomics.

Within the abnormalities detected in U266R by whole exome sequencing diverse mutations including single nucleotide variants, frameshift insertions, frameshift

deletions and structural and numerical aberrations like copy number variations and tetraploidy were found in this model.

## Tetraploidy in U266R

In all clones of U266R a high degree of tetraploidy was observed by interphase FISH and metaphase FISH. Tetraploidy occurs when there is a mitotic arrest, e.g. in absence of microtubules, resulting in failed cell division. Why the U266R cells developed a near-tetraploid karyotype is unclear.

Next generation sequencing confirmed a common polymorphism in TP53, P72R, in U266 cells, which is reported to affect the G1 arrest gene function which may explain why U266R polyploid cells progressed through the cell cycle and proliferated [115,116].

On the other side, hyperdiploidy is frequently reported in multiple myeloma, and is a relevant prognostic factor for the risk stratification of this disease and accounts for up to 50% of MM patients [117]. Moreover, the U266 cell line intrinsically carries a small near-tetraploid population of cells (4-8%), which by clonal evolution may have been enriched by the BRAFi treatment. Polyploidy could provide diverse cancer advantages like chromosomal instability (CIN) that leads to further evolution of the malignancy, and it has been described that tetraploid cells can overcome oncogene-induced senescence by overexpressing DNA repair genes to reduce DNA damage response and have epigenetic modifications to silence p53[118–120]. . To know if this karyotype contributed to the resistant phenotype of U266R cells, naïve U266 cells were induced for tetraploidy with a cytokinesis inhibitor, and treated with dabrafenib. Similar cell viability was observed in tetraploid generated U266 and control cells. Therefore tetraploidy alone did not trigger BRAFi resistance in our model of BRAF mutant multiple myeloma.

## EGR-1 drives resistance to BRAF inhibition in multiple myeloma

Whole exome sequencing to our dabrafenib resistance model U266R led to the identification of aberrant EGR-1 expression in U266R since it overexpresses EGR-1 wild type and truncated EGR-1 (frameshift insertion 994dupC). We could show that this aberrant expression is transcriptionally regulated and overexpression of both protein variants confers dabrafenib resistance to a different degree in multiple myeloma. Noteworthy, EGR-1 is a transcription factor regulated by MAPK/ERK signaling that promotes the expression of factors such as EGF-R ligands resulting in a positive feedback loop within the same signaling pathway.

Interestingly, upregulation of JUN has been shown to be associated with BRAFi resistance[121,122]. One of the target genes of JUN is EGR-1, that in turn upregulates JunB. Some of the targets of JunB include EGF ligands, TNF, CACNA2D3 and STK36. The last two genes were also found to be mutated in WES and validated by Sanger sequencing in U266R (data not shown).

Moreover, EGR-1 overexpression has been reported in prostate cancer where this transcription factor triggers the expression of different targets like IGF-II, PDGF-A and TGF-β leading autocrine cell growth [123]. In melanoma, it has been reported that mutant BRAF activated ERK1/2 leading to EGR-1 overexpression which stimulates the synthesis of fibronectin promoting tumor cell invasion [124]. Recent studies in multiple myeloma identified new frequent gene mutations in EGR-1 including missense mutations[125]. While EGR-1 knockdown in this disease has been associated with bortezomib resistance, this study showed for the first time that EGR-1 overexpression confers dabrafenib resistance in BRAF-driven multiple myeloma.

Diverse posttranslational modifications occur in EGR-1 such as acetylation at the KDKK site by p300/CBP which stabilizes EGR-1 and promotes cell survival. This

protein has few characterized phosphorylation sites. These include S378, T391, and T526, which are phosphorylated by casein kinase II as a stress response favoring cell death. It has been described that p19ARF sumoylates EGR-1 at site K272 and promotes its nuclear translocation. In addition, EGR-1 is ubiquitinated and degraded in the proteasome (Figure 17C) [97, 98,100,101].

The truncated EGR-1 protein in our model loses the zinc fingers and diverse sites for posttranslational modifications that may affect the interaction of this transcription factor to DNA and probably to other protein partners.

A high number of transcription factors are proteins with intrinsically disordered (ID) regions/domains (i.e. not well defined secondary/tertiary structures) which are important for their biological function. The ID sequences are flexible and allow protein-protein and protein-DNA interactions, often accompanied by conformational changes of both, proteins and DNA. The ID regions can be a platform for macromolecular interactions, allowing the cooperation between transcription factors and other coregulatory proteins modifying the chromatin to allow an efficient and selective gene regulation. The case of unbound (free) forms of transcriptions factors with ID regions is poorly studied, but it is likely that the scaffold property is still present [126].

Protein sequence analysis of both EGR-1 wild-type and truncated showed a shared identity of 89.04% (Figure 21A). Analysis of intrinsically unstructured proteins predicts that EGR-1 is a disordered protein along its entire length with a disorder tendency of 0.602 in average (max. 1), this means that in its native unbound state it does not have a well-defined tertiary structure. An advantage of this scenario is that EGR-1 can interact specifically its corresponding interaction partners (Supplementary Fig. 22) and rapidly without excessive binding strength [127,128]. Moreover, unstructured proteins can be flexible linkers suggesting that EGR-1, when unbound to DNA, may work as a scaffold protein. Interestingly, truncated EGR-1 shows higher disorder tendency of 0.685 than the

whole protein length (Figure 21 B). The lack of the zinc fingers of the truncated EGR-1 impede DNA binding, thereby abrogating the conformational changes associated to this interaction and likely leaving the scaffold capacity intact, which may favor the association with other proteins triggering certain cell responses, such as dabrafenib resistance. In contrast EGR-1 wild type retains its DNA-binding capability. However, the excess of EGR-1 wild type protein detected in our U266R model, may also work as a scaffold protein. And therefore possibly explain why also EGR-1 wild type, when overexpressed, confers some resistance to dabrafenib, while the truncated version of EGR-1, losing its DNA-binding capacity, confers even a higher degree of resistance.

Some of the predicted protein partners which may interact with motifs of EGR-1 include GRB2, STAT3, STAT5, TRAF2, TRAF6, CK1, GSK3, NEK2, PKA and SUMO[129]. Although further studies are necessary to fully understand the precise role of EGR-1 (wild type and truncated) in the context of dabrafenib resistance, this is a first approach to explain the complexity of this transcription factor and functional protein association networks.

Furthermore, this is the first study to show that EGR-1 aberrant expression is a BRAFi resistance mechanism in multiple myeloma. Understanding diverse BRAFi resistance mechanisms will lead to new therapeutic approaches.

Strategies to overcome BRAFi resistance include the use pan-RAF-inhibitors which block all RAF isoforms, a combination of BRAF inhibitors with downstream MAPK inhibitors or combinatorial therapy targeting several cell pathways like PI3K/Akt pathway. Another approach to improve patient outcomes is intermittent BRAFi administration[50,54,67,84,130].

**A**



**B**



**Figure 21. Bioinformatic analysis of EGR-1 wild type and EGR-1 mutant.**
A. Multiple-Sequence Alignment of EGR-1 wild type and EGR-1 mutant (indel 994dupC) protein sequences by CLUSTAL MUSCLE (3.8) Asterisks show identical amino acids. Colons and semi-colons display conserved substitutions and semi-conserved substitutions, respectively [134]. B. IUPRED predictions (Long disorder) of intrinsic disorder (ID) for EGR-1 wild type and EGR-1 mutant (indel 994dupC). Values above 0.5 are considered disordered[127,128].

# 6

---

# Outlook

## BRAF V600E

The present work demonstrates that conditional BRAF V600E expression in OPM-2 cells leads to differentially expressed genes and proteins mainly associated with DNA repair mechanisms. Although, the MAPK/ERK pathway was highly activated by this mutation neither a proliferative nor a senescent phenotype was observed in this model. DNA damage has been associated with this aberration in other cancers. However, further validation should be conducted for this disease. On the other side, this model has contributed to further knowledge about this heterogeneous disease and gives a tool to investigate rational therapy approaches. Following this, two BRAF inhibitors showed the paradoxical effect on BRAF wild type in MM cells and how MEK inhibition can abolish the activation of the pathway, which is consistent with previous studies in other types of cancer. Further studies are necessary to fully describe the effect of this mutation in multiple myeloma. Physiologic BRAF V600E models are necessary since there is a lack of MM cell lines carrying this mutation. Different approaches could be followed for this end either by genetic manipulation of MM cell lines or by successful establishment of primary cell lines carrying the BRAF V600E mutation.

## EGR-1 aberrant expression

Overexpression of EGR-1 has been associated with tumor progression and tumor cell invasion in diverse types of cancer. Moreover, EGR-1 mutant (p.332fs) and wild type overexpression lead to dabrafenib resistance in multiple myeloma which is a new BRAFi resistance mechanism. Although an extensive characterization was performed for our U266R model, additional follow-up studies are important to support our findings. Furthermore, the detailed mechanistic role of EGR-1 in a BRAF K601N mutation context needs to be clarified.

A challenge is the lack of BRAF mutant multiple myeloma cell lines. However, there is another BRAF K601N cell line in public depositories, JVM-3, which can be transduced with EGR-1 (wild type and mutant) and tested for dabrafenib resistance. Another point to consider is that BRAF K601N only moderately activates the MAPK/ERK pathway in comparison to BRAF V600E For this reason our group is collaborating to do an *in silico* modeling of the mutant protein to predict how interacts with BRAFi.

Moreover, we examined if the resistance was also found in BRAF V600E and truncated EGR-1 carrying cells, but preliminary data in A375 melanoma cell line showed that is not the case, nevertheless to be certain, additional experiments should be conducted in diverse cell lines under similar conditions. An alternative would be to introduce both mutations to recreate the same conditions and test for drug resistance.

Regarding the study of EGR-1 properties as a disordered and scaffold protein, the first step would be to do bioinformatics analysis to identify EGR-1 critical amino acids residues for the interaction with other proteins and modeling *in silico* of native and truncated EGR-1 to predict the dynamics and biochemical nature of this transcription factor. Another way to characterize ID proteins states is the use of nuclear magnetic resonance. Followed by the analysis of

intracellular protein-protein interactions (co-immunoprecipitation, pull-down assay) and the identification of possible EGR-1 binding proteins by MALDI-QIT/TOF MS. To validate these results, the generation of mutant EGR-1 (native and truncated) lacking the ability to interact with a possible interaction partners could be performed.

This is one of the first studies of BRAF inhibitor resistance mechanisms in multiple myeloma. Discovering a new resistance mechanism such as EGR-1 wildtype overexpression and, even more potent, truncated EGR-1 in a BRAF K601N context allows us to understand more about the biological complexity of this disease and opens an opportunity to design new and better therapeutic approaches.

# 7

# Index

## List of figures

## List of tables

## List of abbreviations

| | |
|---|---|
| AKT | Protein Kinase B |
| ATF3 | Activating Transcription Factor 3 |
| ATF4 | Activating Transcription Factor 4 |
| ATM | Ataxia-Telangiectasia Mutated |
| ATP | Adenosine Triphosphate |
| ATR | Rad3-Related Kinase |
| BRAF | The V-Raf Murine Sarcoma Viral Oncogene Homolog B |
| BRAFi | BRAF Inhibitors |
| CACNA2D3 | Calcium Channel, Voltage-Dependent, Alpha 2/Delta Subunit 3 |
| cBRAF | Conditional BRAF expression |
| CCND1 | Cyclin D1 |
| CCND3 | Cyclin D3 |
| cdk-2 | Cyclin-Dependent Kinase 2 |
| cDNA | Complementary Deoxyribonucleic Acid |
| c-Fos | Fbj Murine Osteosarcoma Viral Oncogene Homolog |
| CIN | Chromosomal Instability |
| c-Myc | V-Myc Avian Myelocytomatosis Viral Oncogene Homolog |
| CNV | Copy Number Variation |
| CR1 | Conserved Region 1 |
| CR2 | Conserved Region 2 |
| CR3 | Conserved Region 3 |
| CREB | Camp Responsive Element Binding Protein |
| cuSCC | Cutaneous Squamous Cell Carcinoma |
| DAG | Diacylglycerol |
| DAVID | Database For Annotation, Visualization And Integrated Discovery |
| DDR | DNA Damage Response |
| DMSO | Dimethyl Sulfoxide |

| | |
|---|---|
| DNM1L | Dynamin 1-Like |
| Dox | Doxycycline Hydrochloride |
| DSBs | DNA Strand Breakings |
| DUSP | Dual-Specificity Phosphatases |
| ECL | Enhanced Chemo-Luminescence |
| ECM | Extracellular Matrix |
| EDTA | Ethylenediaminetetraacetic Acid |
| EGFR | Epidermal Growth Factor Receptor |
| Egr-1 | Early Growth Response 1 |
| Elk-1 | Ets Transcription Factor |
| ER | Endoplasmic Reticulum |
| ERCC1 | Excision Repair Cross-Complementing 1 |
| ERK | Extracellular Signal-Regulated Kinase  ERK1 And ERK2 |
| Ets-1 | Ets Proto-Oncogene 1, Transcription Factor |
| FAM46C | Family With Sequence Similarity 46, Member C |
| FCS | Fetal Calf Serum |
| FGFR | Fibroblast Growth Factor Receptor |
| FGFR3 | Fibroblast Growth Factor Receptor 3 |
| FISH | Fluorescence In Situ Hybridization |
| GEP | Gene Expression Profiling |
| GIN | Genomic Instability |
| GRB2 | Growth Factor Receptor Bound Protein 2 |
| GTP | Guanosine Triphosphate |
| HFG | Hepatocyte Growth Factor |
| HRP | Horseradish Peroxidase |
| IC50 | Half Maximal Inhibitory Concentration |
| IGF-1 | Insulin-Like Growth Factor-1 |
| IgG | Immunglobulin G |
| IL-21 | Interleukin-21 |

| | |
|---|---|
| IL-6 | Interleukin-6 |
| Indels | Insertions And Deletions |
| IPA | Ingenuity Pathway Analysis Software |
| IRES | Internal ribosome entry site |
| IU | International Units |
| KA | Keratoacanthomas |
| KRAS | Kirsten Rat Sarcoma Viral Oncogene Homolog |
| LC-MS/MS | Liquid chromatography–mass spectrometry |
| MAPK | Mitogen-Activated Protein Kinases |
| MEK | Dual Specificity Mitogen-Activated Protein Kinase Kinase |
| MEKi | MEK Inhibitor |
| MGUS | Monoclonal Gammopathy Of Undetermined Significance |
| MH2 | The Avian Retrovirus Mill Hill 2 |
| MKPs | MAP Kinase Phosphatases |
| MLL | Myeloid/Lymphoid Or Mixed-Lineage Leukemia 1 |
| MM | Multiple Myeloma |
| MMSET | Multiple Myeloma SET Domain |
| MSV | Murine Sarcoma Virus 3611 |
| MUT | Mutant |
| MYC | V-Myc Avian Myelocytomatosis Viral Oncogene Homolog |
| NES | Nuclear Export Sequence |
| NRAS | Neuroblastoma Ras Viral Oncogene Homolog |
| NRR | Negative Regulatory Region |
| p8 | Nuclear Transcriptional Regulator Protein 1 |
| PARP1 | Poly(ADP-Ribose)-Polymerase 1 |
| PB04 | Paradox Breaker 04 |
| PBS | Phosphate Buffered Saline |
| PBS-T | Phosphate Buffered Saline - Triton |
| PCR | Polymerase Chain Reaction |

| | |
|---|---|
| PDGF-R | Platelet-Derived Growth Factor Receptors |
| Pen/Strep | Penicillin/Streptomycin |
| PFS | Progression-Free Survival |
| PI | Propidium Iodide |
| PI3K | Phosphoinositide 3-Kinase |
| PTEN | Phosphatase And Tensin Homolog |
| Puma | Bcl2 Binding Component 3 |
| RAF | Rapidly Accelerated Fibrosarcomas |
| Rb | Retinoblastoma Protein |
| RBD | Ras-Binding Domain |
| RNA | Ribonucleic Acid |
| RTK | Receptor Tyrosine Kinases |
| SDF-1 | Stromal Cell Derived Factor-1 |
| SDS-PAGE | Sodium-Dodecyl-Sulfate Polyacrylamide Gel Electrophoresis |
| SHC | Src Homology 2 Domain Containing) Transforming Protein 1 |
| SILAC | Stable Isotope Labeling With Amino Acids |
| SNVs | Single Nucleotide Variants |
| SOS | Ras/Rac Guanine Nucleotide Exchange Factor 1 |
| SP1 | Sp1 Transcription Factor |
| Spry | Sprouty Proteins |
| Spry2 | Sprouty2 |
| SRF | Serum Response Factor |
| Stat-1/3 | Signal Transducer And Activator Of Transcription 1/3 |
| STK36 | Serine/Threonine Kinase 36 |
| Tet | Tetracycline Hydrochloride |
| TNF | Tumor Necrosis Factor |
| TNFα | Tumor Necrosis Factor-A |
| TP53 | Tumor Protein P53 |
| TRB3 | Tribbles Pseudokinase 3 |

| | |
|---|---|
| UV | Ultraviolet Light |
| VEGF | Vascular Endothelial Growth Factor |
| WES | Whole Exome Sequencing |
| WT | Wild type |
| XRCC1 | X-Ray Cross-Complementing 1 |

# 8

## Supplementary information
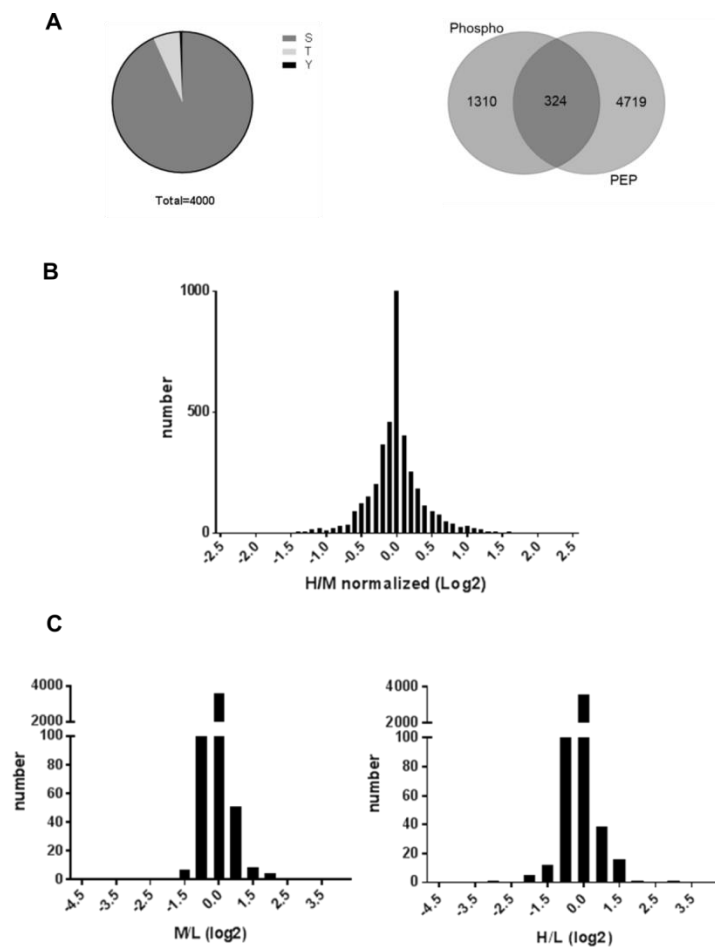


**Figure 21 Protein expression profiling and phosphoproteome of SILAC cBRAF OPM-2**
A. Abundance of phosphorylated aminoacids Serine (S), Threonin (T) and Tyrosine (Y) from phosphoproteome of cBRAF OPM-2cells. B. Distribution of normalized protein expression of cBRAF V600E cells (H) vs. cBRAF wt (M), it follows a normal distribution. C. Distribution of protein expression left, cBRAF wt (M) vs. OPM-2 (L) skewed to the right and right cBRAF mut (H) vs. OPM-2 (L).

**Table 21.Whole exome sequencing single nucleotides variants (SNVs).**

| Gene | Chromosome | Position (bp) | RefSeq | Nucleotide change (bp) | Aminoacid change | Tumor Variant Frequency (TVF) |
|---|---|---|---|---|---|---|
| AAMDC | 11 | 77583291 | NM_024684 | c.C299A | .A100E | 0.1 |
| AKAP3 | 12 | 4736483 | NM_001278309 | c.G1585C | p.V529L | 0.16 |
| AMZ1 | 7 | 2742434 | NM_001284355 | c.G383A | p.R128H | 0.33 |
| ANKMY2 | 7 | 16664685 | NM_020319 | c.T293G | p.V98G | 0.07 |
| ANTXR2 | 4 | 80906014 | NM_001145794 | c.A1045G | p.I349V | 0.38 |
| ANXA1 | 9 | 75777742 | NM_000700 | c.G520A | p.G174R | 0.25 |
| AP1M1 | 19 | 16344329 | NM_001130524 | c.C1109T | p.A370V | 0.22 |
| APBB1 | 11 | 6417099 | NM_145689 | c.G1876A | p.G626S | 0.14 |
| ARMC6 | 19 | 19153596 | NM_001199196 | c.T106G | p.F36V | 0.05 |
| ARSI | 5 | 149676805 | NM_001012301 | c.A1682G | p.N561S | 0.23 |
| ASH1L | 1 | 155451994 | NM_018489 | c.C667G | p.L223V | 0.13 |
| ATG2A | 11 | 64681941 | NM_015104 | c.C203T | p.S68L | 0.14 |
| BCL11A | 2 | 60687763 | NM_022893 | c.A2284T | p.R762X | 0.08 |
| C11orf49 | 11 | 47008832 | NM_001003678 | c.A120C | p.Q40H | 0.2 |
| CCDC141 | 2 | 179702171 | NM_173648 | c.G3775C | p.G1259R | 0.19 |
| CDKL5 | X | 18622565 | NM_003159 | c.A1521T | p.Q507H | 0.43 |
| CELSR2 | 1 | 109807612 | NM_001408 | c.G5587T | p.G1863W | 0.34 |
| CFAP53 | 18 | 47788439 | NM_145020 | c.A220G | p.I74V | 0.28 |
| CNOT3 | 19 | 54647480 | NM_014516 | c.G253C | p.E85Q | 0.1 |
| CNTN2 | 1 | 205034929 | NM_005076 | c.G1708T | p.G570W | 0.24 |
| CR1 | 1 | 207760836 | NM_000651 | c.G5636A | p.G1879E | 0.06 |
| CTRL | 16 | 67963859 | NM_001907 | c.A773T | p.N258I | 0.26 |
| CYP2C8 | 10 | 96827432 | NM_000770 | c.G185T | p.G62V | 0.2 |
| DNHD1 | 11 | 6555133 | NM_144666 | c.G2728T | p.D910Y | 0.07 |
| DNMT1 | 19 | 10246816 | NM_001379 | c.C4589A | p.P1530H | 0.2 |
| DOCK1 | 10 | 129202616 | NM_001380 | c.A3982C | p.I1328L | 0.13 |
| DOCK10 | 2 | 225688253 | NM_014689 | c.A3148G | p.R1050G | 0.26 |
| EIF1B | 3 | 40353004 | NM_005875 | c.G239A | p.G80E | 0.12 |
| EPB41L5 | 2 | 120918480 | NM_020909 | c.T1817A | p.V606E | 0.15 |
| ETV4 | 17 | 41622711 | NM_001079675 | c.C85A | p.R29S | 0.2 |

| FAAH | 1 | 46871718 | NM_001441 | c.G794T | p.G265V | 0.11 |
|---|---|---|---|---|---|---|
| FAM114A1 | 4 | 38910315 | NM_138389 | c.A760G | p.T254A | 0.15 |
| FAM20A | 17 | 66596777 | NM_017565 | c.A31G | p.T11A | 0.26 |
| FMO2 | 1 | 171168615 | | | | 0.1 |
| FOSB | 19 | 45973903 | NM_001114171 | c.G143A | p.G48E | 0.22 |
| GDA | 9 | 74838058 | NM_001242507 | c.T407C | p.V136A | 0.27 |
| GRIA2 | 4 | 158255211 | NM_000826 | c.T1205C | p.L402P | 0.08 |
| HEATR1 | 1 | 236738199 | NM_018072 | c.T3089C | p.V1030A | 0.08 |
| HINFP | 11 | 119001438 | NM_015517 | c.A185G | p.E62G | 0.21 |
| HLA-B | 6 | 31324641 | NM_005514 | c.A167T | p.Q56L | 0.15 |
| HTR1A | 5 | 63257087 | NM_000524 | c.G460A | p.A154T | 0.33 |
| IGHMBP2 | 11 | 68704032 | NM_002180 | c.A2084G | p.K695R | 0.2 |
| IMPDH2 | 3 | 49065219 | NM_000884 | c.G455A | p.S152N | 0.27 |
| IQSEC2 | X | 53280267 | NM_015075 | c.G876T | p.E292D | 0.5 |
| ISM1 | 20 | 13260432 | NM_080826 | c.A530T | p.D177V | 0.19 |
| ITPR2 | 12 | 26811022 | NM_002223 | c.C1928A | p.T643N | 0.32 |
| KCNAB1 | 3 | 156232232 | NM_172159 | c.G684T | p.E228D | 0.04 |
| KCNMA1 | 10 | 78704560 | NM_001161352 | c.G2873A | p.S958N | 0.2 |
| KLHL7 | 7 | 23183521 | NM_001031710 | c.C670G | p.P224A | 0.09 |
| KRT34 | 17 | 39535422 | NM_021013 | c.T1009C | p.S337P | 0.09 |
| KRTAP4-6 | 17 | 39296172 | NM_030976 | c.G568T | p.V190F | 0.44 |
| LMBR1 | 7 | 156516850 | NM_022458 | c.T1181G | p.I394S | 0.18 |
| MAP7 | 6 | 136693664 | NM_001198619 | c.G413A | p.R138H | 0.24 |
| MCC | 5 | 112720680 | NM_001085377 | c.A400G | p.S134G | 0.19 |
| MST1 | 3 | 49725034 | NM_020998 | c.A310T | p.T104S | 0.13 |
| MSX2 | 5 | 174151777 | NM_002449 | c.C115T | p.R39C | 0.11 |
| MTMR10 | 15 | 31240510 | NM_017762 | c.A1372G | p.K458E | 0.22 |
| MUC2 | 11 | 1097266 | NM_002457 | c.G6670T | p.D2224Y | 0.06 |
| MYH10 | 17 | 8473117 | NM_005964 | c.G647A | p.R216Q | 0.73 |
| MYO3B | 2 | 171239640 | NM_138995 | c.G1126C | p.V376L | 0.17 |
| MYRF | 11 | 61549237 | NM_001127392 | c.G2957A | p.R986Q | 0.13 |
| NFE2L3 | 7 | 26224568 | NM_004289 | c.C1250T | p.S417F | 0.12 |
| NKD1 | 16 | 50666257 | NM_033119 | c.A761G | p.E254G | 0.2 |
| OR1D5 | 17 | 2966085 | NM_014566 | c.G817T | p.A273S | 0.48 |
| OR2T34 | 1 | 248737347 | NM_001001821 | c.G712A | p.G238S | 0.09 |
| OR4Q3 | 14 | 20216464 | NM_172194 | c.C878G | p.T293S | 0.1 |

| | | | | | | |
|---|---|---|---|---|---|---|
| PABPC3 | 13 | 25671027 | NM_030979 | c.A691G | p.K231E | 0.06 |
| PANX2 | 22 | 50617645 | NM_052839 | c.A1973G | p.Q658R | 0.16 |
| PCDH18 | 4 | 138452383 | NM_019035 | c.G860T | p.S287I | 0.07 |
| PLA2R1 | 2 | 160832646 | NM_001007267 | c.T2528G | p.L843R | 0.21 |
| PSD4 | 2 | 113956667 | NM_012455 | c.A2777G | p.Q926R | 0.11 |
| PTPRF | 1 | 44086525 | NM_130440 | c.C5354A | p.T1785K | 0.24 |
| PTTG1IP | 21 | 46276150 | NM_004339 | c.C407T | p.A136V | 0.21 |
| RNF170 | 8 | 42711445 | NM_001160223 | c.T634A | p.Y212N | 0.15 |
| RNF217 | 6 | 125397953 | NM_001286398 | c.T1432C | p.Y478H | 0.06 |
| ROR1 | 1 | 64515503 | NM_001083592 | c.C304A | p.P102T | 0.1 |
| RTEL1 | 20 | 62326254 | NM_016434 | c.C3270G | p.D1090E | 0.14 |
| SATL1 | X | 84363163 | NM_001012980 | c.T812A | p.M271K | 0.37 |
| SBNO1 | 12 | 123801894 | NM_001167856 | c.A2809G | p.I937V | 0.2 |
| SFR1 | 10 | 105883785 | NM_145247 | c.A410G | p.Q137R | 0.14 |
| SLC10A4 | 4 | 48485624 | NM_152679 | c.C46T | p.R16W | 0.35 |
| SNX31 | 8 | 101612653 | NM_152628 | c.A698G | p.E233G | 0.2 |
| SPATA31D1 | 9 | 84608678 | NM_001001670 | c.A3293C | p.D1098A | 0.16 |
| SSPO | 7 | 149519194 | NM_198455 | c.C12998G | p.S4333C | 0.2 |
| STK31 | 7 | 23802525 | NM_001260504 | c.C1330T | p.R444C | 0.17 |
| STK36 | 2 | 219540912 | NM_001243313 | c.C595T | p.P199S | 0.1 |
| STRN4 | 19 | 47236473 | NM_001039877 | c.A560G | p.Y187C | 0.35 |
| TMC3 | 15 | 81625596 | NM_001080532 | c.C2467A | p.H823N | 0.27 |
| TMEM245 | 9 | 111782778 | NM_032012 | c.C2602T | p.R868C | 0.17 |
| TOPAZ1 | 3 | 44283561 | NM_001145030 | c.C16A | p.P6T | 0.2 |
| TSPAN17 | 5 | 176083136 | | | | 0.28 |
| TTLL2 | 6 | 167754021 | NM_031949 | c.C633A | p.C211X | 0.24 |
| UHRF2 | 9 | 6460598 | NM_152896 | c.A670T | p.M224L | 0.24 |
| UNC80 | 2 | 210769606 | NM_182587 | c.C4486A | p.L1496I | 0.26 |
| ZNF831 | 20 | 57767600 | NM_178457 | c.T1526G | p.F509C | 0.14 |
| ZYX | 7 | 143080059 | NM_003461 | c.C667T | p.H223Y | 0.05 |

**A**
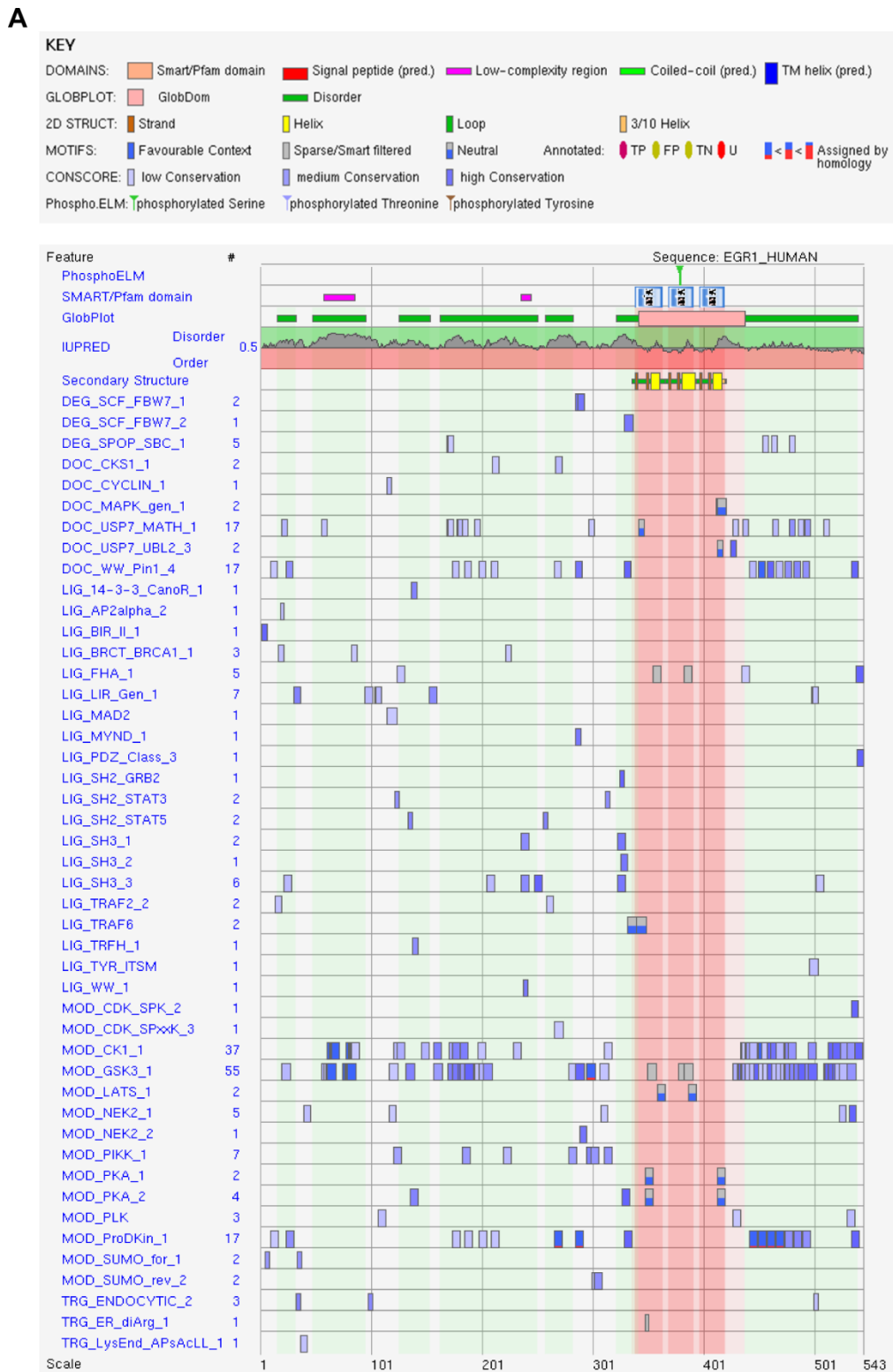


**Figure 22. EGR-1 linear motifs.** [129]

# 9

## Bibliography

1.  Palumbo, A. & Anderson, K. Multiple Myeloma. *N. Engl. J. Med.* **364,** 1046–1060 (2011).

2.  *Multiple Myeloma*. (Springer Berlin, Heidelberg, 2011).

3.  Raab, M. S., Podar, K., Breitkreutz, I., Richardson, P. G. & Anderson, K. C. Multiple myeloma. *Lancet* **374,** 324–39 (2009).

4.  Hideshima, T., Mitsiades, C., Tonon, G., Richardson, P. G. & Anderson, K. C. Understanding multiple myeloma pathogenesis in the bone marrow to identify new therapeutic targets. *Nat. Rev. Cancer* **7,** 585–98 (2007).

5.  Walker, B. a *et al.* Intraclonal heterogeneity and distinct molecular mechanisms characterize the development of t(4;14) and t(11;14) myeloma. *Blood* **120,** 1077–86 (2012).

6.  Bergsagel, P. L. & Kuehl, W. M. Chromosome translocations in multiple myeloma. *Oncogene* **20,** 5611–5622 (2001).

7.  Morgan, G. J., Walker, B. a & Davies, F. E. The genetic architecture of multiple myeloma. *Nat. Rev. Cancer* **12,** 335–48 (2012).

8.  Manier, S., Sacco,  a, Leleu, X., Ghobrial, I. M. & Roccaro,  a M. Bone marrow

microenvironment in multiple myeloma progression. *J. Biomed. Biotechnol.* **2012,** 157496 (2012).

9.    Abdi, J., Chen, G. & Chang, H. Drug resistance in multiple myeloma: latest findings and new concepts on molecular mechanisms. *Oncotarget* **4,** 2186–2207 (2013).

10.   Plotnikov, A., Zehorai, E., Procaccia, S. & Seger, R. The MAPK cascades: Signaling components, nuclear roles and mechanisms of nuclear translocation. *Biochim. Biophys. Acta - Mol. Cell Res.* **1813,** 1619–1633 (2011).

11.   Zhang, W. & Liu, H. MAPK signal pathways in the regulation of cell proliferation in mammalian cells. *Cell Res.* **12,** 9–18 (2002).

12.   Burotto, M., Chiou, V. L., Lee, J.-M. & Kohn, E. C. The MAPK pathway across different malignancies: a new perspective. *Cancer* **120,** 3446–56 (2014).

13.   Platanias, L. C. Review in translational hematology Map kinase signaling pathways and hematologic malignancies. **101,** 4667–4679 (2003).

14.   Caunt, C. J., Sale, M. J., Smith, P. D. & Cook, S. J. MEK1 and MEK2 inhibitors and cancer therapy: the long and winding road. *Nat. Rev. Cancer* **15,** 577–592 (2015).

15.   Lu, Z. & Xu, S. ERK1/2 MAP kinases in cell survival and apoptosis. *IUBMB Life* **58,** 621–631 (2006).

16.   Shin, S.-Y. *et al.* Positive- and negative-feedback regulations coordinate the dynamic behavior of the Ras-Raf-MEK-ERK signal transduction pathway. *J. Cell Sci.* **122,** 425–435 (2009).

17.   Mebratu, Y. & Tesfaigzi, Y. How ERK1/2 Activation Controls Cell Proliferation and Cell Death Is Subcellular Localization the Answer? *Cell Cycle* **8,** 1168–1175 (2009).

18.   Wortzel, I. & Seger, R. The ERK Cascade: Distinct Functions within Various

Subcellular Organelles. *Genes Cancer* **2,** 195–209 (2011).

19.  Kondoh, K. & Nishida, E. Regulation of MAP kinases by MAP kinase phosphatases. *Biochim. Biophys. Acta - Mol. Cell Res.* **1773,** 1227–1237 (2007).

20.  Hadari, Y. R., Kouhara, H., Lax, I. & Schlessinger, J. Binding of Shp2 tyrosine phosphatase to FRS2 is essential for fibroblast growth factor-induced PC12 cell differentiation. *Mol. Cell. Biol.* **18,** 3966–73 (1998).

21.  Yusoff, P. *et al.* Sprouty2 inhibits the Ras/MAP kinase pathway by inhibiting the activation of Raf. *J. Biol. Chem.* **277,** 3195–3201 (2002).

22.  Chapman, M. a *et al.* Initial genome sequencing and analysis of multiple myeloma. *Nature* **471,** 467–72 (2011).

23.  Andrulis, M. *et al.* Targeting the BRAF V600E mutation in multiple myeloma. *Cancer Discov.* **3,** 862–9 (2013).

24.  Lohr, J. G. *et al.* Widespread genetic heterogeneity in multiple myeloma: implications for targeted therapy. *Cancer Cell* **25,** 91–101 (2014).

25.  Kortüm, K. M. *et al.* Targeted sequencing of refractory myeloma reveals a high incidence of mutations in CRBN and Ras pathway genes. *Blood* **128,** 1226–1234 (2016).

26.  Dietrich, S. *et al.* BRAF inhibition in hairy cell leukemia with low-dose vemurafenib. *Blood* **127,** 2847–2855 (2016).

27.  Andrulis, M. & Dex, V. Letters to Blood To the editor : Spatially divergent clonal evolution in multiple myeloma : overcoming resistance to. **127,** 2155–2158 (2016).

28.  Bollag, G. *et al.* Vemurafenib: the first drug approved for BRAF-mutant cancer. *Nat. Rev. Drug Discov.* **11,** 873–86 (2012).

29.  Wagle, N. *et al.* MAP kinase pathway alterations in BRAF-mutant melanoma patients with acquired resistance to combined RAF/MEK

inhibition. *Cancer Discov.* **4,** 61–8 (2014).

30. Chapman, P. B. *et al.* Improved Survival with Vemurafenib in Melanoma with BRAF V600E Mutation. *N. Engl. J. Med.* **364,** 2507–2516 (2011).

31. Lito, P., Rosen, N. & Solit, D. B. Tumor adaptation and resistance to RAF inhibitors. *Nat. Med.* **19,** 1401–9 (2013).

32. Baguley, B. C. in *Methods in Molecular Biology* (ed. Zhou, J.) **596,** 1–14 (Humana Press, 2010).

33. Rapp, U. R. *et al.* Structure and biological activity of v-raf, a unique oncogene transduced by a retrovirus (malignant transformation/transduction/molecular cloning). *Biochemistry* **80,** 4218–4222 (1983).

34. Bateman, A. *et al.* UniProt: A hub for protein information. *Nucleic Acids Res.* **43,** D204–D212 (2015).

35. Cutler, R. E., Stephens, R. M., Saracino, M. R. & Morrison, D. K. Autoregulation of the Raf-1 serine/threonine kinase. *Proc. Natl. Acad. Sci. U. S. A.* **95,** 9214–9 (1998).

36. Treiber, D. K. & Shah, N. P. Ins and outs of kinase DFG motifs. *Chem. Biol.* **20,** 745–746 (2013).

37. Davies, H. *et al.* Mutations of the BRAF gene in human cancer. *Nature* **417,** 949–954 (2002).

38. Greaves, W. O. *et al.* Frequency and spectrum of BRAF mutations in a retrospective, single-institution study of 1112 cases of melanoma. *J. Mol. Diagn.* **15,** 220–6 (2013).

39. Mason, J. M., Morrison, D. J., Basson, M. A. & Licht, J. D. Sprouty proteins: Multifaceted negative-feedback regulators of receptor tyrosine kinase signaling. *Trends Cell Biol.* **16,** 45–54 (2006).

40. Heidorn, S. J. *et al.* Kinase-Dead BRAF and Oncogenic RAS Cooperate to

Drive Tumor Progression through CRAF. *Cell* **140,** 209–221 (2010).

41.  Beck, D. *et al.* Vemurafenib Potently Induces Endoplasmic Reticulum Stress-Mediated Apoptosis in BRAFV600E Melanoma Cells. *Sci. Signal.* **6,** ra7-ra7 (2013).

42.  Laquerre, S. *et al.* A selective Raf kinase inhibitor induces cell death and tumor regression of human cancer cell lines encoding B-Raf V600E. *Mol. Cancer Ther.* **8,** B88 LP-B88 (2014).

43.  Kainthla, R., Kim, K. B. & Falchook, G. S. Dabrafenib for treatment of BRAF-mutant melanoma. *Pharmgenomics. Pers. Med.* **7,** 21–29 (2013).

44.  Menzies, A. M., Long, G. V. & Murali, R. Dabrafenib and its potential for the treatment of metastatic melanoma. *Drug Des. Devel. Ther.* **6,** 391–405 (2012).

45.  Hauschild, A. *et al.* Dabrafenib in BRAF-mutated metastatic melanoma: a multicentre, open-label, phase 3 randomised controlled trial. *Lancet* **380,** (2012).

46.  Huang, T., Zhuge, J. & Zhang, W. Sensitive detection of BRAF V600E mutation by Amplification Refractory Mutation System (ARMS)-PCR. *Biomark. Res.* **1,** (2013).

47.  Flaherty, K. T. *et al.* Improved Survival with MEK Inhibition in BRAF-Mutated Melanoma. *N. Engl. J. Med.* **367,** 107–114 (2012).

48.  Wright, C. J. M. & McCormack, P. L. Trametinib: First Global Approval. *Drugs* **73,** 1245–1254 (2013).

49.  Menzies, A. M. & Long, G. V. Dabrafenib and Trametinib, alone and in combination for BRAF-Mutant metastatic melanoma. *Clin. Cancer Res.* **20,** 2035–2043 (2014).

50.  Morris, E. J. *et al.* Discovery of a novel ERK inhibitor with activity in models of acquired resistance to BRAF and MEK inhibitors. *Cancer Discov.*

**3,** 742–750 (2013).

51.     Ohori, M., Takeuchi, M., Maruki, R., Nakajima, H. & Miyake, H. FR180204, a novel and selective inhibitor of extracellular signal-regulated kinase, ameliorates collagen-induced arthritis in mice. *Naunyn. Schmiedebergs. Arch. Pharmacol.* **374,** 311–316 (2007).

52.     Poulikakos, P. I., Zhang, C., Bollag, G., Shokat, K. M. & Rosen, N. RAF inhibitors transactivate RAF dimers and ERK signalling in cells with wild-type BRAF. *Nature* **464,** 427–30 (2010).

53.     Holderfield, M., Nagel, T. E. & Stuart, D. D. Mechanism and consequences of RAF kinase activation by small-molecule inhibitors. *Br. J. Cancer* **111,** 640–5 (2014).

54.     Spagnolo, F., Ghiorzo, P. & Queirolo, P. Overcoming resistance to BRAF inhibition in BRAF-mutated metastatic melanoma. *Oncotarget* **5,** 10206–21 (2014).

55.     Adelmann, C. H. *et al.* Comparative profiles of BRAF inhibitors: the paradox index as a predictor of clinical toxicity. *Oncotarget* **7,** (2016).

56.     Flaherty, K. T. *et al.* Combined BRAF and MEK Inhibition in Melanoma with BRAF V600 Mutations. *N. Engl. J. Med.* **367,** 1694–1703 (2012).

57.     Le, K., Blomain, E., Rodeck, U. & Aplin, A. E. Selective RAF inhibitor impairs ERK1/2 phosphorylation and growth in mutant NRAS, vemurafenib-resistant melanoma cells. *Pigment Cell Melanoma Res.* **26,** 509–517 (2014).

58.     Zhang, C. *et al.* RAF inhibitors that evade paradoxical MAPK pathway activation. *Nature* **526,** 583–586 (2015).

59.     Straussman, R. *et al.* Tumour micro-environment elicits innate resistance to RAF inhibitors through HGF secretion. *Nature* **487,** 500–504 (2012).

60.     Sullivan, R., LoRusso, P., Boerner, S. & Dummer, R. Achievements and

challenges of molecular targeted therapy in melanoma. *Am. Soc. Clin. Oncol. Educ. Book* **35,** 177–86 (2015).

61.    Mar, V. J. *et al.* BRAF/NRAS wild-type melanomas have a high mutation load correlating with histologic and molecular signatures of UV damage. *Clin. Cancer Res.* **19,** 4589–4598 (2013).

62.    Nissan, M. H. *et al.* Loss of NF1 in cutaneous melanoma is associated with RAS activation and MEK dependence. *Cancer Res.* **74,** 2340–2350 (2014).

63.    Shi, H. *et al.* Acquired resistance and clonal evolution in melanoma during BRAF inhibitor therapy. *Cancer Discov.* **4,** 80–93 (2014).

64.    Gowrishankar, K., S., M. & Rizos, H. Acquired Resistance to Targeted MAPK Inhibition in Melanoma. *Melanoma - From Early Detect. to Treat.* (2013). doi:10.5772/53629

65.    Poulikakos, P. I. *et al.* RAF inhibitor resistance is mediated by dimerization of aberrantly spliced BRAF(V600E). *Nature* **480,** (2011).

66.    Nazarian, R. *et al.* Melanomas acquire resistance to B-RAF(V600E) inhibition by RTK or N-RAS upregulation. *Nature* **468,** (2010).

67.    Shi, H. *et al.* Acquired resistance and clonal evolution in melanoma during BRAF inhibitor therapy. *Cancer Discov.* **4,** 1–15 (2014).

68.    Kaplan, F. M., Shao, Y., Mayberry, M. M. & Aplin,  a E. Hyperactivation of MEK-ERK1/2 signaling and resistance to apoptosis induced by the oncogenic B-RAF inhibitor, PLX4720, in mutant N-RAS melanoma cells. *Oncogene* **30,** 366–71 (2011).

69.    Mulligan, G. *et al.* Mutation of NRAS but not KRAS signi fi cantly reduces myeloma sensitivity to single-agent bortezomib therapy. **123,** 632–640 (2015).

70.    Raab, M. S. *et al.* Spatially divergent clonal evolution in multiple myeloma: overcoming resistance to BRAF inhibition. *Blood* **127,** 2155 LP-2157

(2016).

71.     Montagut, C. *et al.* Elevated CRAF as a potential mechanism of acquired resistance to BRAF inhibition in melanoma. *Cancer* **68,** 4853–4861 (2009).

72.     Villanueva, J. *et al.* Acquired resistance to BRAF inhibitors mediated by a RAF kinase switch in melanoma can be overcome by cotargeting MEK and IGF-1R/PI3K. *Cancer Cell* **18,** (2010).

73.     Johannessen, C. M. *et al.* COT drives resistance to RAF inhibition through MAP kinase pathway reactivation. *Nature* **468,** (2010).

74.     Emery, C. M. *et al.* MEK1 mutations confer resistance to MEK and B-RAF inhibition. *Proc. Natl. Acad. Sci. U. S. A.* **106,** 20411–20416 (2009).

75.     Wang, H. *et al.* Identification of the MEK1(F129L) activating mutation as a potential mechanism of acquired resistance to MEK inhibition in human cancers carrying the B-Raf V600E mutation. *Cancer Res.* **71,** 5535–5545 (2011).

76.     Villanueva, J. *et al.* Concurrent MEK2 Mutation and BRAF Amplification Confer Resistance to BRAF and MEK Inhibitors in Melanoma. *Cell Rep.* **4,** 1090–1099 (2013).

77.     Dankort, D. *et al.* BRAF V600E cooperates with PTEN silencing to elicit metastatic melanoma. *Nat. Genet.* **41,** 544–552 (2009).

78.     Paraiso, K. H. T. *et al.* PTEN loss confers BRAF inhibitor resistance to melanoma cells through the suppression of BIM expression. *Cancer Res.* **71,** 2750–2760 (2011).

79.     Malumbres, M. & Barbacid, M. Cell cycle, CDKs and cancer: a changing paradigm. *Nat. Rev. Cancer* **9,** 153–66 (2009).

80.     Williams, G. H. & Stoeber, K. The cell cycle and cancer. 352–364 (2012).

81.     Smalley, K. S. M. *et al.* Increased cyclin D1 expression can mediate BRAF inhibitor resistance in BRAF V600E–mutated melanomas. *Mol Cancer Ther*

**7,** 2876–83 (2008).

82.     Sewify, E. M., Afifi, O. A., Mosad, E., Zaki, A. H. & El Gammal, S. A. Cyclin D1 Amplification in Multiple Myeloma Is Associated With Multidrug Resistance Expression. *Clin. Lymphoma Myeloma Leuk.* **14,** 215–222 (2014).

83.     Long, G. V *et al.* Increased MAPK reactivation in early resistance to dabrafenib/trametinib combination therapy of BRAF-mutant metastatic melanoma. *Nat Commun* **5,** 5694 (2014).

84.     Greger, J. G. *et al.* Combinations of BRAF, MEK, and PI3K/mTOR inhibitors overcome acquired resistance to the BRAF inhibitor GSK2118436 dabrafenib, mediated by NRAS or MEK mutations. *Mol. Cancer Ther.* **11,** 909–20 (2012).

85.     GlaxoSmithKline. Study to Investigate the Safety, Pharmacokinetics, Pharmacodynamics, and Clinical Activity of GSK2126458 and GSK1120212 Combination Therapy in Subjects With Advanced Solid Tumors. *In: ClinicalTrials.gov [Internet]. Bethesda (MD): National Library of Medicine (US)* (2010). at <https://clinicaltrials.gov/ct2/show/NCT01248858>

86.     National Cancer Institute (NCI). Trametinib and Akt Inhibitor GSK2141795 in Treating Patients With Relapsed or Refractory Multiple Myeloma. *In: ClinicalTrials.gov [Internet]. Bethesda (MD): National Library of Medicine (US)* (2013). at <https://clinicaltrials.gov/ct2/show/NCT01989598?term=GSK2141795&rank=6>

87.     Katagiri, S. *et al.* Two distinct human myeloma cell lines originating from one patient with myeloma. *Int. J. cancer* **36,** 241–6 (1985).

88.     Nilsson, K., Bennich, H., Johansson, S. G. & Pontén, J. Established immunoglobulin producing myeloma (IgE) and lymphoblastoid (IgG) cell

lines from an IgE myeloma patient. *Clin. Exp. Immunol.* **7,** 477–89 (1970).

89.    Gey, G. Tissue culture studies of the proliferative capacity of cervical carcinoma and normal epithelium. *Cancer Res.* **12,** 264–265 (1952).

90.    Giard, D. J. *et al.* In Vitro Cultivation of Human Tumors: Establishment of Cell Lines Derived From a Series of Solid Tumors. *J Natl Cancer Inst* **51,** 1417–1423 (1973).

91.    Kallio, M. A. *et al.* Chipster: user-friendly analysis software for microarray and other high-throughput data. *BMC Genomics* **12,** 507 (2011).

92.    Chen, J., Ozanne, S. E. & Hales, C. N. Methods of Cellular Senescence Induction Using Oxidative Stress. 179–189

93.    Huang, D. W., Lempicki, R. a & Sherman, B. T. Systematic and integrative analysis of large gene lists using DAVID bioinformatics resources. *Nat. Protoc.* **4,** 44–57 (2009).

94.    Thomas, P. D. *et al.* PANTHER: A browsable database of gene products organized by biological function, using curated protein family and subfamily classification. *Nucleic Acids Res.* **31,** 334–341 (2003).

95.    Leich, E. *et al.* Multiple myeloma is affected by multiple and heterogeneous somatic mutations in adhesion- and receptor tyrosine kinase signaling molecules. *Blood Cancer J.* **3,** e102 (2013).

96.    Lodé, L. *et al.* Lack of BRAF V600E mutation in human myeloma cell lines established from myeloma patients with extramedullary disease. *Blood Cancer J.* **3,** e163 (2013).

97.    Yan, S. F., Pinsky, D. J., Mackman, N. & Stern, D. M. Egr-1: Is it always immediate and early? *J. Clin. Invest.* **105,** 553–554 (2000).

98.    Arora, S. *et al.* Egr1 regulates the coordinated expression of numerous EGF receptor target genes as identified by ChIP-on-chip. *Genome Biol.* **9,** R166 (2008).

99. Chen, L. *et al.* Identification of early growth response protein 1 (EGR-1) as a novel target for JUN-induced apoptosis in multiple myeloma. *Blood* **115,** 61–70 (2010).

100. Yu, J. *et al.* PTEN regulation by Akt–EGR1–ARF–PTEN axis. *EMBO J.* **28,** 21–33 (2009).

101. Michaloglou, C. *et al.* BRAFE600-associated senescence-like cell cycle arrest of human naevi. *Nature* **436,** 720–724 (2005).

102. Mooi, W. J. & Peeper, D. S. Oncogene-Induced Cell Senescence — Halting on the Road to Cancer. *N. Engl. J. Med.* **355,** 1037–1046 (2006).

103. Daniotti, M. *et al.* BRAF alterations are associated with complex mutational profiles in malignant melanoma. *Oncogene* **23,** 5968–77 (2004).

104. Mitsutake, N. *et al.* Conditional BRAFV600E expression induces DNA synthesis, apoptosis, dedifferentiation, and chromosomal instability in thyroid PCCL3 cells. *Cancer Res.* **65,** 2465–2473 (2005).

105. Yacoub, A., Park, J. S., Qiao, L., Dent, P. & Hagan, M. P. MAPK dependence of DNA damage repair: ionizing radiation and the induction of expression of the DNA repair genes XRCC1 and ERCC1 in DU145 human prostate carcinoma cells in a MEK1/2 dependent fashion. *Int. J. Radiat. Biol.* **77,** 1067–78 (2001).

106. Hawkins, A., Golding, S., Khalil, A. & Valerie, K. DNA double-strand break–induced pro-survival signaling. *Radiother. Oncol.* **101,** 13–17 (2011).

107. Khalil, A. *et al.* ATM-dependent ERK signaling via AKT in response to DNA double-strand breaks. *Cell Cycle* **10,** 481–491 (2011).

108. Liu D, Song H, X. Y. A common Gain of function of p53 cancer mutants in inducing genetic instability. *Oncogene* **29,** 949–956 (2010).

109. Janku, F., Kaseb, A. O., Tsimberidou, A. M., Wolff, R. A. & Kurzrock, R. Identification of novel therapeutic targets in the PI3K/AKT/mTOR

pathway in hepatocellular carcinoma using targeted next generation sequencing. *Oncotarget* **5,** 3012–22 (2014).

110.  Hyun, T. *et al.* Loss of PTEN expression leading to high Akt activation in human multiple myelomas. *Blood* **96,** 3560–3568 (2000).

111.  Ronchetti, D. *et al.* Deregulated FGFR3 mutants in multiple myeloma cell lines with t(4;14): comparative analysis of Y373C, K650E and the novel G384D mutations. *Oncogene* **20,** 3553–3562 (2001).

112.  Yadav, V. *et al.* Reactivation of Mitogen-activated Protein Kinase (MAPK) pathway by FGF Receptor 3 (FGFR3)/Ras mediates resistance to vemurafenib in human B-RAF V600E mutant melanoma. *J. Biol. Chem.* **287,** 28087–28098 (2012).

113.  Nazarian, R. *et al.* Melanomas acquire resistance to B-RAF(V600E) inhibition by RTK or N-RAS upregulation. *Nature* **468,** 973–7 (2010).

114.  David J. Matthews and Mary E. Gerritsen. *Targeting Protein Kinases for Cancer Therapy*. (John Wiley & Sons, Inc., 2010).

115.  Whibley, C., Pharoah, P. D. P. & Hollstein, M. P53 Polymorphisms: Cancer Implications. *Nat Rev Cancer* **9,** 95–107 (2009).

116.  Pim, D. & Banks, L. P53 Polymorphic Variants At Codon 72 Exert Different Effects on Cell Cycle Progression. *Int. J. Cancer* **108,** 196–199 (2004).

117.  Pavlistova, L. *et al.* Change in ploidy status from hyperdiploid to near-tetraploid in multiple myeloma associated with bortezomib/lenalidomide resistance. *Cancer Genet.* **207,** 326–331 (2014).

118.  Coward, J. & Harding, A. Size Does Matter: Why Polyploid Tumor Cells are Critical Drug Targets in the War on Cancer. *Front. Oncol.* **4,** 1–15 (2014).

119.  Fujiwara, T. *et al.* Cytokinesis failure generating tetraploids promotes tumorigenesis in p53-null cells. *Nature* **437,** 1043–1047 (2005).

120.  Ganem, N. J., Storchova, Z. & Pellman, D. Tetraploidy, aneuploidy and

cancer. *Curr. Opin. Genet. Dev.* **17,** 157–162 (2007).

121. Titz, B. *et al.* JUN dependency in distinct early and late BRAF inhibition adaptation states of melanoma. *Cell Discov.* **2,** 16028 (2016).

122. Ramsdale, R. *et al.* The transcription cofactor c-JUN mediates phenotype switching and BRAF inhibitor resistance in melanoma. *Sci Signal* **8,** ra82 (2015).

123. Gitenay-D. Is EGR1 a potential target fpr prostate cancer therapy? *Futur. Oncol* **5,** 993–1003 (2009).

124. Gaggioli, C. *et al.* Tumor-Derived Fibronectin Is Involved in Melanoma Cell Invasion and Regulated by V600E B-Raf Signaling Pathway. *J. Invest. Dermatol.* **127,** 400–410 (2007).

125. Bolli, N. *et al.* Heterogeneity of genomic evolution and mutational profiles in multiple myeloma. *Nat. Commun.* **5,** (2014).

126. Khan, S. H. & Kumar, R. An overview of the importance of conformational flexibility in gene regulation by the transcription factors. *J. Biophys.* **2009,** 210485 (2009).

127. Dosztanyi, Z., Csizmok, V., Tompa, P. & Simon, I. IUPred: web server for the prediction of intrinsically unstructured regions of proteins based on estimated energy content. *Bioinformatics* **21,** 3433–3434 (2005).

128. Dosztányi, Z., Csizmók, V., Tompa, P. & Simon, I. The pairwise energy content estimated from amino acid composition discriminates between folded and intrinsically unstructured proteins. *J. Mol. Biol.* **347,** 827–839 (2005).

129. Dinkel, H. *et al.* ELM 2016 - Data update and new functionality of the eukaryotic linear motif resource. *Nucleic Acids Res.* **44,** D294–D300 (2016).

130. Villanueva, J. *et al.* Acquired resistance to BRAF inhibitors mediated by a

RAF kinase switch in melanoma can be overcome by co-targeting MEK and IGF-1R/PI3K. *Cancer Cell* **18,** 683–695 (2011).

131. Thevakumaran, N. *et al.* Crystal structure of a BRAF kinase domain monomer explains basis for allosteric regulation. *Nat Struct Mol Biol* **22,** 37–43 (2015).

132. Brummer, T. *et al.* Functional analysis of the regulatory requirements of B-Raf and the B-Raf(V600E) oncoprotein. *Oncogene* **25,** 6262–76 (2006).

133. Yu, J., De Belle, I., Liang, H. & Adamson, E. D. Coactivating factors p300 and CBP are transcriptionally crossregulated by Egr1 in prostate cells, leading to divergent responses. *Mol. Cell* **15,** 83–94 (2004).

134. Li, W. *et al.* The EMBL-EBI bioinformatics web and programmatic tools framework. *Nucleic Acids Res.* **43,** W580–W584 (2015).